Design and Accuracy Assessment of a Multi-Input Single Ended Primary Inductor Converter (SEPIC) for Highly Efficient Output from Hybrid Sources of Renewable Energy

By

Sheikh Mustahsin Ahmed Rakeen
18121029
Tahmin Mahmud
18121027
Afrid Uddin Araf
18121074
Nayeem Ahmed
18121021

A thesis submitted to the Department of Electrical and Electronic Engineering in partial fulfillment of the requirements for the degree of
Bachelor of Science in Electrical and Electronic Engineering

Department of Electrical and Electronic Engineering
Brac University
Summer 2021

Declaration

It is hereby declared that

1. The thesis submitted is my/our own original work while completing degree at Brac University.
2. The thesis does not contain material previously published or written by a third party, except where this is appropriately cited through full and accurate referencing.
3. The thesis does not contain material which has been accepted, or submitted, for any other degree or diploma at a university or other institution.
4. I/We have acknowledged all main sources of help.

Student's Full Name & Signature:

Sheikh Mustahsin Ahmed Rakeen

18121029

Tahmin Mahmud

18121027

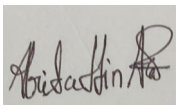

Afrid Uddin Araf

18121074

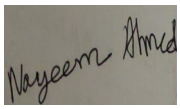

Nayeem Ahmed

18121021

Approval

The thesis/project titled “Design and Accuracy Assessment of a Multi-Input Single Ended Primary Inductor Converter (SEPIC) for Highly Efficient Output from Hybrid Sources of Renewable Energy” submitted by

1. Sheikh Mustahsin Ahmed Rakeen (18121029)
2. Tahmin Mahmud (18121027)
3. Afrid Uddin Araf (18121074)
4. Nayeem Ahmed (18121021)

of Summer 2021 has been accepted as satisfactory in partial fulfillment of the requirement for the degree of Electrical and Electronics Engineering on 3rd October, 2021.

Examining Committee:

Supervisor:

(Member)

Dr. A. K. M. Abdul Malek Azad
Professor
Department of Electrical and Electronic Engineering, Brac University, Dhaka

Program Coordinator:

(Member)

Abu S.M. Mohsin, PhD
Assistant Professor
Department of Electrical and Electronic Engineering, Brac University, Dhaka

Departmental Head:

(Chair)

Md. Mosaddequr Rahman, PhD
Professor and Chairperson
Department of Electrical and Electronic Engineering, Brac University, Dhaka

Ethics Statement

All the resources and data used for our project will be treated as confidential. All the study and work were voluntarily done by us. We carefully observed and examined our data. No payment was made to any person who was directly or indirectly involved in this project work. We carefully avoided any type of discrimination against our members. We focused on minimizing human and animal harm as much as possible and maximizing sheer benefits.

Abstract

In this thesis, a hybrid topology of an off-grid energy-harvesting system (by integrating Solar Photovoltaic (PV) Module with Bicycle Dynamo Generator) using a DC-DC multi-input single-output (MISO) single-ended primary inductor converter (SEPIC) has been proposed for isolated islands. A conventional SEPIC based SISO converter circuit was designed for the boost mode operation and its performance was compared with our proposed hybrid topology of the SEPIC based MISO converter system. The prototype of the proposed hybrid system has been developed by following an optimum design approach for small-scale performance analysis. The MISO SEPIC circuit has been designed to be operated at a practical input voltage of DC 12.1 V and an approximate output voltage of DC 53 V with 10W output power at the load side. To get the maximum voltage at the output end, the operating duty cycle for the proposed converter circuit is recorded as 81.49% with a gain of 4.4. From the hardware analysis and field-test data, we obtain and calculate an efficiency rate of 91.6% for the proposed prototype. A detailed and rigorous investigation of the proposed topology has been carried out through software simulation using MATLAB while considering the Solar PV Panel as Source-I and a feedback-controlled Bicycle Dynamo Generator as the Source-II. Different intermittence conditions, solar irradiance, seasonal variation, day-night behavior, power outage and other factors were taken into consideration while performing both the hardware and software analysis. Moreover, to secure a better understanding of the maximum performance of the two renewable energy sources, separate outdoor analysis was performed for the Solar PV Panel and the Bicycle Dynamo Generator. Solar energy has been a promising tool as an inexhaustible and clean energy for decades. From off-grid small installations to large scale photovoltaic plants, solar energy has become an integral part of our life. Due to the vicissitudes of atmospheric behavior, the PV Module alone can not harvest optimum electrical energy from the sun. So, this is where our proposed topology stands out. Our proposed model instills the

possibilities of renewable energy, with the hope that it would ultimately reduce the total demand from the national grid and ensure utter energy efficiency inside Bangladesh and beyond.

Keywords: Renewable energy sources; Hybrid multi-port converter; SEPIC Converter; Power supplies; Topology; Voltage optimization;

Dedication

We would like to dedicate our research project to our parents as well as to the friends and relatives who have always encouraged us to strive for success and whose never-ending advice through all stages has led us this far in our academic careers. We would also want to dedicate this to our honorable supervisor, who has been very supportive and encouraging throughout the process of developing the final product.

Acknowledgement

We would like to express our gratitude to Dr. A K M Abdul Malek Azad, Professor, Department of Electrical and Electronic Engineering (EEE), School of Engineering, BRAC University, for his constant guidance, supervision and invaluable recommendations throughout the entire project.

Table of Contents

List of Tables

List of Figures

List of Acronyms

SEPIC	Single Ended Primary Inductor Converter
PV	Photovoltaic
MISO	Multi Input Single Output
MIMO	Multi Input Multi Output
MIC	Multi Input Converter
D	Duty Cycle
DC	Direct Current
ESE	East-Southeast
SE	Southeast
SSE	South-Southeast

Glossary

Thesis:	An extended research paper that is part of the final exam process for a graduate degree. The document may also be classified as a project or collection of extended essays.

Chapter 1 Introduction

1.1 Foreword

Climate change, rising oil costs, global warming and the scarcity of fossil fuels have all heightened interests in renewable energy resources such as photovoltaic (PV) panels and electrical power production via bicycle pedals. Numerous renewable energy sources, on the other hand, have fluctuating and intermittent characteristics that change with weather conditions and other environmental factors. To ensure that the local loads may get an uninterruptible, steady and stable power supply, an energy storage system is often needed [1]. When integrated, typical power generators generate low voltage and need high-gain converters to meet load demands. As a result, the development of high static gain DC-DC converters is a significant field of research, owing to the increasing demand for this technology from a variety of applications that are powered by low DC output voltage power sources [2]. It seems that a multi-input converter (MIC) that can handle a range of sources is required in order to allow multi-source technology to be implemented [3].

Considering the fact that MICs can outperform their counterparts in terms of efficiency, size and cost, they are the most often used semiconductor device. The multi-input DC-DC converter, which is a simple device that can be loaded with many input sources, was developed to replace MICs. This project will operate in a boosted converter structure, which has been later shown in this paper. The input current characteristic of these converters is a significant problem [4]. This paper presents the SEPIC, which is one of several DC-DC converters that are available. The step-up capacity of the SEPIC converter is defined in this work without the need to change the polarity of the output voltage. In addition, the capacitor contributes to the

coupling of energy, which simplifies the overall analysis. A converter with two inputs has been shown in this work.

The output voltage of the PV panels, which is one of the sources, supplies a low direct current voltage [6]. It is thus necessary to use a step-up DC-DC converter in order to increase and control the voltage. The voltage conversion gain of the DC-DC converter that has been stated should be high. There is a possibility of connecting the PV panels in series, but this would introduce a number of complications, such as the issue of partial shadowing [1]. Another issue that these DC-DC converters must contend with is the nature of their input current. PV panels need maximum power point tracking (MPPT) in order to function properly. For MPPT to run, the converter's input current must be constant throughout the conversion. A DC-DC converter with a constant input current will also improve the system's dynamic performance by increasing the input current. Overall, a high voltage gain and a constant input current are required for the usage of a DC-DC converter in renewable energy sources [4].

Conventional boost converters may be utilized as a single-switch single-stage designs in the same way that they are used in other applications. Their voltage conversion gains, on the other hand, are insufficient for precise usage in renewable energy applications. However, they are capable of achieving high voltage gains while operating the power switch at high duty ratios. The performance of the converter, on the other hand, will be significantly reduced [7].

As a result, a small, high-profile power electronic interface is required to overcome drawbacks such as size and control complexity resulting from the separation of the transformer and the increased number of components as well as to allow for a flexible integration of a wide range of energy sources with varying characteristics. The majority of multi-input converter (MIC) topologies described in the literature are derived from basic buck–boost topologies, leaving room for future topological structures based on special converters. This paper proposes a

modular, non-isolated converter that can handle varied input sources and output loads derived from a simple SEPIC structure. Due to its unique features, such as improved power factor from continuous input current, non-inverting output, gracious response and true shutdown during short circuits, the SEPIC converter has a wide range of applications, including connecting flexible input voltages with stable outputs, battery-operated equipment and lighting applications [3].

Besides the PV panel, we will also be using a bicycle dynamo generator as a renewable energy source in this research. In rural areas, bicycles are the primary mode of transportation for locals. In order to take advantage of the energy that is generated when humans are pedaling a bicycle, which is almost limitless. When pedaling a bicycle, humans are capable of generating about 150W of power [8]. A dynamo alternator can convert the energy generated by people pedaling their bicycles into electrical energy, which is particularly useful in our rural regions where the majority of people rely on bicycles for transportation. Power from the generator may be used to charge a mobile phone or a small lighting item. Solar energy, which is the cleanest and most plentiful renewable energy source available, is obtained from the Sun. Solar energy has the potential to be converted into electricity. Solar energy is being applied to optimize power in large quantities all around the globe. This has the potential to substantially decrease the energy bills of families while also making a major contribution to the reduction of greenhouse gas emissions. However, we all know that the energy produced by a single renewable resource is insufficient to satisfy the demand for electricity in a given area. In this case, the analytical solution will be the combination of various renewable resources via the use of a converter, which can then be deployed to provide electricity to the surrounding area. Furthermore, the multi-input converter is well-suited for using in a modular configuration [9]. In terms of financial benefits, it is also beneficial to combine various PV modules with other renewable energy sources (generation of electrical power using bicycle pedals in this project). The

multiport converter will decrease the overall number of system components while simultaneously increasing the operating flexibility [4].

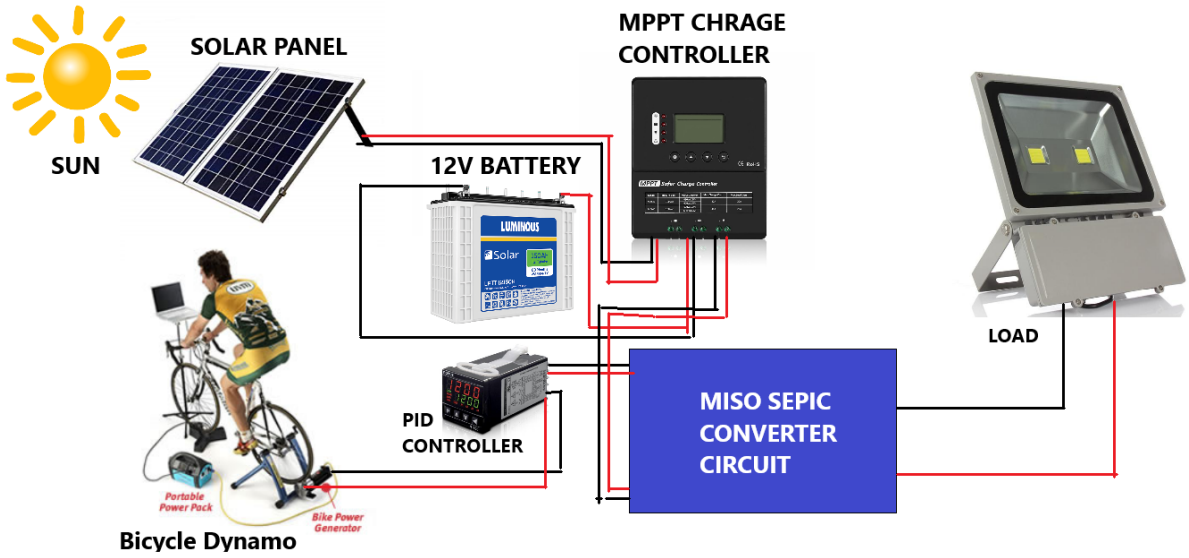

Figure 1.1: Block Diagram of the proposed model

The Figure 1.1 is the block diagram of our proposed model, where we have considered two renewable energy sources as our input to the SEPIC circuit and for the output at the load side, we have used a 10W spotlight. Between the SEPIC circuit and load we proposed integrate a MPPT controller that will resist the battery from being overcharged.

1.2 Background

Bangladesh is especially vulnerable to climate change due to its topography, which is dominated by low-lying delta plains and its dense population. It is one of the ninth most vulnerable countries on the world, according to the Global Climate Risk Index (CRI) [10]. The opportunity to build green infrastructure from the ground up, on the other hand, is the biggest challenge. Adopting electric vehicles, building energy-efficient transportation systems and depending on renewable energy sources are all examples of this. On the other hand, many renewable energy sources have variable and intermittent qualities that vary with the weather and other environmental variables [1]. Government of Bangladesh has adopted a wide range of policies and measures to combat effects of climate change and they have been well praised for its efforts [11]. Conventional power generators generate low voltage when integrated, necessitating the employment of high-gain converters to meet the load's needs. As a consequence, due to the growing demand for this technology from a range of applications that use low DC output voltage power sources, the development of high static gain DC-DC converters has become a major area of study [2]. In order to combat the future's intermittent nature of energy supply, future power systems will also need the interfacing of different renewable energy sources through the usage of multi-source technology. Multi-input converter, as it seems for now, is most capable of handling a variety of sources that is needed in order to deploy multi-source technology [3].

1.3 Motivation

The notion that clean and renewable energy resources and power systems have the potential to make a significant influence on Bangladeshi's lives acts as the motivating factor behind this initiative and its study. Bangladesh aims to generate 40 percent of its electricity from renewable sources by 2041 [10]. Upon a successful testing, debugging and rigorous trial and error method of the prototype, we were able to analyze the performance of a multi-port SEPIC topology.

This may be a silver lining in terms of our knowledge and acceptance of the undergraduate period. The performance evaluation of maximum voltage optimization via an upgraded MISO SEPIC converter will motivate us to carry out further research on this topic on a larger scale in future. Since our government is expanding its investment in the renewable energy sector and considering its potential advantages for billions of rural people, we did not hesitate to select renewable energy as our topic of interest. Solar energy is a tremendous resource for developing nations like Bangladesh and it has taken a prominent position in the ever-growing debate over global warming. The usage of renewable energy will aid rural people to get out of the poverty trap. In order to do this, we have conducted a study and research to collect adequate information on solar photovoltaic (PV) systems, as well as off-grid and on-grid power transmission. In order to get the most out of a solar PV system, we can further continue to empower rural people by inculcating basic standards and core values of renewable energy.

1.4 Literature Review

Renewable energy resources are plentiful and produce zero emissions, yet sporadic in nature. These power generators provide a low voltage when integrated, requiring high-gain converters to satisfy the load demand. Power electronics, therefore, play a key role in interfacing with renewable hybrid power systems, electrical traction and continuous power supply. To address the intermittent nature of energy resources, future power systems will also incorporate multi-source technologies to interface different energy sources. According to project designed by Rehman et al., DC–DC converters have successfully accomplished the leap from SISO to MIMO converters, which he believes is a significant advancement. As a result, these converters may now interface with a variety of different levels of inputs and combine their benefits in order to feed a variety of levels of outputs. While continuing to decrease the cost and quantity

of components, research has also continued to enhance areas such as the overall system's dependability and efficiency while also sustaining continual improvement. Following an examination of different Multi Input Multi Output (MIMO), Multi Input Single Output (MISO) DC–DC converter topologies, we have found that when it comes to fulfilling all of the criteria of expense, durability, adaptability, productivity and versatility in a single topology, it has been found that there is no one topology that can do so [12].

In their paper, Ardi et al. present the concept of a high step-up DC-DC converter. Among the numerous benefits of the converter are its high gain of the voltage and constant input current, both of which make it especially well-suited for renewable energy applications. The converter that is being provided is based on the SEPIC converter. Using a connected inductor in conjunction with two voltage multipliers, on the other hand, the voltage gain of the converter may be enhanced. In addition, a passive clamp circuit is included in the proposed converter, which improves the voltage gain while simultaneously reducing the voltage stress placed on the primary switch [6].

Furthermore, the project of Moradpour et al. included the development of an innovative structure for a boosted DC-DC converter. The SEPIC converter is used as the basis for the structure that is being presented. Thus, the converter takes use of the many advantages offered by a SEPIC converter, such as a constant input current, among other things. Additionally, the suggested converter has a high voltage conversion gain as well as greater efficiency, which are both beneficial. The continuity of the input current makes the converter described ideal for use with renewable energy sources. The use of a linked inductor in conjunction with a voltage multiplier cell in this construction improves the high voltage gain of the construction. In addition, decreased voltage stress on the main power switch results in better conversion

efficiency because of the reduced voltage stress. The steady state analysis as well as the design of the converter are both covered in detail in their research [4].

Zhao et al. described a multiple-input DC-DC converter that was created from a SEPIC configuration that is common in the industry. The suggested design enables the integration of several dispersed generating sources into a single DC main bus. Their paper covers the converter topology, as well as the fundamental dynamic equations that govern it and also explains how it works. They also investigated the stability features of systems using linear techniques [9].

In their work, Anuradha et al. developed and showed an effective technique of fabricating from a basic SEPIC a three-port non-isolated converter. Initially, they divide the SEPIC converter into two cells: a source cell and a load cell. Leveraging DC link capacitors, two of these source cells are connected with a common load cell to form a three-port SEPIC converter with a common input and output. In addition to having a single-stage power conversion with reduced structural complexity, the derived converter has the capability of transferring power in both directions. It includes a battery as well as an auxiliary photovoltaic source to allow for bidirectional power transfer [3].

Mohanty's experiment is based on the multi-input SEPIC converter, which he developed. A positive polarity output voltage is generated that is equal to the polarity of the input voltage, but the output voltage may not always be equal to the value of the input voltage. It operates in the same manner as a buck, boost or buck-boost converter, which means that it may step up the voltage in the same manner as a boost converter and step down the voltage in the same manner as a buck converter. It is also possible to attach a battery storage system to it by using a bidirectional connection in conjunction with the input port. The SEPIC converter has the ability to charge and discharge an energy storage device because of its buck-boost feature. Depending

on the charging conditions of the energy storage device, it may operate in one of two operational modes: steady state mode or dynamic mode [5].

Sangalad et al designed a SEPIC converter with two inputs. It is necessary to utilize the time-sharing switching method in order to produce gate pulses for switching devices. Because it provides for a wider diversity and selection of input sources, this system is more flexible than the previous versions. Instead of utilizing two single input converters for separate power sources, a dual input SEPIC may be used to save money and minimize loss. A simple and low-cost zero-ripple filter method for the load is proposed as a potential future scope of their research and development [13].

1.5 Overview of Thesis Organization

The rest of the dissertation is organized as follows-

Chapter 2: *DC-DC Converter*

In this chapter we have discussed about what is a DC-DC converter, how it works and its mechanism. The applications of DC-DC converter in practical field. We have also focused on different types of DC-DC converter, such as- buck converter, boost converter, buck-boost converter and SEPIC converter. We have explained these converters briefly in this chapter.

Chapter 3: *Single Ended Primary Inductor Converter (SEPIC)*

In chapter 3, we described about SEPIC converter. Moreover, we throw light on the behavior of SEPIC converter when it is in continuous conduction mode. We also described about how this converter conduct in switch on and switch off mode. In addition, we showed the way of designing a SEPIC converter and how its implemented for Solar PV systems.

Chapter 4: *The Proposed Hybrid MISO Converter System*

Throughout this chapter, the explanation about the project that we have built is given. The system we wanted to construct is demonstrated here. Furthermore, the steady state analysis of our system is also shown here. The arrangement and the configuration that was needed to shape our proposed converter is also clarified in this chapter.

Chapter 5: *Renewable Energy Sources: Solar PV Module and Bicycle Dynamo*

In this chapter, the two renewable energy sources that we have used in our project has been described in details. At first, we gave a brief description about the solar energy and the pv panel that we have considered as our first renewable resources. Further, we discussed about the growth of utilizing solar panel for electricity in rural and urban areas of our country. The structure and working principle of a solar panel is also demonstrated in some portions of this

chapter. The characteristics and the efficiency of a solar panel is showed here in details. In addition, different analysis and mathematical calculation of the solar panel that we have used for our proposed system has been attached here with clarification. Secondly, the second renewable resource that we have used for our proposed system is bicycle dynamo which has been described in the late portion of this chapter. Here, we have explicated the mechanism of generator, types of generators that can be involved in constructing bicycle dynamo. Moreover, the working principle of dynamo is presented here, also drawing up an alternative approach of dynamo, which is an alternator. The bicycle dynamo that we have featured is shown here and the working principle of our bicycle dynamo is explained here in details. In addition, we have also done different kinds of analysis through the bicycle dynamo that we have constructed, it is also shown here with clarification,

Chapter 6: *Simulation and result analysis*

In this chapter, the simulation and the design of our system is placed. We have used MATLAB/SIMULINK to simulate our proposed system and to do various kinds of analysis. We have described here, how we have simulated our project in this software and the component and parameters that we have taken into account. Moreover, we have compared many results with each other and briefly clarify them here. The analysis of different models is presented throughout this chapter.

Chapter 7: *Practical field test and result analysis*

In this chapter, as we have also prepared our project through hardware. The components that we have used in our hardware is described here. The implementation of hardware setup of SISO is shown here and explained. Moreover, the construction of bicycle dynamo generator is also presented. In short, the MISO SEPIC hardware is also shown. Finally, the result and analysis of all the hardware that was build is clarified in this chapter.

Chapter 8: *Conclusion and future work*

In this chapter, the difficulties and challenges that we have faced while constructing our project in pandemic situation is shared. The overall idea of our project is briefly described here. It is also described how this project will be beneficial for human being. Moreover, the idea of future work that can be operated in this project is narrated here elaborately.

Chapter 2 DC-DC Converter

2.1 Introduction

A DC-DC converter is a typical DC converter circuit that transforms high-frequency power by utilizing fast switching, inductors, and capacitors to smooth out any anomalies at the DC voltage circuits. It may be thought of as the direct current counterpart of an alternating current transformer with a continuously changing turn ratio. When working with dc voltage sources, it is mainly utilized to step-up or step-down voltage. Vehicle traction motor control, voltage regulators, and DC current source converters are all examples of applications for DC-DC converters. Prior to the introduction of power semiconductors, DC voltage supply conversion for low-power applications was accomplished by combining a vibrator with a transformer and a rectifier to create a bridge. This indicates that the direct current voltage was changed to alternating current voltage, which was then rectified and filtered to convert back to direct current voltage. In order to achieve the necessary direct current voltage for high-power applications, an electric motor was used to drive a generator of the appropriate voltage. Such methods of stepping up or down DC voltage were very expensive, and the procedures themselves were extremely time-consuming to begin with. These procedures became less expensive and more efficient as a result of the development of power electronic integrated circuits and solid-state switch-mode circuits, respectively [31-32].

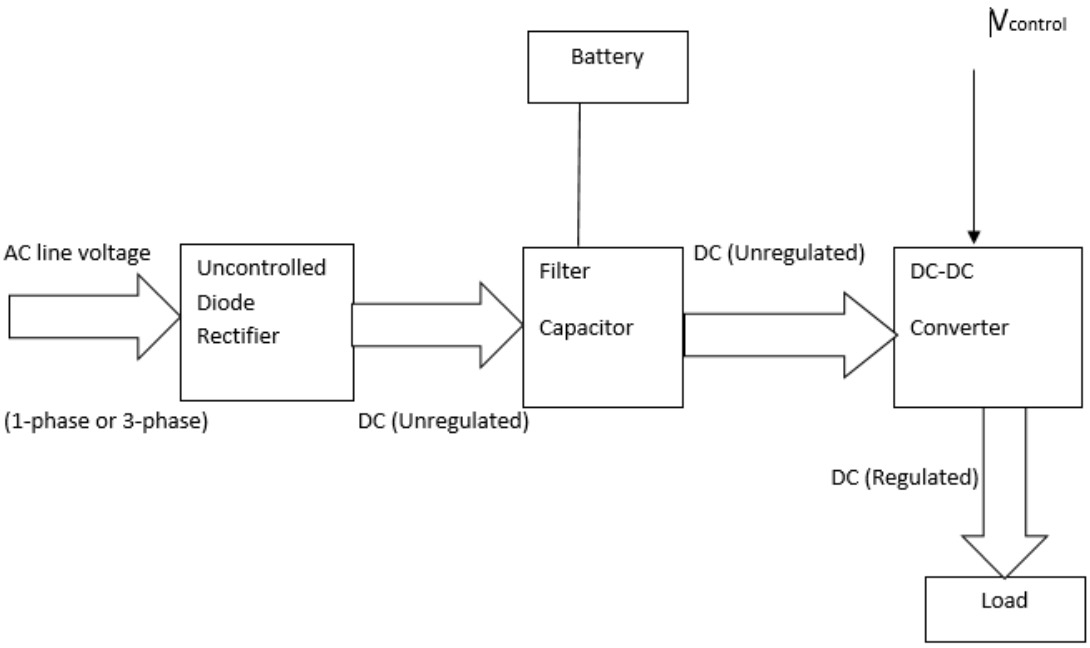

Figure 2.1: Block Diagram of DC-DC Converter

2.2 Applications of DC-DC Converters

DC-DC converters are used in a wide range of applications, ranging from small electronic circuits to high-power supply systems and everything in between. DC-DC converters have a multitude of purposes in the automobile industry. Boost converters are utilized in hybrid electric vehicles (HEVs), adaptive control applications such as those found in spacecraft, airbuses, and jets, and robotics [33]. Furthermore, Solar panels typically provide a low amount of voltage as their output. A boost converter is needed in order to achieve the higher voltage that is required by the majority of loads. A DC-DC converter is also used to ensure that a solar panel produces the greatest amount of electricity possible. DC-DC converters are utilized in digital devices such as computers, mobile phones, PDAs, and other handheld electronic devices. When a laptop battery has a voltage as high as 10.8 V, the CPU may only need 3.3 V or even lower voltages in order to function properly. Because of this, a DC-DC converter is required to lower the input voltage [37].

2.3 DC-DC Converter Topologies

DC-DC converters may be divided into two categories based on the way in which transistors are used in the converter circuits.

1. Voltage Regulators

2. Switched Linear -mode Voltage regulators

Linear voltage regulators are so called because the mode of operation of the transistor employed is in the linear area, which is where they operate. The basic linear voltage regulator is shown in the figure 2.1. The output voltage is $V_O=I_LR_L$, which means it is across the load. The output voltage of a transistor may be varied between 0V and close to V_S by varying the base current of the transistor (source voltage). The variable resistance is provided by the transistor that is utilized in the circuit. Despite the ease with which such a circuit may be constructed, the inefficiency caused by the power loss across the transistor can be a significant problem when it comes to reducing massive losses in high-power applications. In this case, it can be seen that the transistor absorbs about 70-75 percent of the entire power provided by the source. As a result, only low-power applications may benefit from this kind of converter [34].

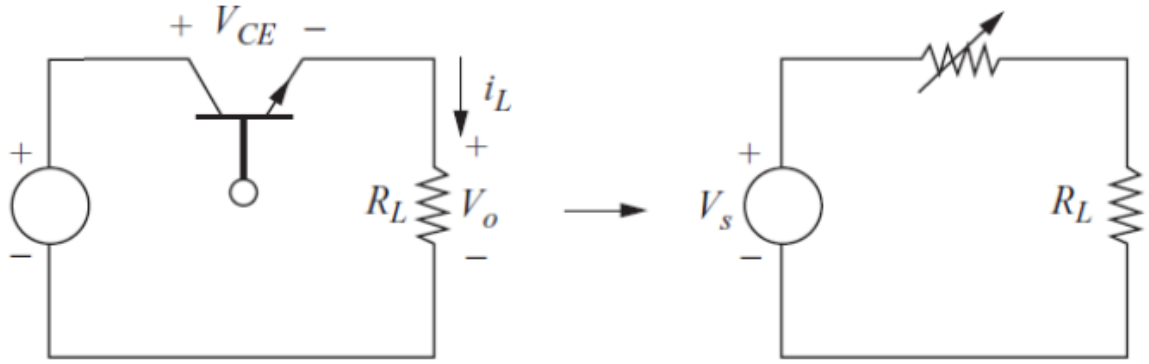

Figure 2.2: Basic Linear Voltage Regulator Circuit [34]

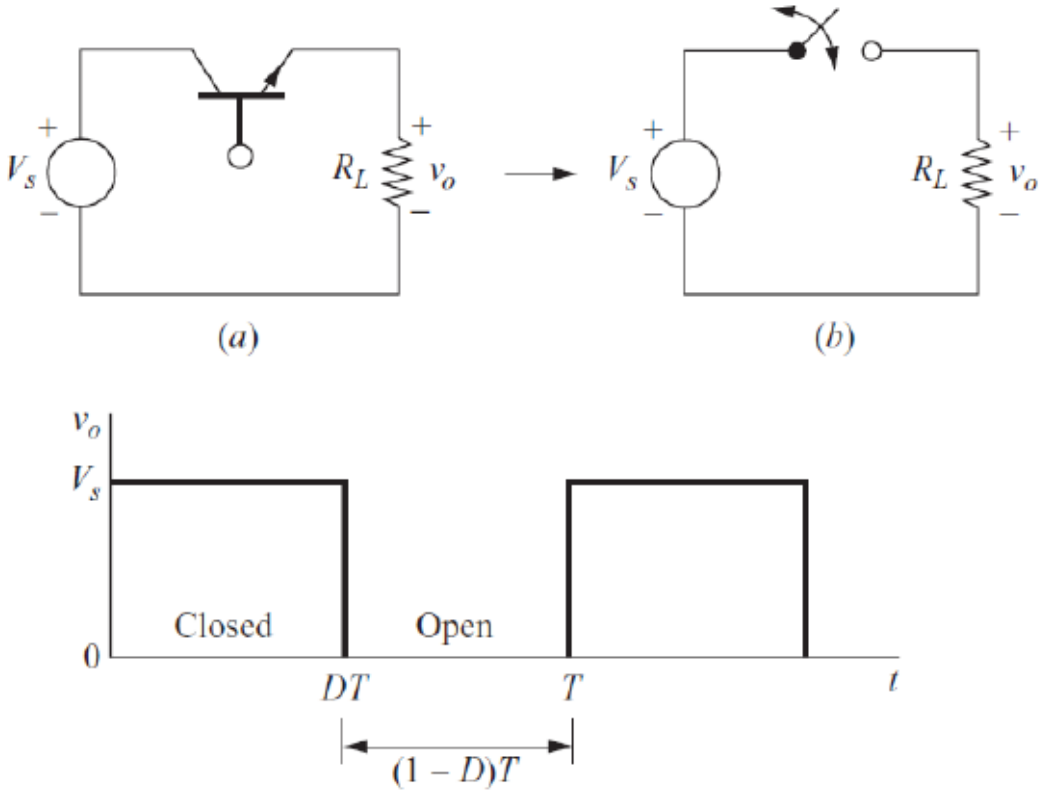

Figure 2.3: Basic Switched-mode Converter [34]

The switched mode voltage regulators, on the other hand, operate the transistors as if they were an electronic switch, and have proved to be a more efficient and practical alternative to linear voltage regulators. In this kind of converter, the transistor is both fully on and completely off at all times. This happens because the transistor is in the saturation or cut-off (in the case of a BJT) or triode and cut-off regions (in MOSFETS). The dissipation of heat in the circuit is minute and practically insignificant owing to the small transience across the linear area of the transistor and the absence of resistive components inside the input and output, and the efficiency is much higher.

In Figure 2.2, a basic switching converter is shown, where V_o represents the output voltage and V_S represents the source voltage, and T represents the time period. The duty cycle (D) shows

how much of the time period T the switch is closed, and it is measured in percentages. Assume that the switch is in perfect condition. Continuum operation of the switch results in an average output voltage of when it is opened and closed repeatedly will be:

$$V_O = \frac{1}{T}\int_0^T v_{o(t)}dt \quad \text{.....(I)}$$

$$= \frac{1}{T}\int_0^T v_s dt$$

$$= V_S D$$

It is possible to regulate the DC component or the average output voltage by varying the duty cycle according to the requirements.

$$Duty\ Cycle, D = \frac{t_{ON}}{t_{ON}+t_{OFF}} \text{.....(II)}$$

$$= \frac{t_{ON}}{T}$$

$$= t_{ON} f$$

The switching frequency is denoted by f. The power absorbed by real switches will not be zero since the voltage across the switch will not be zero, and the switch will still have to pass through the linear area during every transitional state. However, because the losses are so insignificant, they can be overlooked. The switched-mode power converter topologies are available in both isolated and non-isolated versions, and there are many of them. The four most frequent and beneficial topologies, which are often utilized in the majority of situations, are as follows:

1. Buck

2. Boost

3. Buck-Boost

4. Single-ended primary inductor converters (SEPIC)

2.4 Buck Converter

The buck or step-down converter controls the average DC output voltage at a level that is lower than the input or source voltage. For variable speed drive applications, the buck converter supplies a variable DC voltage to the armature of a DC motor. This is achieved via controlled switching, in which the DC input voltage is switched on and off at regular intervals, resulting in a lower average output voltage on the output side of the system.

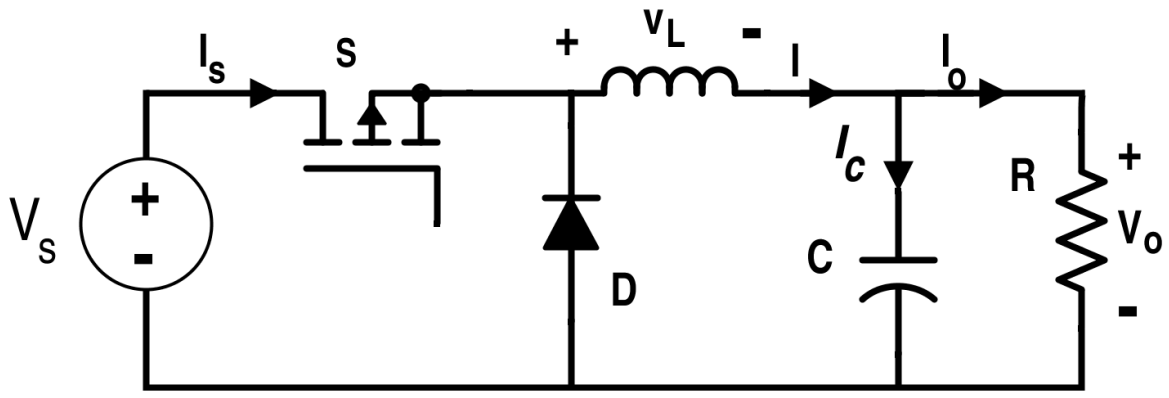

Figure 2.4: Buck converter circuit diagram [source: google]

The buck converter, shown in Figure 2.4, is a kind of power converter that is frequently used in regulated DC power supply, such as those found in computers and instruments [35].

2.5 Boost Converter

In a boost converter, the average output voltage is regulated at a level that is greater than the input or source voltage. When referring to the boost converter, the terms step-up converter and regulator are often used interchangeably. The DC input voltage is connected in series with an

inductor, which serves as a current source for the circuit. A switch connected in series with the current source and the output is intermittently switched off, allowing the energy from the inductor and the source to be used to raise the average output voltage. The boost converter shown in Figure 2.5 is a kind of power converter that is frequently used in regulated DC power supply and regenerative braking of DC motors.

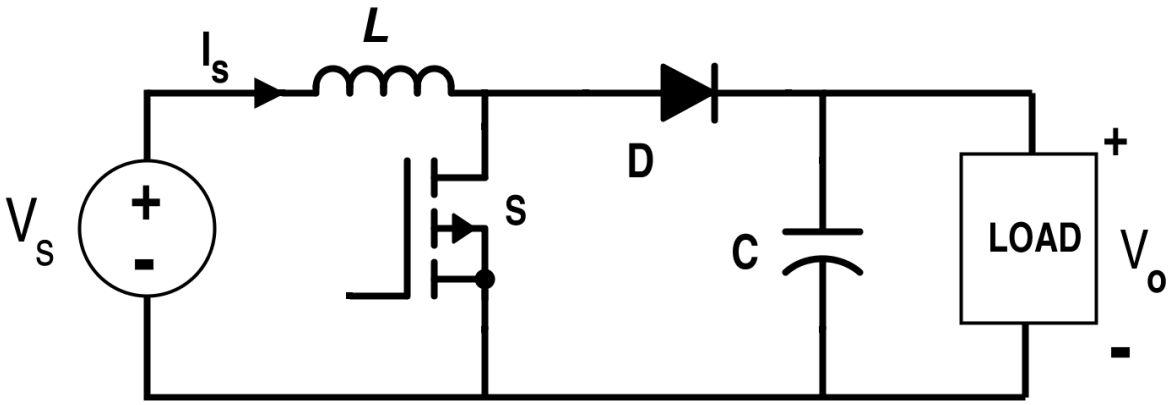

Figure 2.5: Boost converter circuit diagram [source: google]

The boost converter, shown in Figure 2.5, is a kind of power converter that is frequently used in regulated DC power supply and regenerative braking of DC motors.

2.6 Buck Boost Converter

When the DC-DC converter circuit is linked to the DC power source and the load, it transforms the uncontrolled DC input into a controllable DC output converter by adjusting the voltage of the input. Traditional buck-boost converters, which have a straightforward construction and are simple to build, have been extensively utilized in a variety of applications. Although the switching frequency has increased in recent years, the power required to switch has decreased, making the switching process lighter and more efficient. However, the relationship between switching frequency and switching losses is inverse, meaning that as the switching frequency

increases, the switching loss also increases. The conventional buck-boost converter is used in order to increase conversion capacity, changeable range, and overall efficiency of the system.

It is a kind of DC-to-DC converter, and the output voltage is of a certain magnitude. It is possible that it is more or less than the magnitude of the input voltage. The buck boost converter, which is a single inductor, is utilized in lieu of the transformer in this application. There are two types of features in the buck-boost converter.

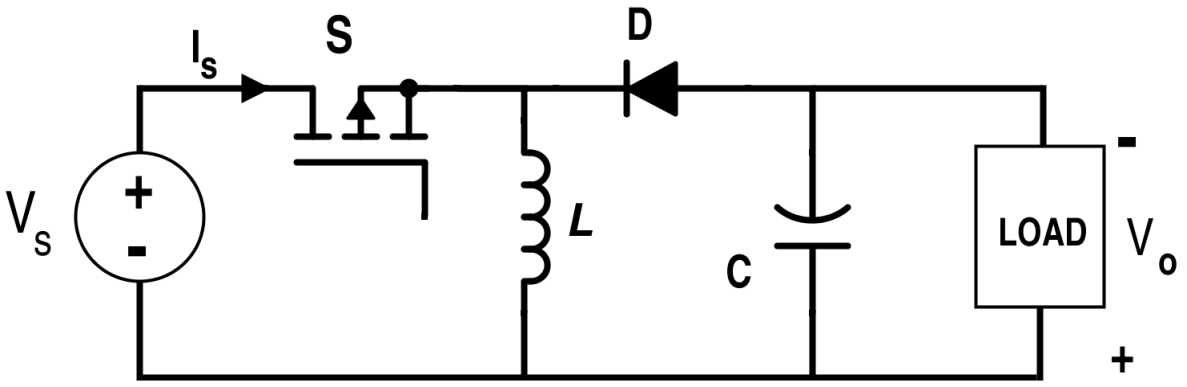

Figure 2.6: Buck-Boost converter circuit diagram [source: google]

The basic buck boost converter is shown in the Figure 2.6. One of the features of this converter is, it can step down the input voltage like buck converter or it can step up the voltage level like boost converter depending on the duty cycle that is being provided to this converter. If the percentage of duty cycle is above 50% then it will act like a boost converter and if the percentage is below 50% then it will act like a buck converter.

2.7 SEPIC Converter

The single-ended primary inductor converter (SEPIC) operates on both the step-up and step-down principles. Two inductors are used to either buck or boost the input voltage to the output voltage, and the output voltage is not reversed in polarity as a result of this configuration. Due to the fact that it transmits energy through capacitor C1 and inductor L1, the switching voltage is greater than that of the boost converter. For broad input voltage applications, the static gain of the converter is employed. It is almost exactly equal to the sum of the input and output voltages in the switch due to the voltage flow in the switch. When compared to a boost converter, the inrush input current is modest, but the voltage stress is significant due to the high voltage stress [32].

Some converter applications just need the bucking or boosting of voltage, and these applications may be served by using the appropriate converters. However, it is possible that the required output voltage will be within the range of the input voltage at some point. Whenever this is the case, it is generally preferable to use a voltage converter that has the ability to reduce or raise the voltage as needed. Because they only need a single inductor and a single capacitor, buck-boost converters may be more cost-effective. These converters, on the other hand, suffer from a significant degree of input current ripple. A big capacitor or an LC filter may be required in many applications because of this ripple's ability to cause harmonics to occur. As a result, the buck-boost is often either costly or inefficient. Another problem that may make the use of buck-boost converters more difficult is the fact that they invert the voltage when they are used. Cuk converter overcomes both of these issues by including an additional capacitor and inductor. However, the functioning of both the Cuk and the Buck-boost converters puts a significant amount of electrical stress on the components, which may result in device failure or excessive heating.

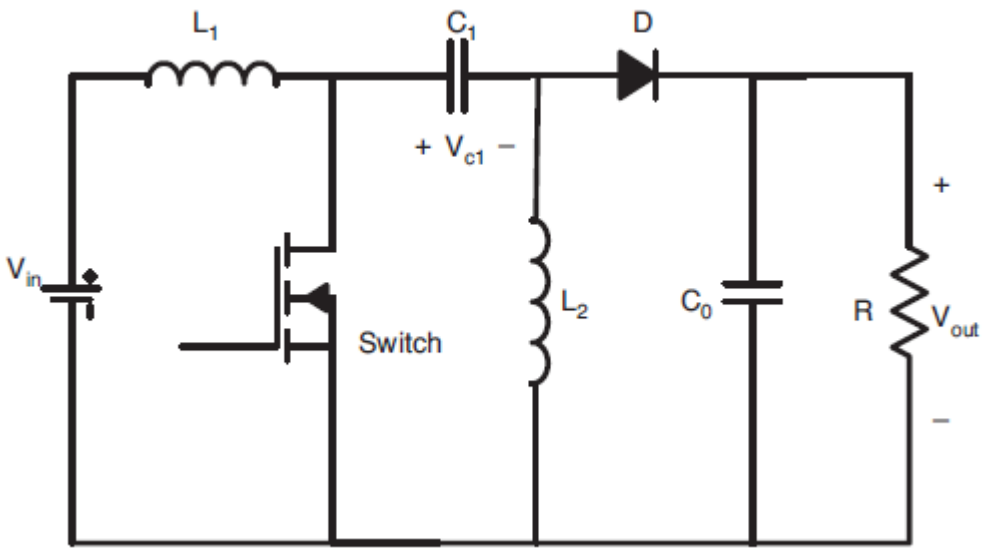

Figure 2.7: SEPIC circuit diagram [source: google]

The SEPIC, shown in Figure 2.7, provides a solution to each of these issues, which will be explored in more depth in the next chapter.

2.8 Conclusion

A DC-DC converter is an electromechanical device that can shift the voltage level of a DC source. This converter plays a very major role to regulate the output voltage of multiple appliances. There are various types of DC-DC converter, each type has its own specialty and importance.

Chapter 3 Single Ended Primary Inductor Converter (SEPIC)

3.1 Introduction

The DC-DC converter is a type of voltage converter that is extensively utilized in a variety of applications [4]. The Buck converter, a Boost converter, a Buck-Boost converter, a Cuk converter and the SEPIC are the most common DC-DC converters [15]. The SEPIC (single ended primary inductor converter) is a DC-DC converter. The output voltage of the SEPIC converter may be less than, equal to, or higher than the input voltage. The duty cycle of the control transistor is responsible for controlling the output of the SEPIC converter [14].

The SEPIC may be used as a boost, buck and buck-boost converter, among other things. It functions in the same way as a buck-boost converter, but it has certain benefits, such as the fact that its output is non-inverting (the polarity of output voltage of SEPIC converter is the same as the input voltage of SEPIC converter). Energy is transferred between inductors and capacitors in the SEPIC converter in order to convert from one voltage source to another using the converter.

SEPIC's duty cycle is critical to the operation of the system. It is possible to alter the magnitude of the output voltage by varying the duty cycle. When compared to other converters, the SEPIC converter achieves a superior result in terms of efficiency as well as input current purity, which is a desirable characteristic. The SEPIC converter has a very low switching loss and a very low overshot compared to other converters.

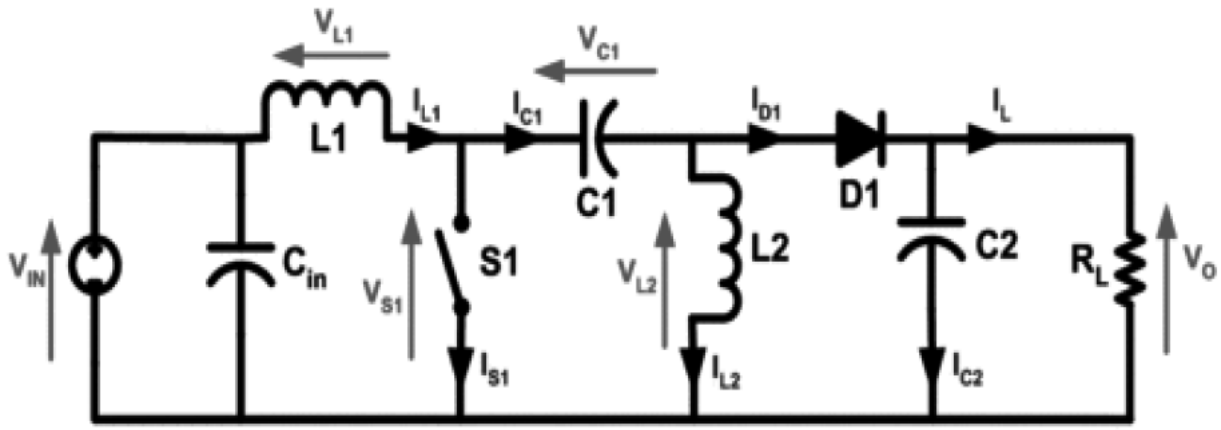

Figure 3.1: Schematic Diagram of SEPIC [18]

When using the SEPIC, shown in Figure 3.1, it is feasible to operate the output noise at a considerably higher frequency than when using conventional converters [5].

3.2 Continuous Conduction Mode

Figure 3.1 depicts a schematic circuit design of a basic SEPIC dc-dc converter with a dc-dc output. The SEPIC converter works in the same way as other DC-DC converters in that it transfers energy between capacitors and inductors in order to convert voltage and current. Typically, a semiconductor switch such as a MOSFET controls the amount of energy transferred through the switch S_1. MOSFETs have a higher input impedance and a smaller voltage drop than bipolar junction transistors, making them more efficient (BJTs). BJT switching is controlled by current driving, whereas MOSFET switching is controlled by voltage changes between the gate and source.

Any time that the current flowing through the inductor L_1 does not decrease to zero, the SEPIC converter is in continuous-conduction mode (sometimes referred to as "continuous mode"). During the steady-state functioning of a SEPIC, the average voltage across capacitor C_1 (V_{C1}) is equal to the input voltage of the circuit (V_{in}). Because the capacitor C_1 prevents direct current (DC) from flowing across it, the average current across it (I_{C1}) is zero, resulting in the inductor L_2 being the only source of load current. The average current through inductor L_2 (I_{L2}) is

therefore the same as the average load current, and the average load current is therefore independent of the input voltage [20].

When average voltages are considered, the following may be written:

$$V_{in} = V_{L_1} + V_{C_1} + V_{L_2} \ldots\ldots\ldots\ldots (I)$$

Since the average voltage of V_{C1} equals the voltage of V_{IN}, $V_{L1} = -V_{L2}$. As a result, the two inductors can be wrapped together on the same core. Since these voltages are of equal magnitude, the mutual inductance effects of the two windings will be zero, provided that the polarity of the windings is accurate. Furthermore, since the voltages are of similar size, the ripple currents produced by the two inductors will be of same magnitude [21-22].

$$I_{D_1} = I_{L_1} - I_{L_2} \ldots\ldots\ldots\ldots (II)$$

3.3 Operation

3.3.1 Mode A: When switch is ON

When the switch S_1 is turned on, the inductor L_1 is charged by the voltage supplied by the source, V_S. Given that the coupling capacitor C_p is originally charged to the source voltage V_{in}, with S being on, the coupling capacitor discharges via the inductor L_2 to discharge the coupling capacitor.

$$V_{in} = (L_1)\frac{d}{dt}\left(i_{L_1}\right) \ldots\ldots\ldots\ldots (III)$$

$$V_{C_1} = (L_2)\frac{d}{dt}\left(i_{L_2}\right) \ldots\ldots\ldots\ldots (IV)$$

$$\frac{V_{C_2}}{R} = -(C_2)\frac{d}{dt}\left(V_{C_2}\right) \ldots\ldots\ldots\ldots (V)$$

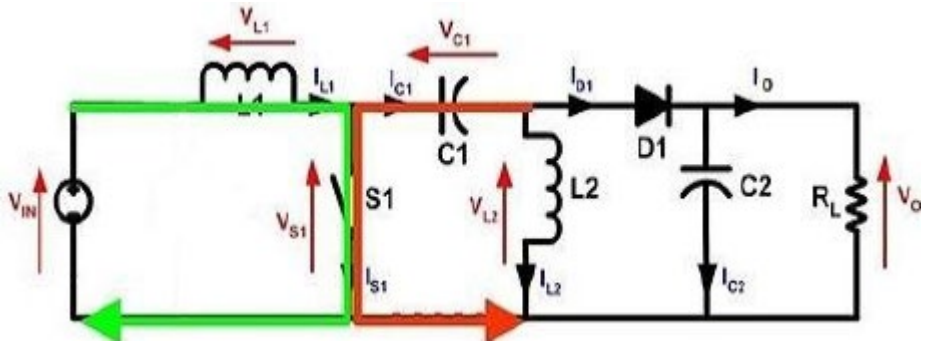

Figure 3.2: SEPIC when switch S1 is on [18]

As it can be seen in Figure 3.2, the diode is reverse biased and the output capacitor supplies power to the load as a result of this [17].

3.3.2 Mode B: When switch is OFF

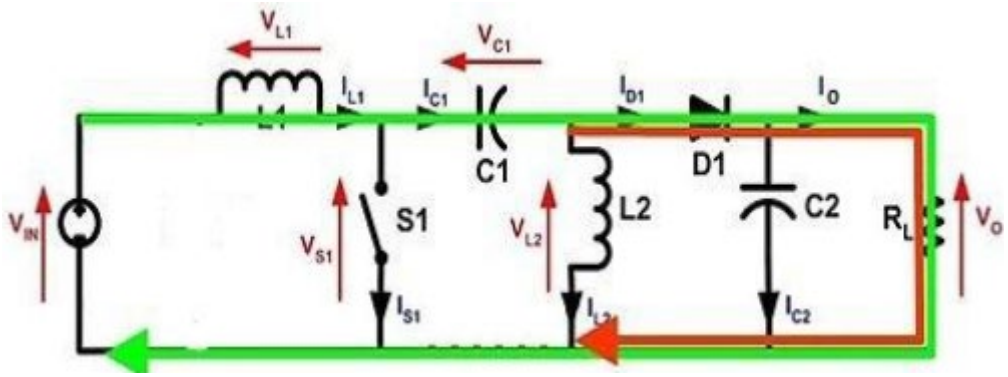

Figure 3.3: SEPIC when S1 is off [18]

As the circuit illustrated in Figure 3.3, when switch S1 is turned off, the inductor L1 discharges via coupling capacitor Cp. As a result, it will be charged. Because the inductor L2 changes polarity in order to resist the change in current direction, the diode D is activated as a result. The inductor L2 discharges via the output capacitor as well as through the load and the output capacitor [18].

$$V_{in} + (L_1)\frac{d}{dt}(i_{L_1}) = V_{C_1} + V_{C_2} \ldots\ldots\ldots\ldots (VI)$$

$$(C_2)\frac{d}{dt}\left(V_{C_2}\right) + \frac{V_{C_2}}{R} + i_{L_1} + i_{L_2} \ldots\ldots\ldots\ldots \text{(VII)}$$

$$V_{C_2} = (L_2)\frac{d}{dt}\left(i_{L_2}\right) \ldots\ldots\ldots\ldots \text{(VIII)}$$

3.4 Ideal Voltage and Current Gain Equations of the DC-DC SEPIC

The SEPIC DC-DC converter is depicted in Figures 3.2.1 and 3.2.2 in both the switch ON and switch OFF modes, respectively. As shown in the accompanying diagrams, the volt-sec balance for each switching cycle may be performed in order to get the optimal voltage and current gain equation of the converter.

For inductor L_1,

$$V_{in}DT + (V_{in} - V_C - V_O)(1 - D)T = 0 \ldots\ldots\ldots\ldots \text{(IX)}$$

Which yields,

$$V_C = \frac{V_{in}}{1 - D} - V_O$$

$$I_C = \frac{1 - D}{I_{in}} - I_O$$

For inductor L_2,

$$-V_C DT + V_O(1 - D)T = 0 \ldots\ldots\ldots\ldots \text{(X)}$$

Which yields,

$$V_C = \frac{V_O}{D} - V_O$$

$$I_C = DI_O - I_O$$

Solving the equations of Voltage simultaneously

$$\frac{V_{in}}{1-D} - V_O = \frac{V_O}{D} - V_O$$

$$V_O = \frac{D}{1-D} V_{in}$$

Solving the equations of Current simultaneously

$$\frac{1-D}{I_{in}} - I_O = DI_O - I_O$$

$$\frac{I_O}{I_{in}} = \frac{(1-D)}{D}$$

According to the voltage and current equations, an ideal SEPIC DC-DC converter has a Buck-Boost voltage and current gain relationship.

3.5 Design of SEPIC

Measuring the duty cycle to design a SEPIC circuit is crucial for a designer. Basically, the duty cycle of is the ratio of the total time when the pulse is high over the time when the pulse is low. The duty cycle, also known as the "duty factor," is represented as a percentage of the total time spent ON. Duty cycle can be calculated from the equation:

$$D = \frac{V_O}{V_O + V_{in}} \text{.....(XI)}$$

Average inductance current can be calculated using:

$$I_{L_1} = \frac{Output\ Power}{V_{in}} \text{ .....(XII)}$$

$$I_{L_2} = \frac{Output\ Power}{V_O}$$

Maximum inductance current can be found by:

$$I_{L_{1max}} = I_{L_1} + \frac{\Delta i_{L_1}}{2}$$

$$I_{L_{2max}} = I_{L_2} + \frac{\Delta i_{L_2}}{2}$$

Minimum inductance current can be found by:

$$I_{L_{1min}} = I_{L_1} - \frac{\Delta i_{L_1}}{2}$$

$$I_{L_{2max}} = I_{L_2} - \frac{\Delta i_{L_2}}{2}$$

Value of inductor can be determined by:

$$L_1 = \frac{V_{in}D}{f\Delta i_{L_1}}$$

$$L_1 = L_2$$

Value of capacitor can be determined by:

$$C_1 = \frac{V_O D}{Rf\Delta V_{C_1}}$$

$$C_1 = C_2$$

Value of load resistor can be determined by:

$$R = \frac{(V_O)^2}{P}$$

3.6 SEPIC for Solar PV Systems

Solar photovoltaic technology has risen to the top of the list of power production options among the many renewable energy sources available. Being an environmentally friendly and secure investment option for both individuals and companies, it can help consumers with having a decrease in their power costs, a new experience with more energy independence and contribute to lower the global pollution levels to a great extent.

Solar panels are made up of photovoltaic (PV) cells, which are solar cells that collect direct sunlight or photons. The PV cells transform the collected energy into direct current electricity by using a semiconductor material such as silicon. A DC-DC converter is then used to increase the voltage of the DC electricity to the desired level, after which an inverter is used to transform the DC energy into useable Alternating Current (AC) [19].

A PV module is made up of a number of PV cells and a PV array is made up of a combination of PV modules that produce the necessary electricity for specified loads. In general, solar PV modules are linked in series to enhance the PV output voltage as the existing PV modules can only produce a much lower DC output voltage ranging from 12V to 75V, which makes it necessary to connect them in series. As a result, in order to convert this low DC output to the necessary usage voltage level, a suitable power electronic DC-DC converter is required. Furthermore, the low DC output voltage produced by the PV panel is quite unpredictable and depends on a variety of factors such as solar irradiance, shadowing effects, ambient temperature, mismatches between PV modules, the cleanliness of the PV module surface and so on. Furthermore, the selection of an appropriate DC-DC converter architecture is particularly crucial when it comes to effectively harvesting solar energy from solar PV arrays.

As a result, a sheer urgency growing for the development of a highly efficient DC-DC converter to control the low and variable DC output voltage produced from PV arrays. The converters

that are now available on the market are costly, but their efficiency is poor. As a result, in order to meet the aforementioned requirements, a Single-Ended Primary Inductance Converter (SEPIC) is recommended. The SEPIC converter may be used with a PID controller to guarantee that the voltage output from a solar PV array remains consistent even when the irradiance levels fluctuate dramatically during daytime. Furthermore, an inverter may be connected after the SEPIC converter to convert DC power into Alternating Current, which is then supplied to household electrical loads [19].

3.7 Conclusion

SEPIC converter is a special kind of buck-boost DC-DC converter. It has an advantage of having a non-inverted output. As it consists of two inductors, if the current flows in both the inductor then it will be in continuous conduction mode. The SEPIC converter operates in two modes (switch on and switch off) with the help of switching of its MOSFET. Moreover, this converter can be easily design by considering some formulas that are stated here in this chapter. A SEPIC converter can play a very vital role in obtaining a modified output from solar PV panel.

Chapter 4 The Proposed Hybrid MISO Converter System

4.1 The Conceptual Topology of the Proposed SEPIC based MISO Converter System

Figure 4.1 shows a simplified visual representation of the proposed topology. The hybrid topology that we are proposing is a single-ended primary inductor converter (SEPIC) based multi-input single-output (MISO) converter for photovoltaic (PV) based bicycle dynamo system. The proposed system configuration shows that the number of ports may be increased or lowered even further by connecting or detaching the extra pulsating voltage cells (PVC), depending on the availability of the power and data input sources [3].

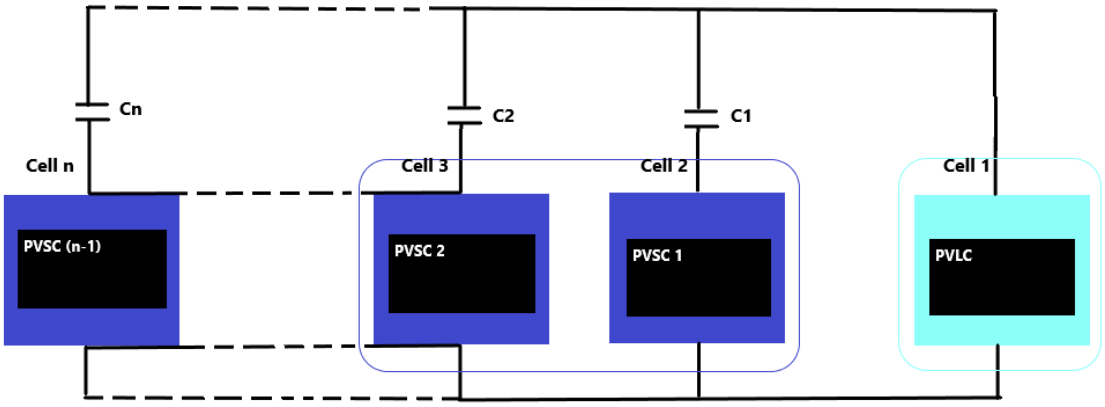

Figure 4.1: Generalized Diagram of n-port SEPIC converter

In this paper, we have proposed a unidirectional SEPIC based MISO converter with three ports (2 inputs and 1 output), as seen in Figure 4.2. A multi-input converter is essentially a circuit structure that integrates various input voltage sources with varied voltage levels and delivers

an output dc load to a single output voltage source [27]. The suggested model is having a PV cell at the input side. PV cells are classified into two types: Pulsating Voltage Source Cells

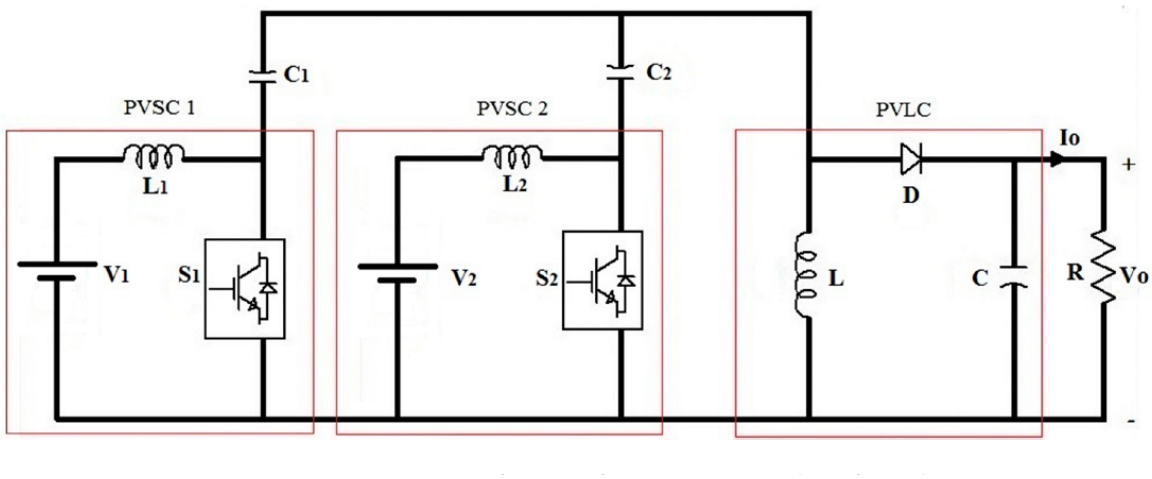

Figure 4.2: Three-port SEPIC Converter

(PVSC), they are basically used for the input side, and Pulsating Voltage Load Cells (PVLC), which are used for the output side. Since it is a MISO structure, each PVSC is connected to a common PVLC by a coupling capacitor, resulting in a full SEPIC structure when combined.

4.2 Steady State Analysis of the Proposed SPEIC based MISO Converter Circuit

During the steady state phase, the voltages on the input capacitors on C_1 and C_2 are the source voltages V_1 and V_2 respectively. If both of the integrated two sources are the renewable energy sources (for example, if V_1 is a solar photovoltaic system and V_2 is a bicycle dynamo), the converter operates as a unidirectional converter, with current flowing solely from the source to the load in our proposed system. When the voltage magnitudes of both sources are equivalent, the switches S_1 and S_2 functions with the similar amount of duty cycle. We can calculate different parameters of the proposed dual input SEPIC converter by using the following expressions.

The output voltage expression for our modified dual input SEPIC converter that we have developed for our project is represented by the equation below:

$$V_o = \frac{D_2V_2+D_{eff}V_1}{1-D_1} \text{ .....(I)}$$

Where D_{eff} is the effective duty and is deduced by:

$$D_{eff} = D_2 - D_1 \text{ .....(II)}$$

The current across the input inductors can be calculated by:

$$i_{L_1} = \frac{D_1V_o}{(1-D_2)R} - \frac{(D_1D_{eff}V_2T)(L_1L_2+LL_2+LL_3)}{2L_1L_2L} \text{ .....(III)}$$

$$i_{L_2} = \frac{D_{eff}V_o}{(1-D_2)R} - \frac{(D_1D_{eff}V_1T)(L_1L_2+LL_2+LL_3)}{2L_1L_2L} \text{.....(IV)}$$

Likewise, we can also calculate the voltage ripples from the steady-state equations. Assuming that, the voltage across C_1 rises linearly from a lower value to a upper value. This condition creates a chance to rise the ripple voltage, the expression is as below:

$$V_{C_1} = \frac{i_{L_1}}{fC_1}(1 - D_1) \text{.....(V)}$$

$$V_{C_2} = \frac{i_{L_2}}{fC_2}\left(1 - D_{eff}\right) \text{.....(VI)}$$

The output capacitor C discharges during a certain period, providing load current. Therefore, the voltage ripple can be defined by:

$$V_C = V_{C_2} - V_{C_1} = \frac{D_1V_1+D_{eff}V_2}{fRC}(D_1 + D_{eff}) \text{ .....(VII)}$$

4.3 Design Considerations of the Proposed SEPIC based MISO Converter Circuit

The design of the different components that are included in the suggested converter topology is covered in this section. Dual input SEPIC converters are DC-DC converters that generate output voltages that are either less than or larger than the voltages supplied by the inputs. The duty cycle of the switches, the values of the input inductors and capacitors, and the shape of the output LC filter are all important parameters to design for the modelling of the converter circuit.

The duty cycle for the two switches, D_1 and D_2 can be calculated from the output voltage equation mentioned earlier.

The input inductance is given by

$$L_1 = \frac{V_1 D_2}{f I_{L_1}}$$

$$L_2 = \frac{V_2 D_2}{f I_{L_2}}$$

The input capacitance is given by

$$C_1 = \frac{i_{L_1}}{f V_{C_1}} (1 - D_1)$$

$$C_2 = \frac{i_{L_2}}{f V_{C_2}} \left(1 - D_{eff}\right)$$

The output LC filter can be deduced by

$$L = \frac{D_1 V_1 + D_{eff} V_2}{f * i_{L_1}}$$

$$C = \frac{\left(D_1 V_1 + D_{eff} V_2\right)}{f R V_c}$$

The load resistor can be easily calculated by

$$R = \frac{(V_o)^2}{P}$$

4.3.1 A Brief Idea: LC Filter for DC-DC Converters and Relevant Applications

According to the study of the electrical engineering, an LC filter or LC network is a typical electrical circuit. This circuit is made up with basic passive elements such as an inductor (L) and a capacitor (C). Figure 4.3 depicts a typical LC Filter circuit

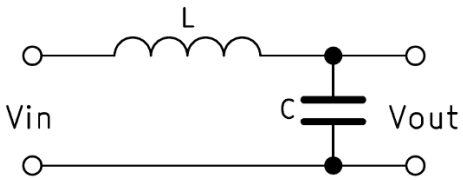

Figure 4.3: LC Filter Circuit

Inside an LC filter, the charges can flow back-and-forth between the two conducting plates of the capacitors and through the inductors. The energy that is being stored inside the capacitors and flowing through the inductors, keeps oscillating between them until the internal resistance of these two components and the overall connecting wires extincts. The operation mode of this circuit seems like a tuned action. This tuned action for the LC circuit is known as harmonic oscillation and this is why the LC circuits are called tuned or tank circuit [36]. The series or parallel LC circuit configuration is designed to create different types of filters like low-pass filters, high-pass filters, multiplexer, band-pass filters, or even band-rejection filters [59].

One of the most crucial appliances of these LC filters is to create an LC effect to filter out certain frequency levels. As the LC filters incorporate coil and capacitors, the inductive and capacitive resistances vary with different frequency levels of the input voltage. For designing general DC-DC converters, we use LC filters to have a smooth output voltage at the output side. These filters can curb the ripple effect (ripple currents and ripple voltages) at the output side. LC filters in DC-DC converters can reduce switching harmonics in the output voltage and

current. The design approach of the LC filter is crucial for DC-DC converters because it affects the overall functionality, power density and even the cost of the converter. Usually, high rated coils are expensive and it takes a lot of effort to build them. The general appliances of these LC filters include but not limited to wireless transmission of signals with different attenuation effects, control of unwanted frequencies, radio communication and satellite communication etc. [60].

4.4 The Advantages of MISO Topology over the SISO Topology

SISO topology of DC-DC converters can be implemented in such a way that the voltage of the battery can reach either above or below to the regulator's desired output. Suppose, if we take that our output requirement is 5V and the battery that we are using discharges from 10 V DC to 4.3 V DC, this is the case where we can measure and observe the SISO circuit's operation mode. A general SEPIC based DC-DC SISO converter is useful for small projects like LED blinking applications, NiMH chargers, handheld devices or laboratory testing/measurement analysis. The SISO topology can not produce enough optimum output voltages that can be paired with other renewable energy sources or even any kind of voltage sources. For better precision and analysis, it is advised that the SEPIC based SISO converter circuit should be designed with minimum component values. For this reason, the operating input voltage to the SISO topology is kept as much as low. This configuration has only one input port at the input side and only one output port at the output side. This is where the need of a SEPIC based MISO topology steps in. The MISO topology is a cost-effective and feasible solution because, we can study the utilization of other renewable sources that are connected at the input of the MISO DC-DC converter circuit. The MISO topology can be used for analyzing large voltage increment at the output side. The MISO topology incorporates effective combination of a variety of other renewable energy sources that is undeniably beneficial for people who are

living in remote area or even villages [61]. We have found a fundamental study [62] on effective approaches and design guidelines of different topologies of the MISO converters over the SISO converters. Also, this paper [63] shares necessary design methodologies to achieve high efficiency from a MISO converter circuit. However, we have still managed to design a SISO converter and the necessary analysis and results have shown in the hardware result analysis section.

4.5 The Drawbacks and Challenges of a SEPIC based SISO Converter Circuit

Although the general SEPIC based SISO topology has several features like providing a stable operation, non-inverting voltage at the output and stable gain for a given duty cycle etc., it has some drawbacks too. The SEPIC based SISO converter circuit has a pulsating output current at the output end just like the conventional buck-boost converter. Therefore, in a SISO topology, the converter actually uses the series capacitors to transfers all the energy after the switching mode is turned ON. This is why in a SISO topology, there needs to have a high capacitance in the converter as well as current handling capability.

The SISO topology is restricted to operate in a very slow varying applications due to the fourth-order nature. We can overcome these problems by incorporating multiple renewable energy sources that makes the overall system more stable and feasible. The control method of the SEPIC based SISO converter has several drawbacks. For example, the SISO converter circuit controls the output voltage automatically. To have a full control on the controlling part of the SISO SEPIC converter, we can rely on the input side but there is no circuit feedback. So, we need a feedback for the circuit to step down the voltage. Otherwise, once the switching mode is turned on in the boost phase, the circuit will automatically increase the output voltage to the maximum and a huge heat will dissipate from the switch (if we use a MOSFET as a switch). The main challenge is while using a potentiometer, the operator needs to be watchful on the

output reading to adjust the proper output voltage. It is better for SISO topologies to have a static voltage at the output without the necessity to have a control over it [64]. Furthermore, the SISO topologies can often get disrupted by electromagnetic interferences. In contrast, we can say that SISO topology can be implemented as per the requirement of the load, yet, the total number of components increases with incurring high-costs. Additionally, the harmonics are also increased in the output voltage for a single renewable energy application [65].

4.6 A Comparative Study: SEPIC Converter vs Different Features of the Commercial Converters

In this section we have presented a comparative tabular analysis, in the Table 4-1 of the features of different converters. Several DC-DC, as shown in figure 4.4, converters are present in the current power-electronic device market. The usual *Buck* converter is used to have a reduced input voltage. The *Boost* converter can only function to increase the input voltage to a certain level. On the contrary, the *Buck-Boost, Cuk and SEPIC* converters can either increase or decrease the output voltage. It is to note that, these converters need additional feedback system to lower the output voltage.

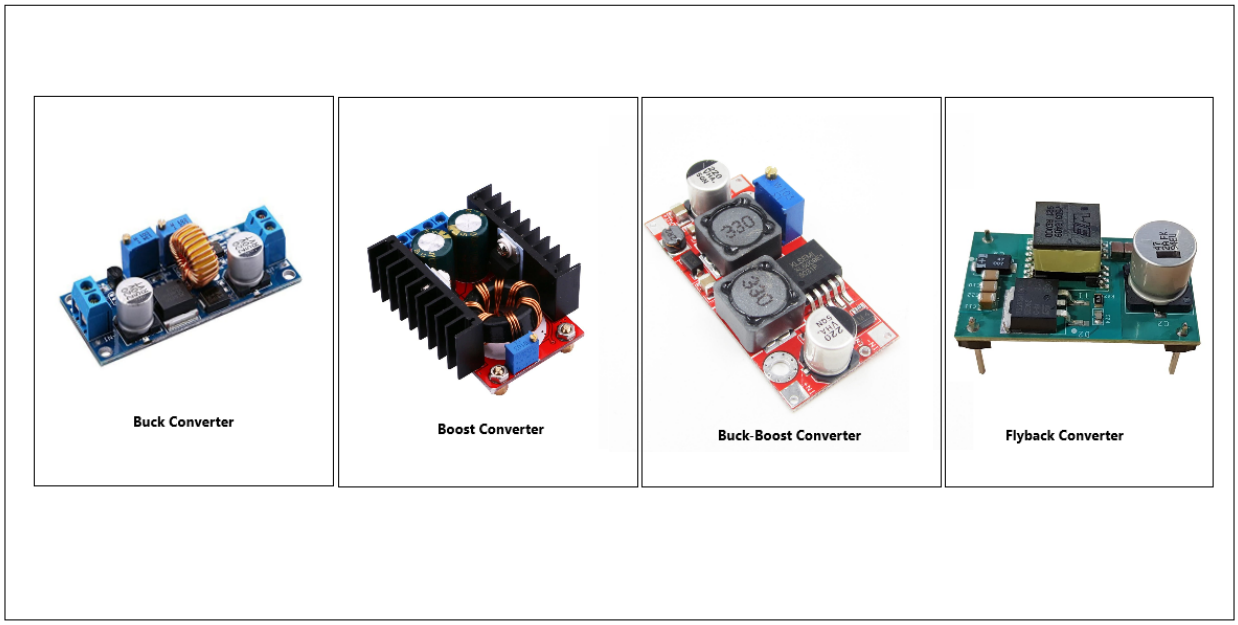

Figure 4.4: Different Types Commercial of DC-DC Converters (Sources: Pinterest)

We have decided to study the SEPIC converter because it can act like a Buck-Boost converter but the specialty is it has a non-inverting output. Although, the Buck-Boost converters are cheap because they have only one inductor and a capacitor connected with it. But the main drawback is that, these converters usually produce a high input current ripple at the output side. The ripple effect can introduce anomalies in the output reading [10] The SEPIC converter design uses minimal active components. SEPIC converter also utilizes the 'clamped' switching waveforms. This feature reduces additional noises if the converter performs high frequency switching.

Converters / Features	Buck-Boost	Cuk	Positive Buck-Boost	SEPIC	Flyback
Output Voltage Polarity	Invert	Invert	Non-Invert	Non-Invert	Non-Invert
Input Current	Pulsating	Nonpulsating	Depends on operation mode	Nonpulsating	Pulsating
Switch Drive	Floated	Floated	One floated the other is grounded	Grounded	Grounded
Efficiency	Low	Medium	High with only one stage is active	Medium	Low
Cost	Medium due to float drive	Medium due to additional block capacitor	High due to an additional switch and diode, complexity in the drive circuit	Medium due to an additional block capacitor	Low due to a grounded switch and no block capacitor

Table 4-1: The tabular analysis of the existing feature of different converters [66]

From the Table 4-1, we can understand that the efficiency of the SEPIC converters are medium yet we are considering this converter because it has no pulsating input current and a non-inverting output voltage at the output side. Still, the SEPIC topology is not suitable for the proposed MISO hybrid system. We could implement MISO SEPIC-Cuk converter. For the time being, in order to avoid further complexity, we have opted into the implementation of both of the SEPIC based DC-DC SISO SEPIC topology as well as the MISO SEPIC topology. In the upcoming section we will explain different aspects of other hybrid configuration that we couldn't incorporate within our hardware implementation and software simulation.

4.7 Additional Improvement of the Proposed MISO Topology

In this section, we have explained several aspects of the improved design considerations and any additional factors that could stir the efficiency of the proposed hybrid MISO system.

4.7.1. Distributed MPPT based MISO hybrid topology

As mentioned earlier, in our proposed hybrid topology, we have included the application of a Solar Photovoltaic (PV) Cell as a renewable energy source. The Solar PV modules can not be operated efficiently due to intermittence conditions. So, we have to ensure that the Solar PV module is equipped with proper features that can make them energy-efficient. The Maximum Power Point Tracking (MPPT) is a special feature that can be incorporated with Solar PV module. This feature ensures that during the sun-hours, the Solar PV module is providing maximum power. Under operating conditions, the Solar PV panel needs to be operated at MPPT. We can also utilize several MPPT algorithms like Perturb & Observe (P&O) and Incremental and Conductance (I&C) can maximize the Solar PV module's efficiency [67].

4.7.2. SEPIC Integrated CUK Topology

From this paper, [8] we got to know that the SEPIC converter can also be paired with a CUK Converter. Necessary diagram and detailed design considerations has been discussed. This

SEPIC-CUK converter circuit had both Solar PV module and Wind as sources. This fusion of the two converters can eliminate input filters that can ultimately reduce harmonics. The converter can both operate simultaneously and individually. Furthermore, it can either increase the input voltage and decrease the input voltage to a specific level according to the requirements. In the circuit diagram, there are two coils, L_1 and L_2. These two coils are located at the input end of the converter. These coils reduce the requirements of any input filters to control the harmonics at the output side of the converter. [67]

4.8 The Selection Criteria of Renewable Energy Sources: A Comparative Analysis of Wind, Solar PV, Bicycle Dynamo and Biomass Waste

Renewable energies are abundant in the earth. The nimble growth rate of the global population over the last few decades sends us an ominous message. With the incremental population growth rate, the decremental amount of fossil fuels and mineral resources have become a global issue. The existing pressure on fossil fuels and the dire need of the mineral resources can be altered if renewable energy sources like the Sun, wind, biomass wastes, geothermal energy etc. are promoted globally.

4.8.1 Wind Energy: An Overview and Pitfalls

Wind energy is harvested as mechanical power by the conversion of kinetic energy of wind turbine. Offshore wind turbines can be seen in the Irish Sea. As the wind passes by, these turbines can harvest wind power. The wind power is pure and clean. There are two major disadvantages of wind power. Firstly, the construction of wind turbine stations is extremely expensive. Secondly, the wind turbine system highly depends on geographical position, longitude and latitudes [68]. Additionally, wind turbines can be disrupted by flying animals and it can be a threat for flying birds. Furthermore, these turbines can create noises. This is why we have decided to not choose this resource as a small-scale study.

Figure 4.5: An Offshore Wind-Turbine (Source: Pinterest)

4.8.2 Biomass Waste Energy: An Overview and Pitfalls

Bioenergy is a special form of renewable energy that is converted from biomass to heat, electricity, biogas or other fuels. Biomass can be collected in the form of human waste/animal stools, leaves and other vegetable wastes, agriculture waste etc. [69]. Bioenergy is not easy to harvest as it needs additional technologies, setups, projects, space and chemical reactions. By thinking about the area, Dhaka, the place where we have carried out the field test of this study, it was not feasible for us to equip so many side projects to harvest bioenergy from different bioresources.

Figure 4.6: A Biomass Powerplant (Source: Google Image)

4.8.3 Solar PV: An Overview and Prospects

Solar PV based projects and field study is handy. There are a lot of researches currently going on Solar PV. Solar energy is the knight of the energy efficiency movement. Harnessing energy from the solar or the Sun is very easy and available. Solar energy is the best renewable energy source. Considering the availability of the Solar PV modules, we have decided to introduce Solar PV modules in our hybrid topology.

Figure 4.7: Solar PV Installed on a Rooftop (Source: Google)

4.8.4 Bicycle Dynamo: An Overview and Prospects

Bicycle dynamo is a common renewable energy source. The dynamo generated power is harnessed as a form of electrical energy converted from mechanical/rotational pedaling power of a human. The alternative to a bicycle dynamo is an alternator. An alternator is a special form of generator that produces huge power to be fed in the load side. We have selected the bicycle-dynamo as the second renewable energy source because it has zero emission like the solar power.

Figure 4.8: A Simple Bicycle Dynamo (Source: Google)

The dynamo system configuration is clean and it can be converted into AC voltage by using a simple inverter. For small scale study and a small load requirement, we have decided to implement the bicycle dynamo generator that is being fed into the SEPIC based MISO converter input side.

4.9 Target Group and Beneficiaries of the Proposed Hybrid MISO System

The idea of the Solar PV Module and the Bicycle Dynamo based hybrid MISO system was first originated when we were exposed to a study [70], where the researchers carried out a pre-feasibility analysis on an off-grid electrification using hybrid renewable technology in Nijhum Dwip (an isolated island in the southern part of Bangladesh Bay Area). Our proposed hybrid MISO system can be implemented in such distant islands where people solely depend on solar energy. The island people get electricity in day-time from the solar panel. If we can introduce the MISO hybrid topology in such islands, people will be highly benefited and they can use the efficient output power to charge their multiple devices like cellphones, torch light and rechargeable bulbs etc. The MISO topology can be extended by incorporating a Solar PV module that has 100W optimum power.

4.10 Conclusion

The feasibility of our proposed hybrid MISO converter system can benefit thousands of rural people who are deprived of on-grid electrification. The proposed MISO tropology including the two renewable energy sources that we have integrated serves the best outcome and optimum solution.

Chapter 5 Renewable Energy Sources: Solar PV Module and Bicycle Dynamo

5.1 A Brief Introduction to the Renewable Energy Sources

The renewable energy sources are booming with time to time and gradually earning people's trust due to its strong position in the environmental protection. Also, renewable energy is attracting global attention due to a predictable shortage of conventional energy sources as well as fossil fuels. It can stabilize the energy market in near future. Our world has abundant renewable sources. Humans waste countless energy resources. Burning fossil fuels creates air pollution and changes the global climate by emitting different greenhouse gases in the air. We can utilize existing renewable energy sources like solar, wind, biomass waste, geothermal energy, biofuels, woods etc. Non-renewable sources are limited and our world is having a huge shortage of energy. The optimum conversion of energy and proper appliance can mitigate energy wastage to a great extent. Further, the continuing process of energy harvesting from renewable energy resources can be utter helpful in removing the scarcity of different fossil fuels like coal, petroleum, natural gas and nuclear electric power. We highly encourage the usage of renewable energy sources because they are plentiful and the energy conversion process is 100% natural and emission-free. For our proposed MISO system, we are using the Solar PV module as our Source-I. Likewise, we have also integrated the bicycle dynamo as our Source-II of the MISO System. In the upcoming sections, we will elaborately explain and discuss about the prospects and feasibility of these two sources. We will also present the outdoor analysis of the Solar PV panel as well as the Bicycle Dynamo in this section. The outdoor field study has been analyzed carefully. We have attached necessary calculation methods, mathematical data table, error analysis, efficiency calculation, graphs etc. The field

analysis of these two sources prove that they are feasible enough to integrate into the proposed MISO SEPIC converter hybrid topology.

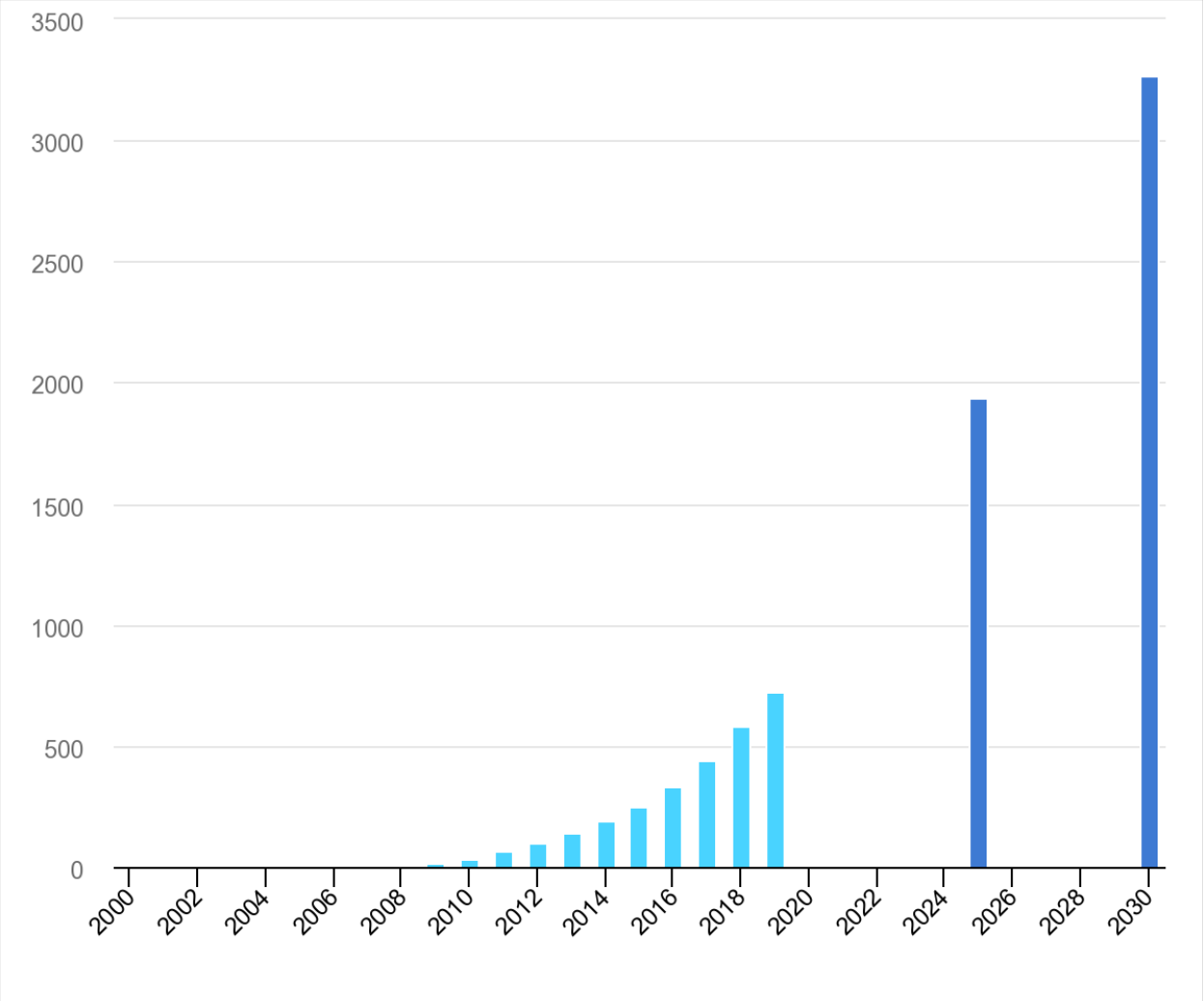

Figure 5.1: Solar PV power generation in the Sustainable Development Scenario, 2000-2030 (Source: IEA)

The graph in Figure 5.1 shows a growth rate of the Solar PV based power generation in the developed countries. From this graph, we can deduce that Solar PV based electricity generation will take all over the next energy efficiency movement.

5.2 Solar Photovoltaic (PV) Module: An Overview

Solar photovoltaic (PV) modules are commonly known as *Solar Panels*. A PV module is nothing but an assembly of Solar PV cells. The main resource of Solar PV cells is an abundant semiconductor material, known as Silicon. Silicon is used in almost 95% of PV modules that have a huge demand in the global market. These PV cells are usually mounted on thin solid frames that can be installed into any surface area. The Solar PV cells are protected with resistive coating to avoid any unexpected mechanical damage due to overheating or dampness. This gives the module an extra strength to operate irrespective of the transition of weather. The main source of wafer-based crystalline silicon PV modules are the electromagnetic radiation released by the sun that is called sunlight. This means PV cells take sunlight as inputs. When the sunlight is fed into the PV module, it gives direct-current (DC) electricity as output followed by Einstein's photoelectric effect. It is important to note that, PV panel is the collection of PV cells and the system of panels is generally called an array. Solar PV cells have multi-faceted implementations in our day-to-day life. For example, small wearable electronic devices, calculators, home appliances, refrigeration, boats etc. The appliances of Solar PV panel systems can vary based on the consumer's demand. The most common ways of applying PV systems are of two kinds. The first one is an on-grid system and the second one is an off-grid system. When a Solar Power Plant is directly connected to the main grid, it's an on-grid system. At night, when the PV panels are in resting mode, consumers can use the electricity drawn from the main grid which is previously stored as an output from the PV panel system. For small domestic appliances, a PV panel system can be set up on the rooftop with an additional battery as a storage device. The nominal voltage of the PV panel should match with the nominal voltage of the battery. After the charging mode, when the battery discharges, the consumers can get the electricity that can power up any loads connected with the battery. The most popular PV panels for domestic appliances are the monocrystalline PV panels, polycrystalline PV

panels and thin-film PV panels. Among them, the monocrystalline PV panels are the most efficient and the thin-film panels are cost-effective. In our proposed system, we have used a SunPower polycrystalline PV panel that is of 12V-10W rating. For a small-scale testing purpose, we are using the smaller PV panel. Larger PV panels are way efficient and they can be used in domestic appliances, but the prices are a bit high. Another reason for which we are using a smaller PV panel at the input side is because of the load requirement. We are using a very small load at the output side. Additionally, our proposed system is a complete off-grid model. That's why we are using a smaller PV panel. But in the following sections, we have discussed and showed a mathematical calculation of Solar PV system for domestic appliances. Nonetheless, for rural or remote areas, the off-grid PV panel system can play an incredible role as an alternative source of non-renewable energy. As technology advances, scientists and researchers are now mostly focused on the development of IoT enabled PV panel system. For example, an IoT enabled PV panel system can be the appliance of the Maximum Power Point Tracking (MPPT) charge controller for each individual PV module within a PV system. Also, new inventions like the typical DC-DC hybrid SEPIC converter and its multiple source topologies combined with a PV panel system can maximize the power harvesting mechanism are now taking the lead. The main challenge of electrical energy harvesting from the PV panel is the volatile weather conditions and intermittence problem. Scientists are now working on a responsive PV panel system that can change its orientation according to the sun. These panels can respond to the sunlight and change its tilt angle.

5.2.1 Solar Power based projects inside Bangladesh: Recent updates, Prospects and Challenges

According to the Renewable Energy (RE) generation report of Sustainable and Renewable Energy Development Authority (SREDA), Solar Power encompasses a total 67.4% share

among other Renewable Energy resources. It is clear that Solar Power is the highest generated energy resource among other renewable energy resources inside Bangladesh. The government of this country has taken significant initiatives that have helped this sector to grow and made an enormous impact on millions of lives mostly in the rural areas. These initiatives have alleviated the total demand of electricity from the national grid creating opportunities for hundreds of thousands of people in the job sector. As of 2021, the online archive of SREDA shows that the off-grid installation of Solar Power is nearly 346.19 MW. Whereas, the on-grid installation of Solar Power is nearly 136.6 MW. The total combined installation of Solar Power all over the country is 482.79 MW [47]. The government of Bangladesh promised to accomplish a total number of 19 Solar Power projects that is worth generating nearly 1070 MW electricity [48]. Some notable Solar Power projects inside Bangladesh are the 200 MW (AC) Solar Park by Beximco Power Co. Ltd. in Sundarganj, Gaibandha, the 200 MW (AC) Solar Park by SunEdison Energy Holding (Singapore) Pvt Ltd in Teknaf Upazila, Cox's Bazar, the 100 MW (AC) Solar Park by Zhejiang Dun An New Energy Co., Ltd, China National Machinery Import & Export Corporation, Solar Tech Power Limited, & Amity Solar Limited in Aditmari, Lalmonirhat, the Ashuganj 100 MW Grid Tied Solar Park in Katiadi Upazila, Kishoreganj etc. [49]. A total number of 8 Solar Power projects is to be accomplished by 2021. Solar power has played a vital role as an alternative source of energy mostly for rural people inside Bangladesh. The Bangladesh Rural Electrification Board (BREB) has taken numerous resourceful initiatives to equip remote areas like detached islands with solar power-based electrification. These people have whole-heartedly accepted Solar Power due to its ease of access and appliance. However, the main drawback of ground mounted on-grid Solar PV Park is that it puts an additional pressure on land which is dire in the context of an intemperately populated country like Bangladesh. As an alternative to ground mounted Solar PV systems, floating Solar PV technology can be an option. In 2019, the Mongla Port Municipality took an

initiative to establish a 10kWp floating Solar PV system on the water surface of the reservoir of its water treatment plant [50]. Thus, it paves the way to install more floating Solar PV projects even in the megawatt-scale. As the total demand of electricity is increasing each year, floating Solar PV projects can be a viable option that can put zero pressure on land and simultaneously generate electricity. The government of Bangladesh is investing more and more on Solar Power based mega projects.

5.2.2 A review on Solar PV Technology

In this section, we will give a brief idea on the Solar Photovoltaic (PV) technology as well as the common technical terms related to it. A Solar PV system generates its power through crystalline or thin sheet film-like PV modules. Inside each PV cell, there are semiconductor materials that triggers photons as sunlight. These photons can get into the depletion region of the sandwiched P-N junction of the PV module. These photons can break the neutrons into holes as cations and free moving electrons as anions. The photons coming from the sunlight can further dislodge the electrons in order to drive an electric current [51].

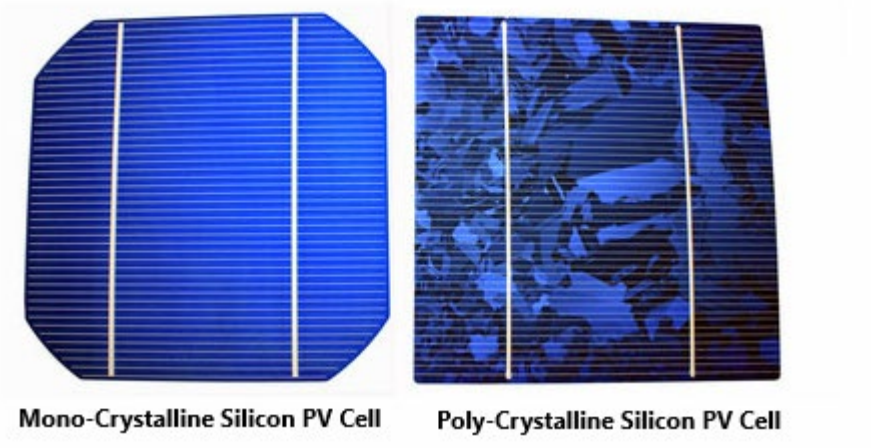

Figure 5.2: Mono- and Poly-Crystalline Silicon PV Cell (Source: Pinterest)

The two common categories of PV technology used for PV modules are shown in the above Figure 5.2.

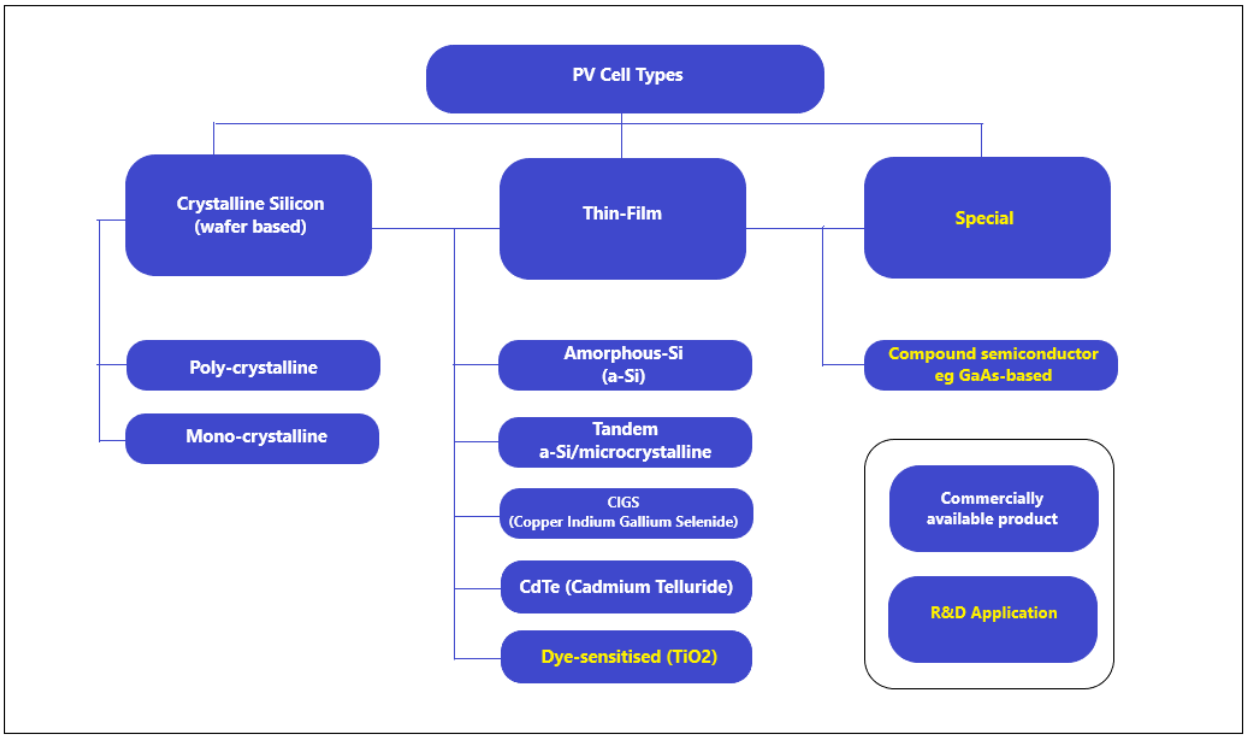

Figure 5.3: PV Technology Family Tree

The preceding Figure 5.3 shows an overview of the existing Solar PV technologies. We have also shown sub-categories through a chart model. The key technologies have been divided into three different parts.

5.2.3 Solar Radiation

The sunlight that directly comes off of the Sun that we call a solar energy is the result of solar radiation. Actually, with the process of solar radiation, sunlight is mixed with many colors. It carries low-energy infrared photons of 1.1 eV along with several high-energy ultraviolet photons of 3.5 eV [52]. The sunlight also carries several visible-light photons. The solar

radiation is crucial to maintain an ecological balance and it also stirs a biological process like photosynthesis. The solar radiation keeps the air temperature compatible with human life and other living beings. In the following Figure 5.4, the area under the curve is the total energy in the spectrum that is known as the *Solar Constant,* G_0. This value is equal to 1367 Watts per square meter (W/m^2) [52].

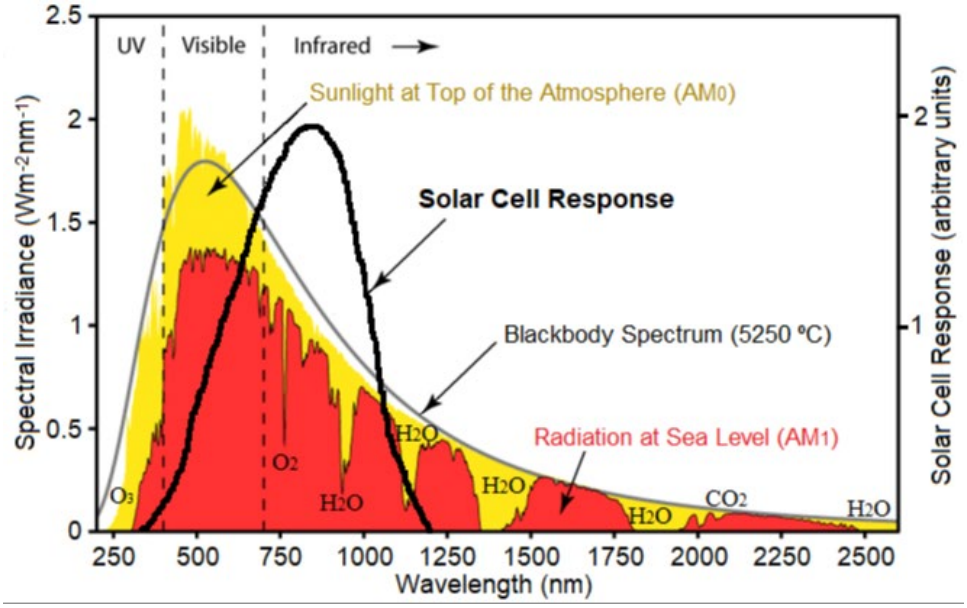

Figure 5.4: Extraterrestrial Solar Spectrum (Source: Wikipedia)

The above Figure 5.4 represents the spectrum of the solar energy that is directly facing the sun and affecting an imaginary plane outside the Earth's atmosphere at the Earth's mean distance from the Sun [52]. The total solar radiation is categorized into three different parts (direct radiation, diffused radiation and reflected radiation). The solar radiation is dependent on several factors like atmospheric conditions (cloud coverage, Ozone layer etc.), earth's rotation (daylight, time of a particular day, twilight, solar activity etc.) and earth's orbital revolution (the net distance between earth and sun, seasons, angle of inclination of earth's surface etc.)

5.2.4 Solar Irradiance and Solar Insolation

We define *solar irradiance* as the net amount of radiant energy that is directly coming from the Sun in different wavelengths. The emitted sunlight carries not only visible light but also it is highly attenuated by noises and other particles. We calculate the solar irradiance by assuming that this sunlight is falling each second on a one-square meter perpendicular plane that is likely to be estimated outside of Earth's atmosphere to a certain distance from the Sun. The solar irradiance is almost a constant value. Solar irradiance and the term *solar insolation* can often be used interchangeably. We define the solar insolation as the net amount of solar energy or the sunlight coming from the Sun, that is actually penetrating through the atmosphere and hits a certain area (mostly an imaginary plane on the Earth's surface) over a brief period of time with varying latitude, seasonal constrains and weather conditions. We assume that when the Sun is directly overhead, the incident energy touching the Earth's surface which is perpendicular to the Sun's projecting rays is 1000 Watts per square meter. The insolation value increases with altitude [52].

5.2.5 Air Mass Coefficient (Solar Energy)

The *air mass coefficient* is one of the most significant values related to Solar Energy. We define the air mass coefficient as the direct optical path length (it is the product value of the geometric length of the path followed by the light through a given system and the refractive index of the medium through which it propagates) through the Earth's atmosphere [53]. It is expressed as a ratio of a relative path length that is vertically upwards. Let's take L is the imaginary path length through the atmosphere and z is the solar radiation incident angle relative to the normal to the Earth's surface. The air mass coefficient is thus [53]:

$$AM = \frac{L}{L0}$$

L_0 is the path length at zenith. In our solar panel, the Standard Testing Condition (STC) air mass coefficient is 1.5. The AM1.5 denotes that the atmospheric thickness is 1.5 corresponding to a zenith angle of z = 48.2° [54]. The commercialized solar modules have a STC AM1.5 value. This specific value has been selected in the 1970s as a standardized value. The air mass coefficient depends on altitude and latitude position. Solar output power decreases with an increased air-mass coefficient.

5.2.6 Solar Panel Temperature Coefficient

The solar *panel temperature coefficient* necessarily determines how much power we are losing from the PV module at a certain temperature. The parameter is key for a designer who wants to get the best out of a Solar PV module. So, seemingly the better understanding of this parameter can help a designer who would like to maximize the amount of energy he wants to generate from a Solar PV module. For loss estimation, this value can help a consumer who is planning for a bigger Solar PV based home appliance. For our PV panel, the solar panel temperature coefficient is rated at -0.41%/°C that is the STC parameter for a poly-crystalline silicon wafer-based PV module [55]. In the upcoming field-study section, we have shown how this value has helped us finding the electrical solar efficiency.

5.2.7 I-V Characteristics of a Solar Cell

The Solar Cell I-V characteristics symbolizes the operation phase of the solar panel and its existing current-voltage relationship in accordance with irradiance and temperature.

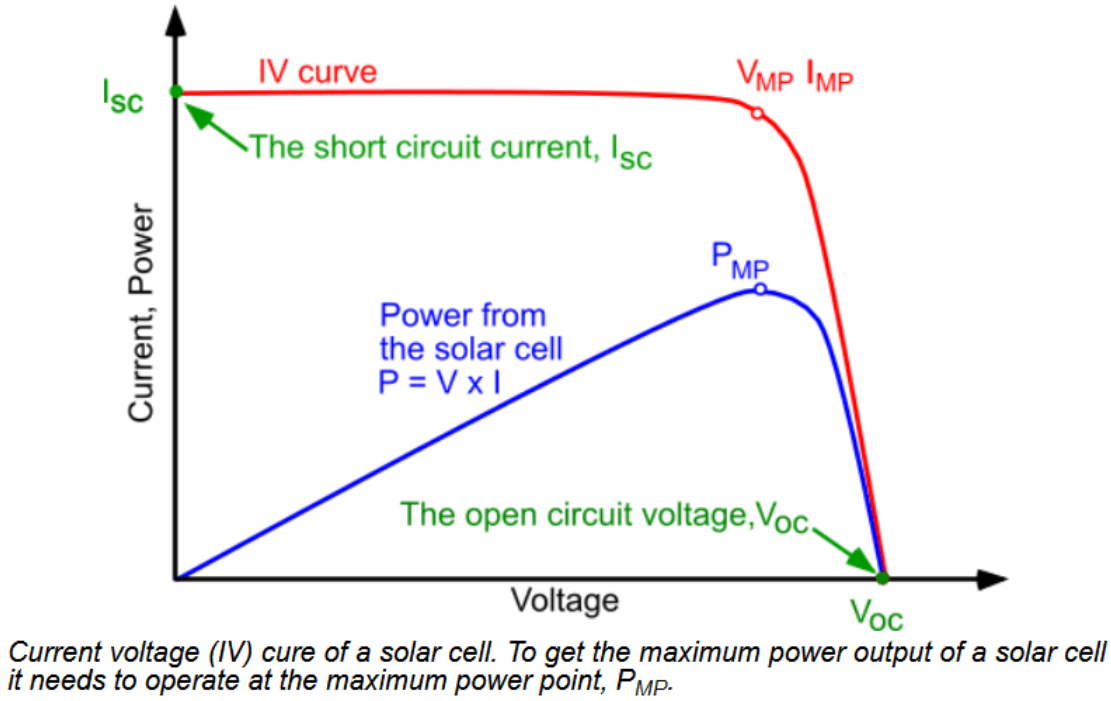

Figure 5.5: Solar Cell I-V Characteristic Curve (Source: winaico.com.au)

From the I-V curve of Figure 5.5, we get an idea that in what way the solar panel should be configured so that it can provide with an optimal peak power point (MPP).

Short-Circuit Current, I_{SC} of a solar module is the net current when the module is connected to a low impedance forcing the voltages across the device to V = 0. The open-circuit voltage, V_{OC} is the voltage when the module is connected with a high impedance keeping the electrical current I = 0.

5.2.8 Dust Accumulation on Solar Panel

The effects of dust accumulation on solar panel are a great concern because we are conducting the field study inside Dhaka and the air quality is very poor here. Dust accumulation can degrade the solar panel efficiency to a great extent. Dust can reduce the overall performance of the module (both efficiency and output power) by at least 50% over a period of six months

[56]. The only way to avoid the dust accumulation affect is to use a solar tracker that can improve power output.

5.2.9 Solar Panel Efficiency: An Overview and Mathematical Calculation of our PV Panel Electrical Efficiency

The efficiency of the Solar PV module greatly depends on the weather conditions and the temperature of the PV cells. The efficiency measurement is crucial for a consumer or a designer who wants to keep track of his/her solar PV system's optimal peak power point. The electrical efficiency can be calculated using this expression [57]:

$$Electrical\ Efficiency = \frac{(\frac{Pmax}{Area})}{Solar\ Irradiance,E} \times 100\% \ldots\ldots\ldots\ldots\text{(I)}$$

From our solar panel STC datasheet, the rated maximum power, P_{max} is 10W, Area is 0.1068 m^2 and Solar Irradiance, E is 1000 W/m^2. By using this expression, we get our electrical efficiency as P_{el} = 9.36%.

The other method to find the operating efficiency is to deduct the STC temperature from an estimated temperature of 25°C, then if we multiply this value with the temperature co-efficient $P_{max,}$ the calculation will yield a negative percentage. If we subtract this negative percentage from the initial electrical efficiency, then we get the operating efficiency of the PV panel at varying temperatures.

5.2.10 Best Orientation for Solar Panels

Choosing the best angle/orientation for a solar panel is key to harvest the most energy from the Sun. The sunlight strikes the PV panel in different angles from dawn till dusk. In this section

we will discuss the step by step (azimuth angle) and possibly the best inclination angle for any panel (tilt angle) in accordance with seasonal variation.

5.2.10.1 The Most Effective Direction for a Solar Panel

While preparing for a solar panel installation in the rooftop of a building, a consumer must consider several aspects and choosing the best roof-side is one of them. We must know from which side the solar radiation is achieved more. The best roof-side for solar radiation can confirm maximum power production for our home appliances. According to a scientific data, it is proved that the South is the best direction for installing a Solar PV panel with an azimuth angle of 180° [58]. If any Solar PV panel is placed focusing the South, it is true that approximately 45% of the direct solar radiation would be accepted with a very minimal amount of reduction.

5.2.10.2 The Optimal Tilt-Angle for a Solar Panel

Just like the direction of a solar panel, the optimal tilt-angle is also another key point that a designer/engineer/consumer must consider before opting into an installation phase. So, before jumping to install the Solar PV panel, we must consider the rooftop that has already its own inclination and slope. At midday, when the Sun reaches its maximum altitude on the horizon, we get the maximum output from a PV module. We should also consider the winter solstice and summer solstice when there are days that are longer than night and vice-versa. This phenomenon will guide us to what angle the solar panels need to be tilted. Additionally, the longitude and latitude position of the solar home system should be considered. Because, according to the latitude, the maximum and minimum annual altitude of the sun also varies at midday.

5.2.11 Solar Panel for Home Appliance: An Estimation for the Local Consumer Demand

For home appliance, solar panel system has been a resounding success for detached island or isolated places and even for the remote villages in the subcontinent area.

If we assume that the peak sun-hours for Dhaka in the month of September is 5 hours. Then the watt-hour conversion of our PV panel is:

$$Pout\ (per\ day) = 5\ hours\ \times 10\ watts$$

$$= 50\ watt - hours$$

= 0.05 kWh energy per day

Now, we are going to calculate how much power this PV panel can produce in a single year:

$$Pout\ (per\ year) = 0.05 \times 365$$

= 18.25 kWh of energy per year

For home-appliances, we usually consider using a larger solar panel that have higher maximum rated power. With the same calculation, in the following table we have shown different PV panel requirements for getting maximum power at yearly basis:

Solar Panel rated maximum power $P_{max,}$ W	Number of Panels	Connection	Maximum Peak Sun-Hours in a Single Day, Hr	Generated Power in a Single Day, kWh	Generated Power (Year), kWh
400	25	Series	5	50	18250
400	1	Do	4	1.6	584
400	1	Do	6	2.4	876
400	1	Do	6.5	2.6	949
200	2	Do	5	2	730
150	3	Do	3	1.35	492.75
150	3	Do	4	1.8	657
150	3	Do	5	2.25	821.25
150	3	Do	6	2.7	985.5
100	4	Do	5	2	730

Table 5-1: Different PV panel requirements for getting maximum power at yearly basis

According to the year 2020 data of the World Bank, the per capita electricity consumption in Bangladesh per year is 325.76 kWh. Now, from the above data analysis, we can understand that a consumer can easily use a 400W solar panel or three series connected 150W solar panels to generate a yearly power of 584 kWh and 657 kWh respectively, that is more than sufficient for a single household appliance in the context of Bangladesh.

5.2.12 STC parameters of the Solar PV panel

Parameter	Value
Rated Maximum Power at STC (P_{max})	10W
Tolerance (Tol)	0~+3%
Optimum Operating Voltage at P_{max} (V_{mp})	17.35V
Optimum Operating Current at P_{max} (I_{mp})	0.577A
Open-Circuit Voltage (V_{OC})	21.2V
Short-Circuit Current (I_{SC})	0.625A
Nominal Operating Cell Temperature (NOCT)	47±2°C
Maximum System Voltage	1000VDC
Maximum Series Fuse Rating	10A
Operating Temperature	-40°C to +85°C
Application Class	Class A
Protection Class	⊡
Cell Technology	Poly-Si
Weight (Kg)	1.22
Dimensions (mm)	356*300*25
Air Mass (Solar Energy) Coefficient	1.5
Solar Irradiance, E	1000 W/m^2
Temperature in Celsius, TC	25°C
Electrical Efficiency, η_{el}	9.363%
Maximum Power temperature coefficient at P_{max}	-0.41%/°C

Table 5-2: STC Performance of the SunPower 10W 12V Solar PV Panel

These parameters are rated for this SunPower 12V-10W PV panel. For this PV panel, there was no rated electrical efficiency. So, we have calculated the electrical efficiency and it is assumed

that the actual electrical efficiency of this panel is ~10%. The Standard Test Conditions (STC) are the industry standard conditions. The rated parameters are analyzed values under factory manufacturing conditions. The STC values are not ideal. Hence, we can not only rely on these values, because, the solar PV panel efficiency is heavily dependent on the latitude, weather conditions and solar irradiance. This is why we have successfully carried out field analysis of the single 12V-10W PV panel. The hardware analysis reports are shown in the next section.

5.2.13 Outdoor Analysis of Solar PV Panel and Meteorological Data Analysis with Simulation Result

We have collected the hourly weather condition report of the very day on which we carried out the Solar PV Panel hardware analysis.

Data	**Value**
Sunrise	5:45 AM
Sunset	5:58 PM
Moonrise	5:15 PM
Moonset	3:55 AM
Average Humidity	74%
Pressure	1009 mb
Dew Point	23°
UV Index	8 – Very High

Table 5-3: 20th September, 2021 GFS Data

This data from the Table 5.3 has been collected from the Meteorological Report of the Bangladesh Meteorological Department.

Current Location:

Latitude: 23.8045, Longitude: 90.3607

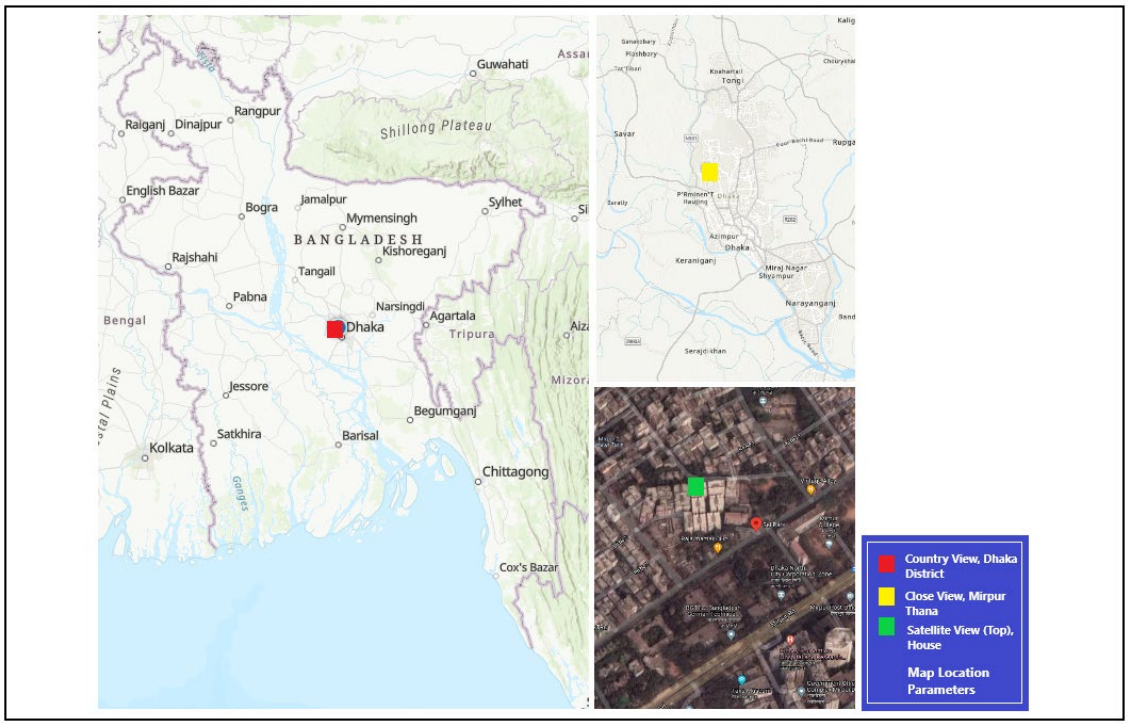

Figure 5.6: The area where the PV panel analysis has been carried out

The map in the Figure 5.6 is simulated in ArcGIS Online Software and the satellite imagery was taken from the Google Map.

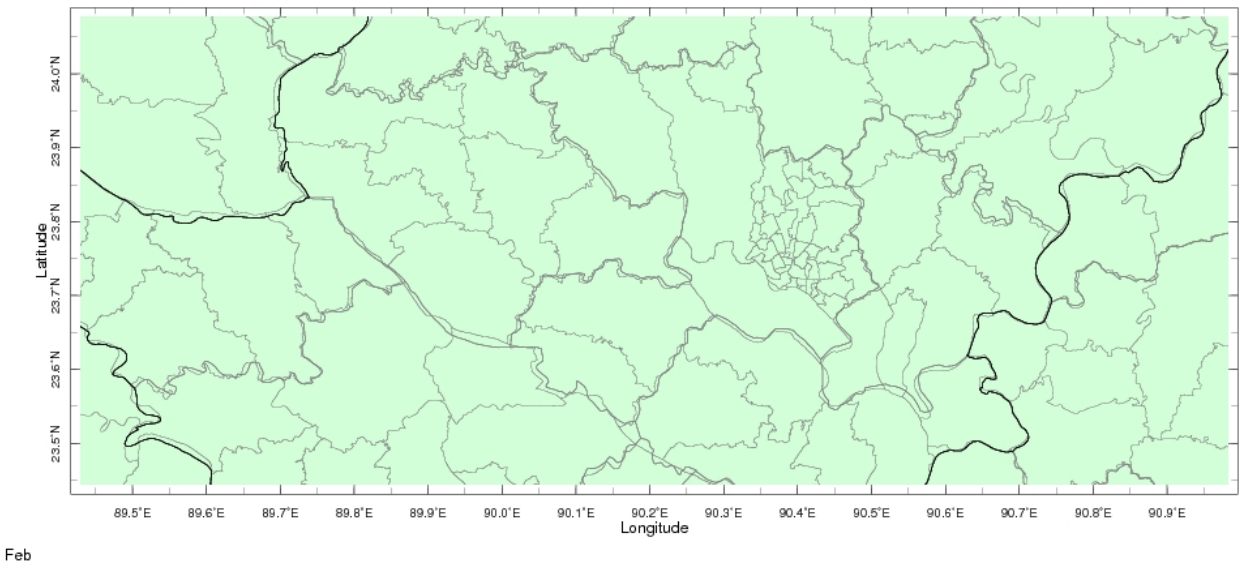

Figure 5.7: The Longitude and Latitude position of the district Dhaka

This graph was collected from the online archive of the National Meteorological Report of Bangladesh. In this graph, we can observe the longitude and latitude parameters within the Dhaka district.

Other Data:

In this section we have attached some important meteorological data that we have collected to analyze the characteristics of the month September.

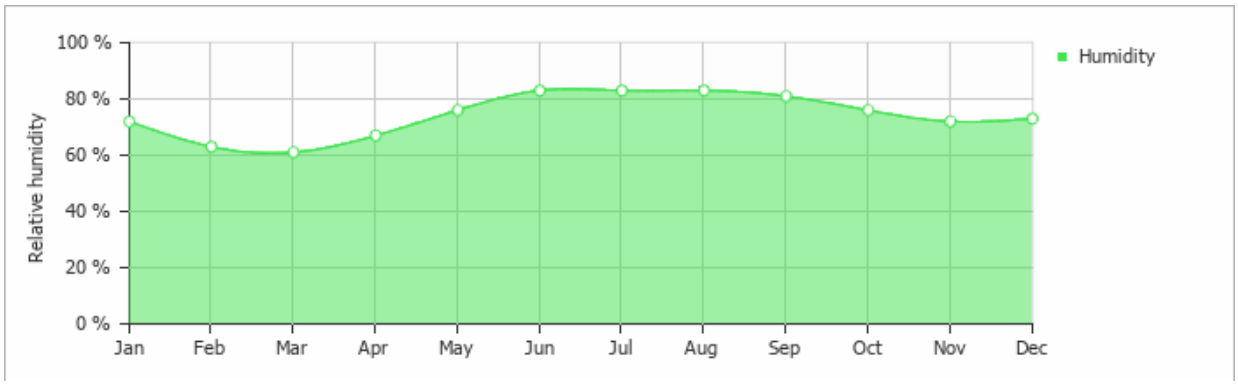

Figure 5.8: Average Relative Humidity in Dhaka for the year 2021 (Source: weatherandclimate.com)

The graph in Figure 5.8, we can see that the relative humidity is nearly 80% in the month of the September. Actually, summer is the best time period to analyze the Solar PV panel. The months are between late January to May according to the Bangladeshi climatic conditions.

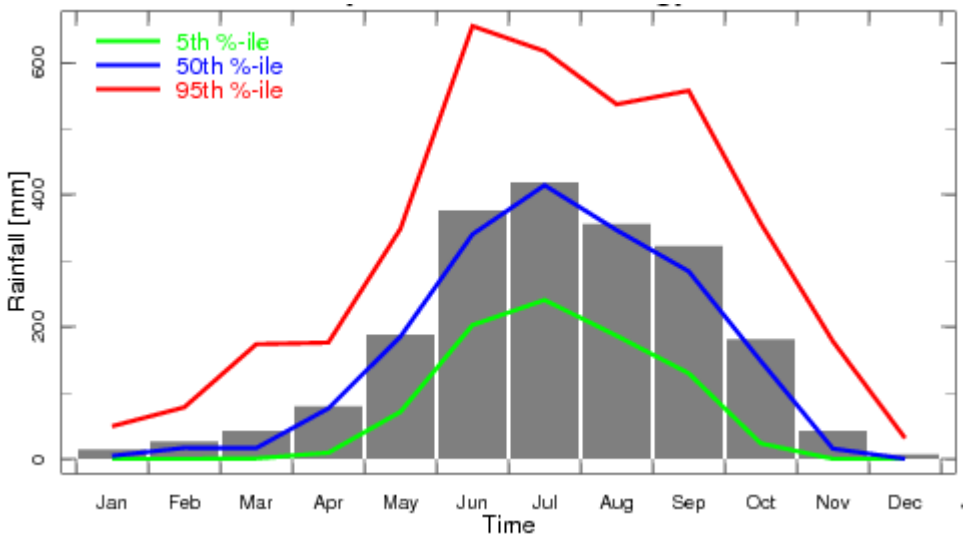

Figure 5.9: The Monthly Rainfall Climatology (Source: Meteorological Report, Bangladesh)

The graph in Figure 5.9, we can understand that the month of September is not the efficient month to study a solar panel. It is because solar panels are either studied in the summer or either in the winter.

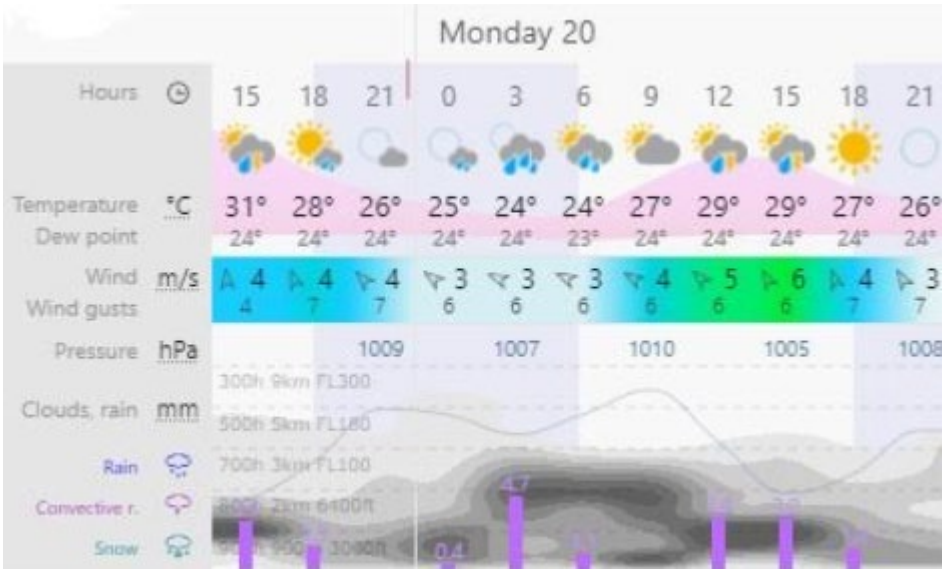

Figure 5.10: The simulation of hourly wind speed variation on Windy Software

In Figure 5.11, it is showed a wind speed data from the Windy Software to analyze the change of wind during the day when outdoor analysis was performed.

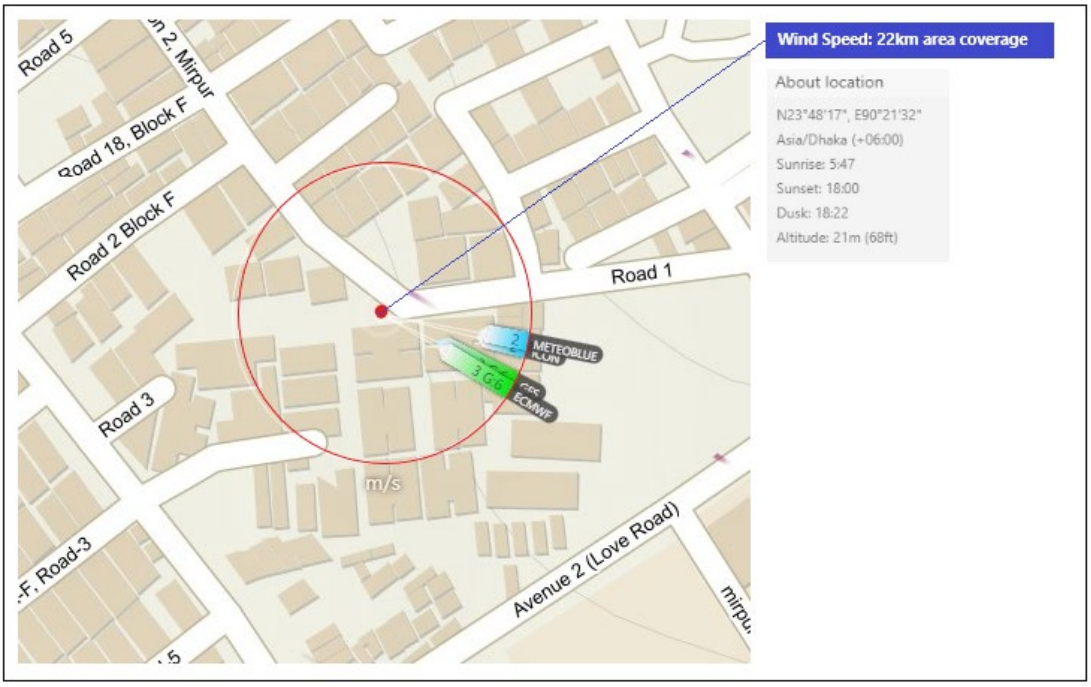

Figure 5.11: The Wind-Speed Data Simulation using Windy Software, the figure is showing the location

The Figure 5.11 shows that wind speed has been measured surrounding 20km from the field test area.

Open-Circuit Voltage V_{OC}, VDC vs Time Data Table:

Time (half-hour interval)	V_{OC} (VDC)
07:06 AM	18.57
07:30 AM	19.10
07:44 AM	19.63
08:00 AM	19.35
08:30 AM	19.70
09:00 AM	18.87
09:30 AM	19.97
10:00 AM	20.80
10:30 AM	20.50
11:00 AM	19.80
11:30 AM	20.40
12:00 PM	20.12
12:30 PM	20.00
01:00 PM	19.91
01:30 PM	19.70
02:00 PM	17.70
02:30 PM	18.52
03:00 PM	20.00
03:30 PM	19.64

04:00 PM	19.30
04:30 PM	17.20
05:00 PM	16.80
05:30 PM	11.20
06:00 PM	8.23
06:30 PM	4.30

Table 5-4: VOC, VDC vs Time Data Table

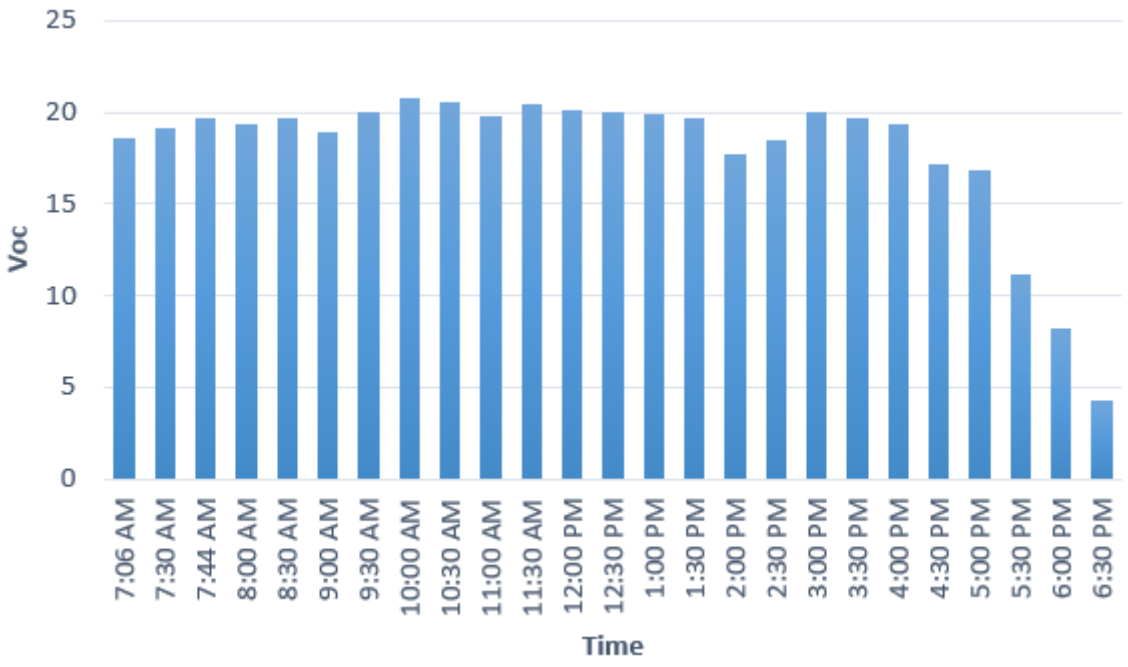

Figure 5.12: Graphical Representation of VOC, VDC vs Time

The Open-Circuit Voltage has been measured by disconnecting the PV panel completely from the hybrid MISO system. Then, the positive probe of the Digital Multimeter has been connected with the positive pole of the PV panel and the negative probe has been connected with the negative pole of the PV panel output. We have set the panel angle to approximately 20°-30° to record the readings. From the Table 5.4 and Figure 5.12 we can see that several disruptions

occurred during 9 AM and 2 PM respectively. At these times, the sky was covered with dark and thick clouds. For that reason, the output voltages dropped dramatically. The optimum voltage was generated at 10 AM and it was 20.8 V. The sky was clean.

Short-Circuit Current I_{SC}, A vs Time Data Table:

Time (half-hour interval)	I_{SC} (A)
07:06 AM	0.07
07:30 AM	0.09
07:44 AM	0.12
08:00 AM	0.09
08:30 AM	0.18
09:00 AM	0.08
09:30 AM	0.25
10:00 AM	0.37
10:30 AM	0.35
11:00 AM	0.22
11:30 AM	0.30
12:00 PM	0.28
12:30 PM	0.29
01:00 PM	0.23
01:30 PM	0.19
02:00 PM	0.04
02:30 PM	0.06
03:00 PM	0.19

03:30 PM	0.13
04:00 PM	0.11
04:30 PM	0.03
05:00 PM	0.02
05:30 PM	0.01
06:00 PM	-
06:30 PM	-

Table 5-5: Short-Circuit Current ISC, A vs Time Data Table

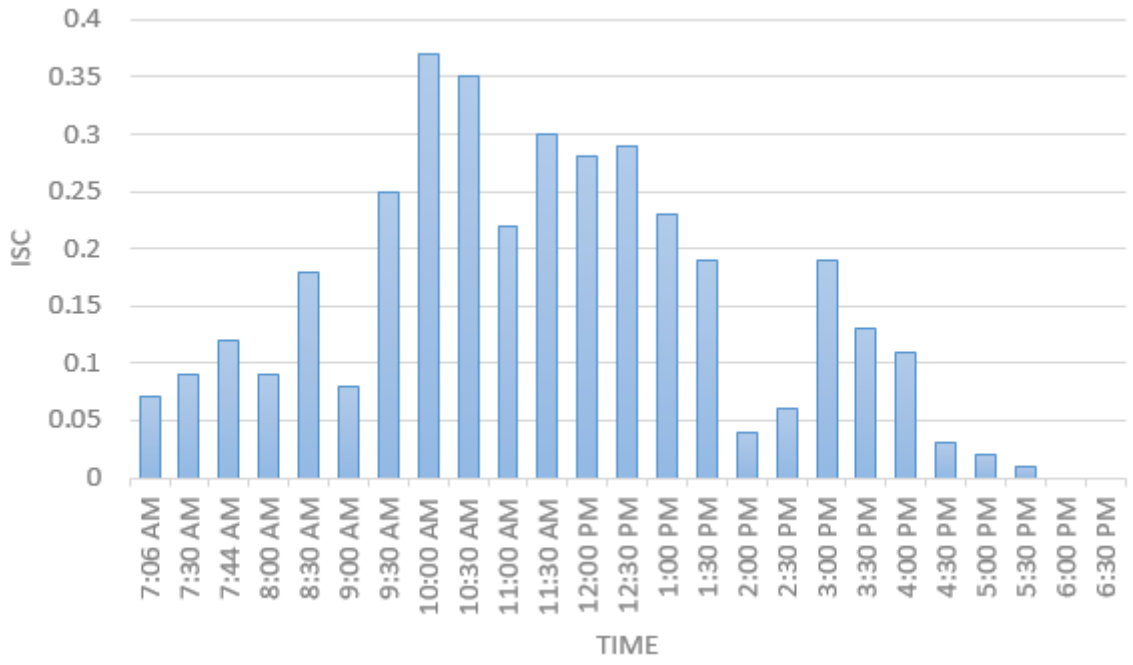

Figure 5.13: Graphical Representation of Short circuit current vs Time

The Short-Circuit Current has been measured by disconnecting the PV panel completely from the hybrid MISO system. Then, the positive probe of the Digital Multimeter has been connected with the positive pole of the PV panel and the negative probe has been connected with the negative pole of the PV panel output. The positive probe was connected to the 20A rating of

the multimeter end. We have again set the panel angle to approximately 20°-30° to record the readings. From the Table 5.4 and Figure 5.12 we see that the highest short-circuit current was measured at 10 AM and that is 0.37 A. The multimeter did not show any result for I_{SC} values after 05:30 PM as it was evening and the PV was generating voltages below the input level.

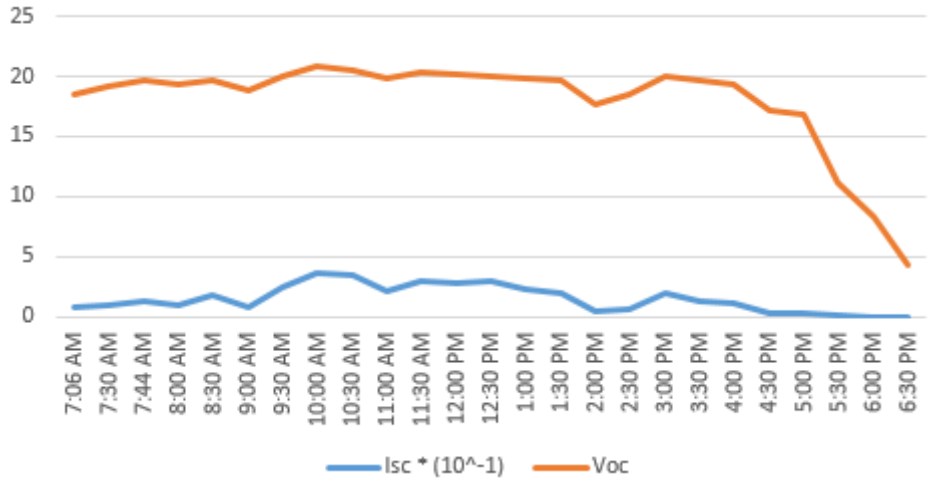

Figure 5.14: Isc and Voc with respect to Time

The preceding graph in Figure 5.14 is the comparative data representation of Isc and Voc of our PV panel. Since, during the conduction of the test, we haven't got proper irradiation due to cloudy sky and also the temperature is lower so that the output voltage is quite low and same goes for the output current. We have multiplied current value with 10 to get more understandable graph. In this graph, since at 10AM to 11AM irradiation is higher, output voltage is also higher comparing to other time frame of the day. And also, after 5PM the voltage along with current decreases because irradiation at that time starts to fall to zero as the output voltage and current is very much dependent on the amount of irradiation the solar panel receives.

Fill Factor FF, vs Time

Time (half-hour interval)	FF
07:00 AM	7.69
07:30 AM	5.18
07:44 AM	4.24
08:00 AM	5.74
08:30 AM	2.82
09:00 AM	6.62
09:30 AM	2.00
10:00 AM	1.29
10:30 AM	1.39
11:00 AM	2.29
11:30 AM	1.63
12:00 PM	1.77
12:30 PM	1.72
01:00 PM	2.18
01:30 PM	2.67
02:00 PM	14.12
02:30 PM	8.99
03:00 PM	2.63
03:30 PM	3.91
04:00 PM	4.71
04:30 PM	19.37
05:00 PM	29.76
05:30 PM	89.28

06:00 PM	-
06:30 PM	-

Table 5.5-6: Fill Factor FF, vs Time

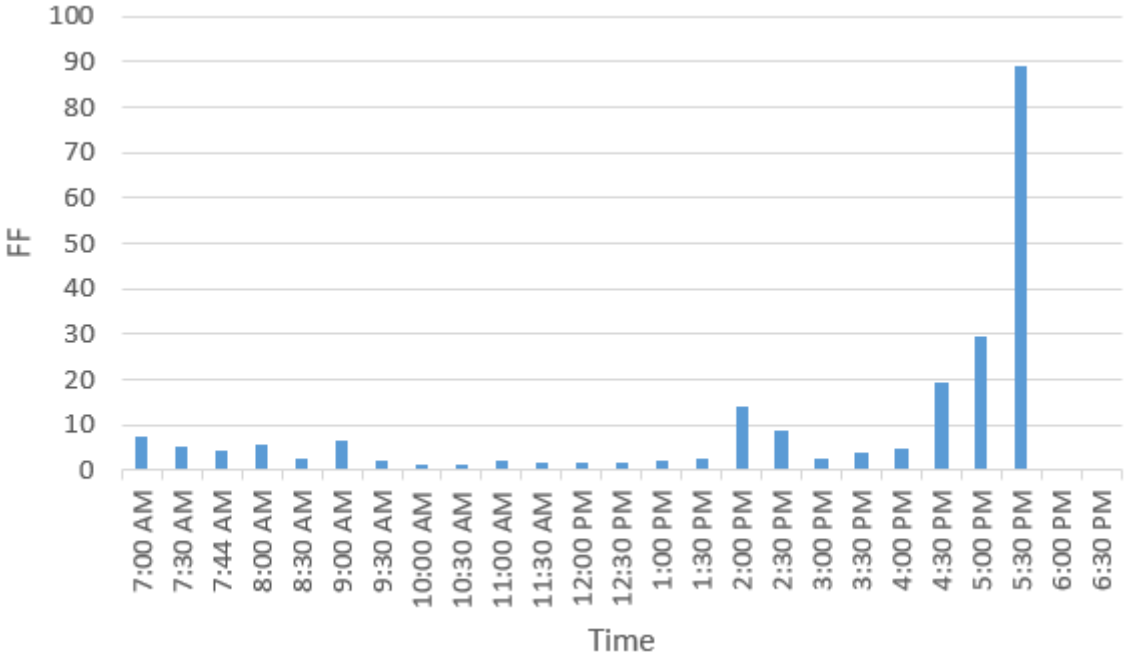

Figure 5.15: Graphical representation of FF vs Time

The fill factor has been calculated by this expression:

$$\text{Fill Factor (FF)} = \frac{Pmax}{Voc \times Isc}$$

Where, Pmax is 10W for our case. The data tables of open-circuit voltages and short-circuit currents have already been showed. The FF increases when the irradiation is less than 500 watts/$m^{2.}$ Subsequently, the FF decreases for irradiation greater than 500 watts/m^2. The fill factor of an ideal solar cell is exactly equal to 1 with no losses.

Wind Velocity Vw, m/s vs Time

Time (half-hour interval)	Vw
07:00 AM	ESE 2.4
07:30 AM	ESE 2.6
08:00 AM	ESE 2.7
08:30 AM	ESE 3.0
09:00 AM	ESE 3.05
09:30 AM	SE 3.06
10:00 AM	SE 3.07
10:30 AM	SE 3.4
11:00 AM	SE 3.6
11:30 AM	SE 3.5
12:00 PM	SE 4.0
12:30 PM	SE 4.2
01:00 PM	SE 4.6
01:30 PM	SE 5.2
02:00 PM	SSE 5.2
02:30 PM	SSE 5.6
03:00 PM	SSE 5.9
03:30 PM	SSE 6.0
04:00 PM	SSE 4.6
04:30 PM	SSE 4.3
05:00 PM	SSE 4.1
05:30 PM	SSE 4.2
06:00 PM	SSE 3.5

06:30 PM	SSE 3.0

Table 5-7: Wind Velocity Vw, m/s vs Time

The values are generated according to the real-time Global Forecast System (GFS). The total area coverage for the wind was 22km. Due to not having an *Anemometer,* we have opted into simulating the real-time data from the Windy Software and the AccuWeather Software for better precision and accuracy.

Ambient Temperature T_a, °C vs Time

Time (half-hour interval)	Ambient Temperature (°C)
07:00 AM	26
07:30 AM	26
08:00 AM	27
08:30 AM	27
09:00 AM	27
09:30 AM	28
10:00 AM	28
10:30 AM	29
11:00 AM	29
11:30 AM	30
12:00 PM	31
12:30 PM	31
01:00 PM	31
01:30 PM	31

02:00 PM	31
02:30 PM	31
03:00 PM	30
03:30 PM	30
04:00 PM	30
04:30 PM	30
05:00 PM	29
05:30 PM	29
06:00 PM	28
06:30 PM	27

Table 5-8: Ambient Temperature Ta, °C vs Time

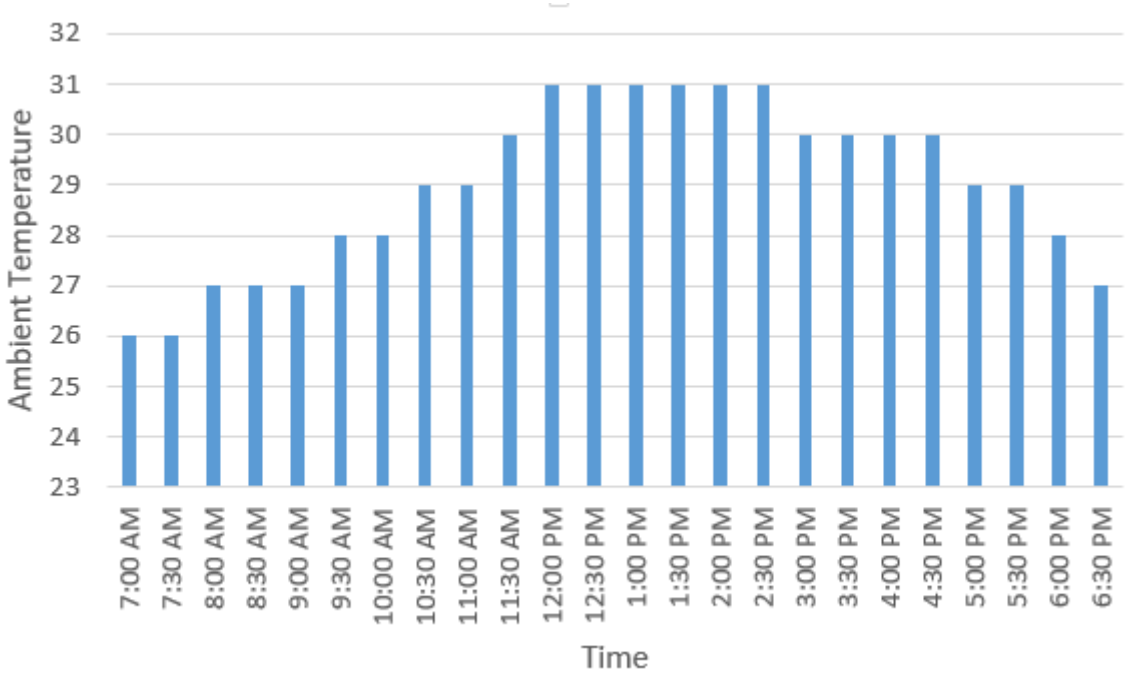

Figure 5.16: Graphical representation of Ambient Temperature Ta, °C vs Time

The temperature has been measured using an HTC-2 Indoor LCD Digital Temperature/Humidity Meter. We could implement different sensors or transducers by

interfacing an Arduino UNO board to analyze the ambient temperate. That would be more feasible analysis. But we thought that this would create additional complexity of the overall analysis process.

Cells Temperature $T_{cell,}$ °C vs Time

Time (half-hour interval)	T_{cell} (°C)
07:00 AM	33.2
07:30 AM	36.1
07:44 AM	36.5
08:00 AM	36.2
08:30 AM	36.7
09:00 AM	33.8
09:30 AM	41.8
10:00 AM	47.5
10:30 AM	46.9
11:00 AM	43.1
11:30 AM	46.3
12:00 PM	45.1
12:30 PM	41.9
01:00 PM	41.6
01:30 PM	35.1
02:00 PM	32.3
02:30 PM	33.1
03:00 PM	37.5

03:30 PM	35.2
04:00 PM	33.1
04:30 PM	31.5
05:00 PM	28.2
05:30 PM	-
06:00 PM	-
06:30 PM	-

Table 5.5-9: Cells Temperature Tcell, °C vs Time

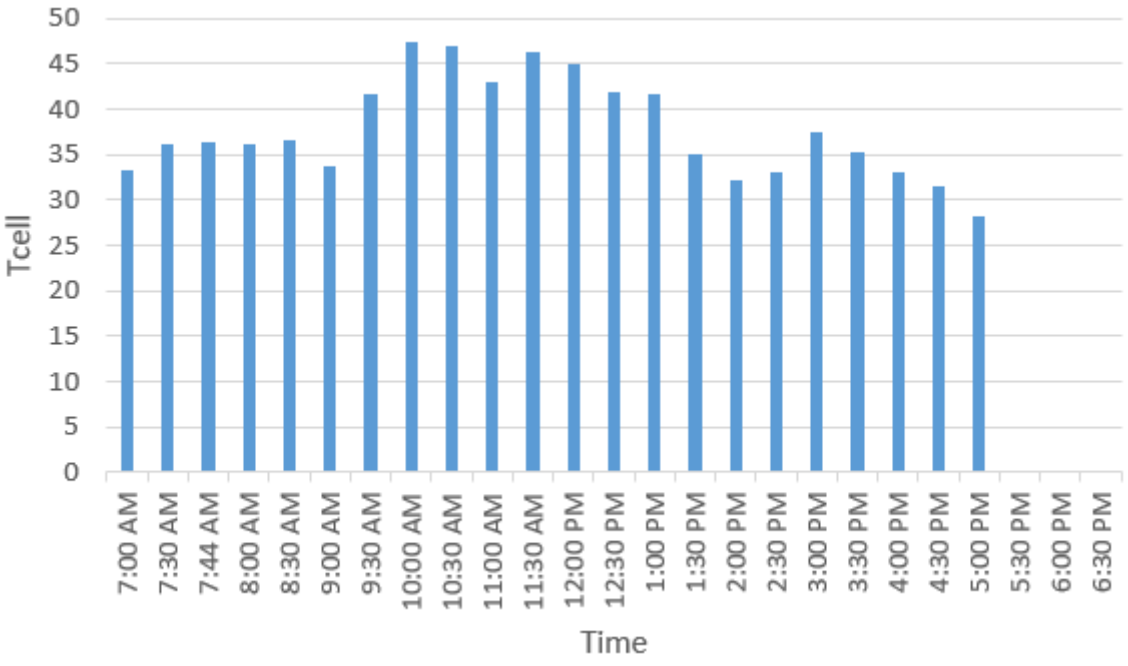

Figure 5.17: Graphical representation of Cells Temperature Tcell, °C vs Time

The cell temperature has been measured using an infrared thermometer. It has a laser pointer and when the IR laser hits a certain point, it can measure the surface temperature. The measured temperature values were pointed at the center of the PV panel. However, this does not symbolize the overall temperature of the PV panel. The initial measured temperature values

were in Fahrenheit values. Later, we have converted the reading parameters to corresponding Celsius values.

Fill Factor, FF vs Open-Circuit Voltage V_{OC}, VDC

Time (one-hour interval)	V_{OC}	FF
07:00 AM	18.57	7.69
08:00 AM	19.35	5.74
09:00 AM	18.87	6.62
10:00 AM	20.80	1.29
11:00 AM	19.80	2.29
12:00 PM	20.12	1.77
01:00 PM	19.91	2.18
02:00 PM	17.70	14.12
03:00 PM	20.00	2.63
04:00 PM	19.30	4.71
05:00 PM	16.80	29.76
06:00 PM	8.23	-

Table 5-10: Fill Factor, FF vs Open-Circuit Voltage VOC, VDC

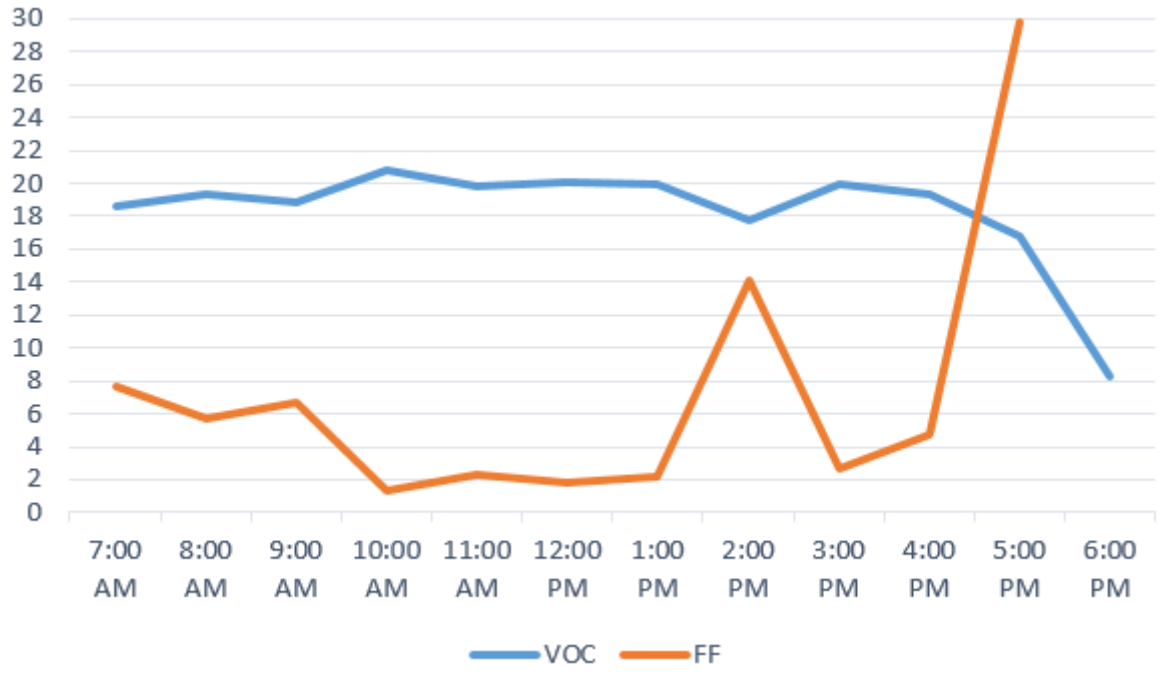

Figure 5.18: Graphical representation of Voc and FF with respect to Time

In Table 5-10 and Figure 5.18, we have represented the fill factor values and the open-circuit values and their variance with time to time from 07 AM up to 06 PM. We can show that there is an anomaly in the fill factor at 2 PM and 6 PM. It is because at 2 PM, light rains were falling and the sky was filled with black clouds. The open-circuit voltage dramatically changed. Again, at 5 PM, the solar panel open-circuit voltage and short-circuit current was not sufficient enough to produce a smooth result at the output.

Operating Efficiency η_{op}, % vs Time

Time (half-hour interval)	η_{op} (%)
07:00 AM	8.95
07:30 AM	8.95
08:00 AM	8.54
08:30 AM	8.54
09:00 AM	8.54
09:30 AM	8.13
10:00 AM	8.13
10:30 AM	7.72
11:00 AM	7.72
11:30 AM	7.31
12:00 PM	6.90
12:30 PM	6.90
01:00 PM	6.90
01:30 PM	6.90
02:00 PM	6.90
02:30 PM	6.90
03:00 PM	7.31
03:30 PM	7.31
04:00 PM	7.31
04:30 PM	7.31
05:00 PM	7.72
05:30 PM	7.72

06:00 PM	8.13
06:30 PM	8.54

Table 5-11: Operating Efficiency ηop, % vs Time

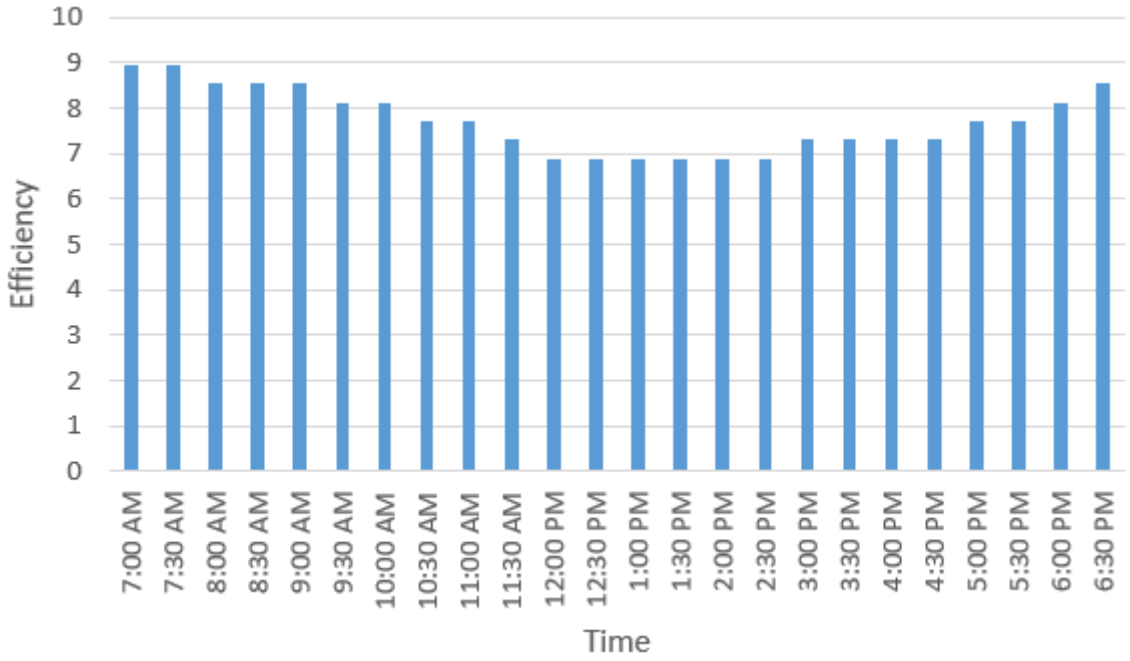

Figure 5.19: Graphical representation of Operating Efficiency ηop, % vs Time

The operating efficiency that is shown in Table 5.11 and Figure 5.19 of the Solar Panel has been calculated using the ambient temperature values. Firstly, we have taken a certain ambient temperature, then we have deducted the STC rated ambient temperature (25°C) from this temperature. Then we multiply the value with the maximum power temperature co-efficient. This process yields a negative value. Finally, we get the operating efficiency by subtracting the modulus of this negative value from the initial electrical efficiency of the solar panel that is η_{el} = 9.363%. This operating efficiency actually indicates that the more the temperature rises, the solar panel will lose more power comparing with the actual electrical efficiency. The difference of the two temperatures will increase if the operating ambient temperature is high. In this calculation, we also find that the negative value actually denotes as for a certain value of the

negative result, a certain amount of power will be lost in that ambient temperature. For case-I at 7:00 AM, our ambient temperature was 27°C and after multiplying the difference with the maximum power temperature co-efficient the result becomes -0.82%. This means, 0.82 wattage of power will be lost from the maximum operating power, P_{max} at 27°C.

5.3 Brief Introduction to Bicycle Dynamo

Humans can generate power from general bicycle but most of it is actually wasted. The mechanical energy from a general bicycle can be converted into electrical energy and it can remove the problem of electricity insufficiency in remote areas. We can harvest the energy that we get from the output of the bicycle dynamo. This output power generated from a bicycle can be paired with the energy of other renewable sources and we can further run basic devices of household appliances for example- fans, lights, etc. Additionally, this generated power can be directly used to charge a mobile or a small lighting device, because, the output we get from the bicycle dynamo is a DC voltage. However, in village areas bicycle is a commonly used transportation and there are some areas where there is no electricity or huge load shedding problem, in such places the energy can be very much productive.

5.3.1 Mechanical Power Generation

When a magnet is placed in close proximity to a conductive item (such as an iron nail), the magnet attracts the object because the electrons in the object have inherent magnetic fields around them. The magnet causes the electrons in the item to realign themselves and traverse towards the magnet, resulting in the two objects being drawn together [38]. A wire that has been moved in a magnetic field will cause electrons to begin to flow through it if the conductive item is one that has electrons. This motion through a magnetic field is the fundamental concept that underpins the operation of generators. The flow of electric charge is denoted by the unit

amperes (amps), while the "pressure" that causes electrons to move is denoted by the unit voltage, which is measured in volts [39].

Generators are devices that transform mechanical energy into electrical energy, which may then be utilized to power electronics in a circuit. The word "generator" is usually used in a broad sense to cover a wide range of devices that generate electricity via the use of magnets and wire coils. In all cases, permanent magnets or electromagnets are used in conjunction with an armature composed of wire coils to form the generator's output. These two components may be located on either the rotor (the spinning portion of the generator) or the stator (the stationary section) of a generator, depending on the generator [40].

Permanent magnets are used in the construction of small and relatively low-power generators, while electromagnets are used in the construction of bigger and higher-power generators. During the operation of a basic generator, such as the one shown in Figure 5.20, the rotor, also known as the armature, is a wired coil that spins in the magnetic field generated by the stator magnets. The armature is rotated by an external mechanical power source that is situated outside of the main assembly. The armature spins using mechanical energy from sources such as a wind or water turbine, or simply by manually cranking the rotor assembly. The revolving armature rotor is represented by the "loop" in Figure 5.20, and the stators are represented by the magnets on each side of the loop.

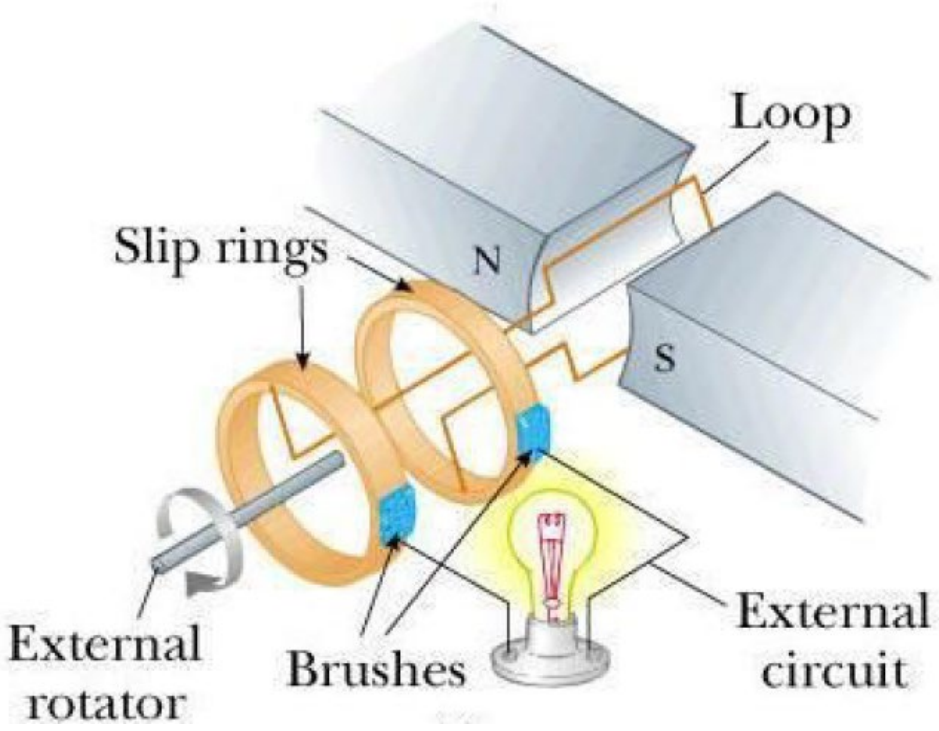

Figure 5.20: Simple Generator [40]

In a basic generator that is shown in Figure 5.20, when the armature spins in a magnetic field, electrons in the coils of armature-wire travel, resulting in the generation of electrical current. Metal slip rings are mounted on the shaft of the motor to transport energy from the spinning armature to an external circuit. Stationary brushes, usually made of graphite, come into contact with the slip rings to transfer power. Using the brushes, electrical current is transferred to the stationary external circuit, where it may subsequently be utilized to power external devices such as lights, fans, and other home appliances [40].

The energy generated by a generator, such as the one shown in Figure 5.21, is alternating current (AC), which means that the current travels in both directions via the wires of the generator. According to Figure 5.21, an alternating current is produced owing to an angle formed by the armature and the magnetic field; since these two components continuously cross each other at various angles, the voltage output of the generator changes, as can be seen in the figure.

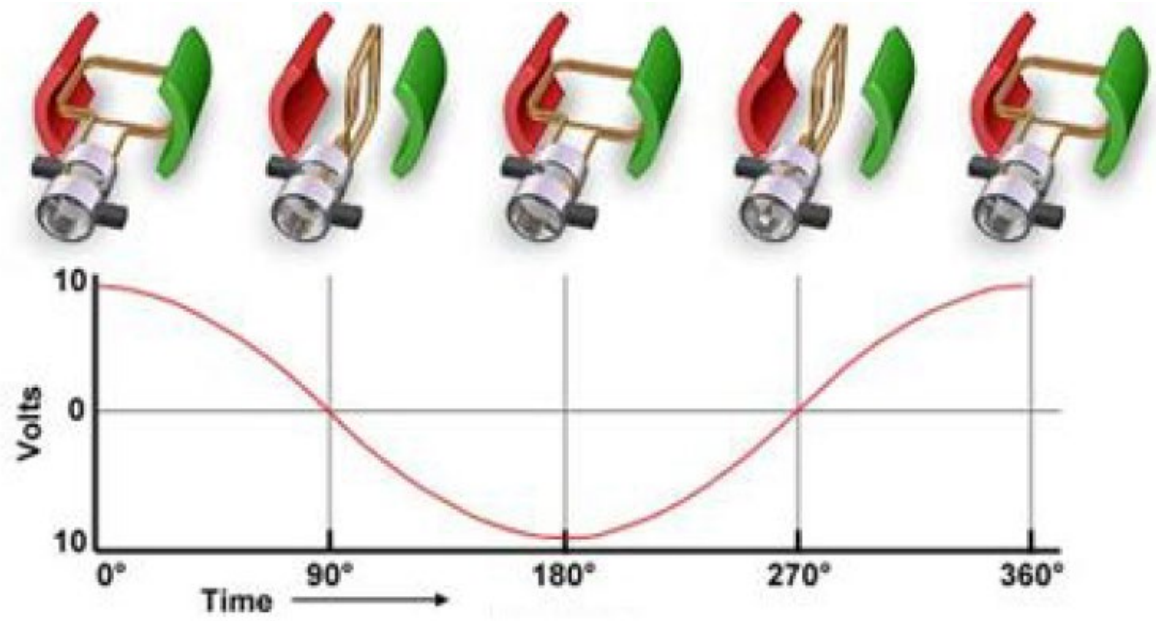

Figure 5.21: Sine Waves produced by AC Generator [40]

The majority of electrical equipment of the late 1800s, on the other hand, could only operate on direct current (DC), thus early designers utilized commutators and brushes instead of slip rings and brushes to physically convert alternating current (AC) to direct current (DC) [40]. Commutators, as shown in Figure 5.22, are identical to slip rings, with the exception that there are at least two breaks in the rings. Every half turn, the breaks in the rings serve as switches, reversing the connection of the armature windings and allowing electrical current to flow in just one way, as shown by the symbol. The voltage waveform produced by the DC generator is shown in Figure 5.23. A dynamo is a generator that generates direct current (DC) electricity using a commutator [41].

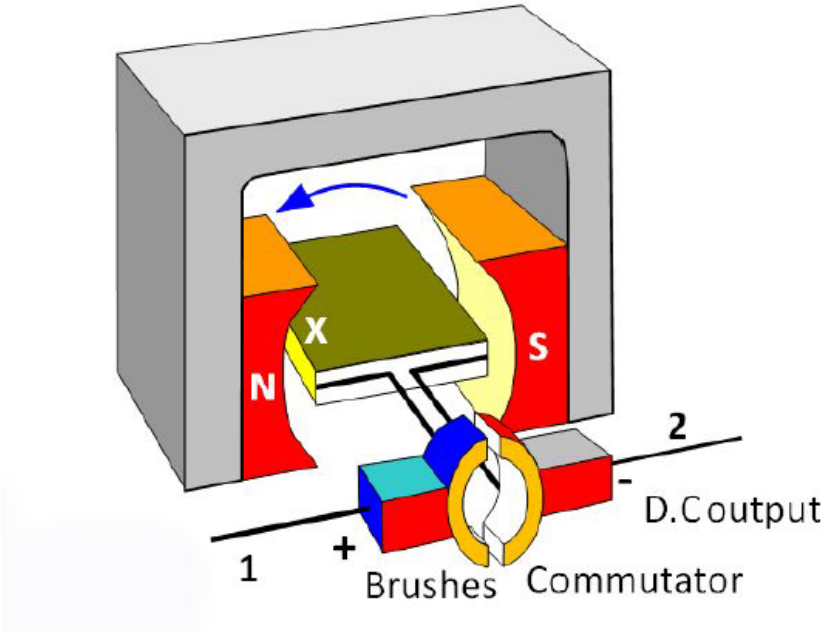

Figure 5.22: DC Generator with Split Ring Commutator [41]

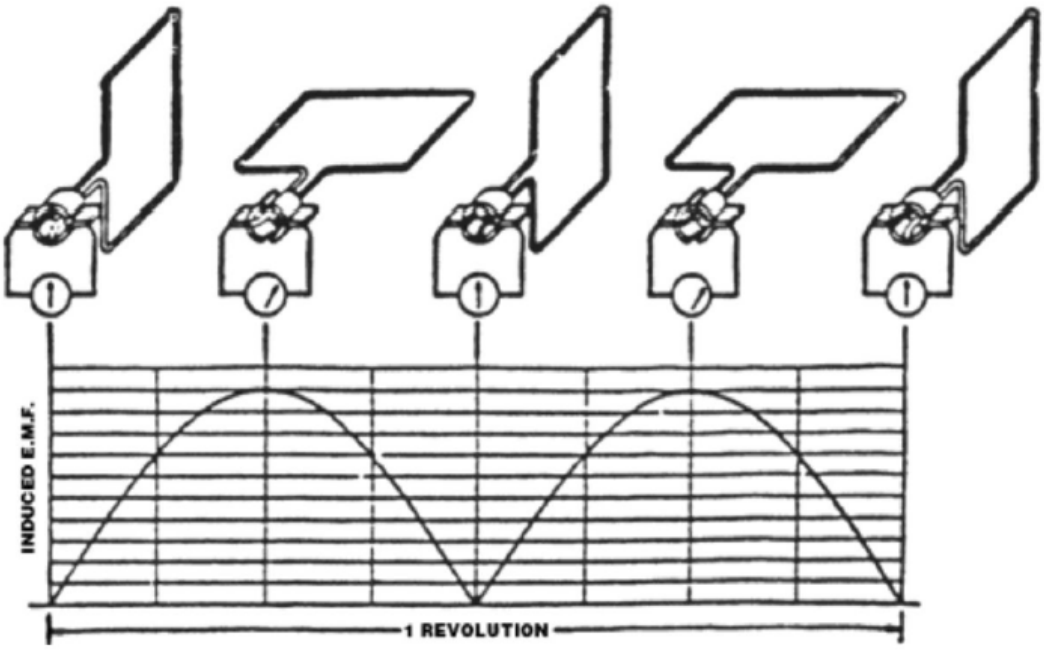

Figure 5.23: Voltage Waveform produced by DC Generator [41]

It is because standard wall outlets provide 220V alternating current, a typical household generator that produces power during an electricity outage, as well as generators used in power

plants and other similar applications, do not require the conversion of alternating current to direct current [39].

An alternator is a kind of generator that is shown in Figure 5.24. In an alternator, a magnetic field rotates within stationary wire coils, which means that the magnet, which is typically an electromagnet, is the rotor and the wire coils are the stators, which is the polar opposite of the design of simple generators and dynamos, which is the rotor and the wire coils are the stators. The output voltage of this kind of generator is generated in the stator, rather than the rotor, as in the previous type. Generators, like alternators, contain brushes and slip rings. In an alternator, these components serve to transfer electricity into the rotor to power the rotor's electromagnets, whereas slip rings and brushes in a generator serve to transfer electrical energy out of the rotor to an external circuit [42].

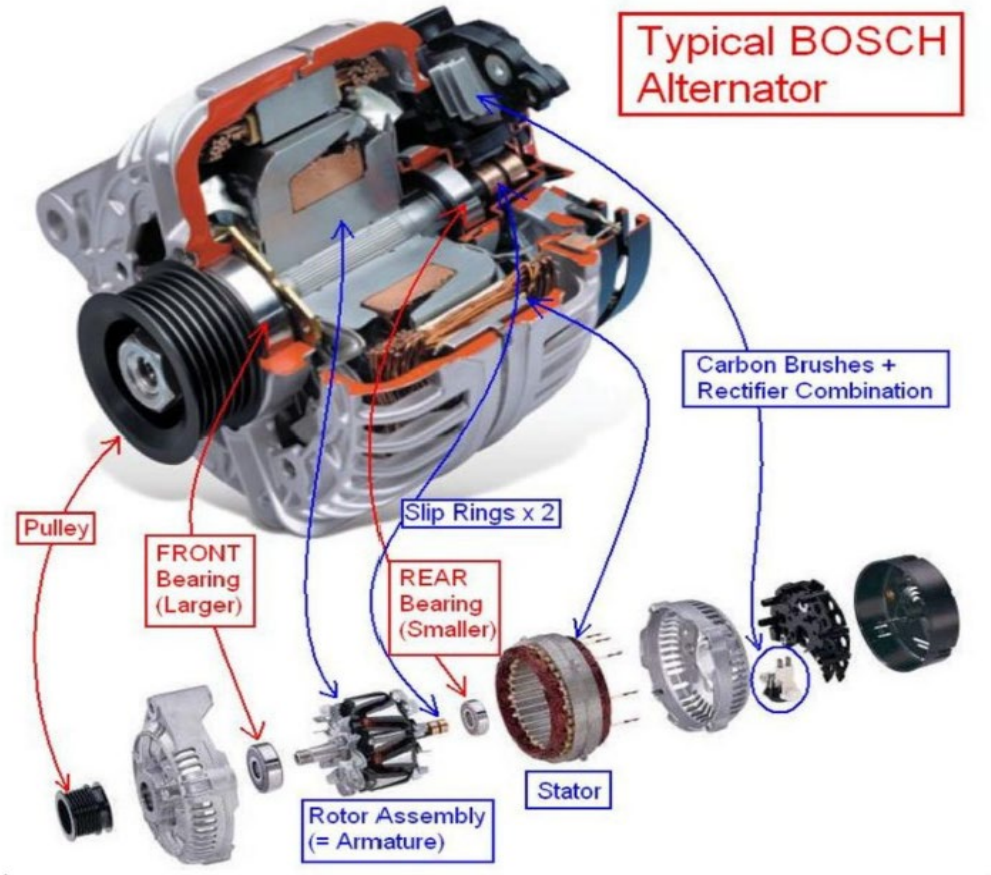

Figure 5.24: Car Alternator [43]

In Figure 5.24 the Alternator that is basically used in car is shown. Alternators are commonly used in modern cars because of their small size and high efficiency. However, electronics of vehicle such as the radio and lights require DC power to function, car alternators are equipped with additional circuitry that converts the alternator's alternating current (AC) power to direct current (DC) [43].

5.3.2 Dynamo

In order to improve the safety of cyclists at night, lights are frequently installed on their bicycles. Bicycle lights can be powered by batteries or by a dynamo, depending on the manufacturer. The advantage of using dynamo driven lights is that they do not require batteries [44]. While they are similar in appearance to real dynamos, bicycle dynamos are not the same thing. Bicycle dynamos are actually magnetos (a generator with a permanent magnet), but when used on a bicycle, magnetos are referred to as dynamos. Magnetos do not have commutators; thus, they generate pulse alternating current power by spinning a wire armature within the magnetic field of permanent magnets and connecting the revolving armature to an external load via slip rings. All bicycle dynamos generate some degree of drag on the bicycle, which causes the rider to exert additional effort.

Dynamos are used for converting mechanical energy to electrical energy. There are two types of dynamos available they are- hub dynamo and bottle dynamo. The dynamo that will be placed in bicycle should have permanent magnets which can generate ac current. Bottle dynamos, as seen in Figure 5.25, are often connected to the seat stay or fork of a bicycle's rear tire and contain a small wheel that makes contact with the tire’s sidewall to generate electricity. In conjunction with the tire rotation, this wheel spins which in turn, turns the armature in the dynamo, generating enough electrical energy to power the bike's lights. The drawbacks of this

method include the fact that the dynamo's wheel might wear down the sidewall of the tire, resulting in the tire failing prematurely. It is also less dependable in wet weather due to the possibility of the ribbed wheel getting in touch with the tires' skidding, resulting in the dynamo not producing any power.

Figure 5.25: Bottle Dynamo (Source: Google)

Both dynamos are suitable for bicycle and has its own advantages.

Figure 5.26: Hub Dynamo (Source: Google)

Hub dynamos, such as those seen in Figure 5.26, are more efficient than bottle dynamos since they are not impacted by wet circumstances. As they are installed inside either the back or front wheel hub of the bicycle, as indicated. Unlike batteries, these dynamos are directly linked to the bicycle wheels, making them a dependable supply of electrical energy for the bicycle. These

bicycle dynamos, on the other hand, are the least flexible of the bunch, as they are generally integrated into the bicycle wheel hub and so cannot be readily removed [25].

5.3.2.1 Working Principle of Dynamo

A bicycle dynamo works by using a magnet to transform the revolving wheel's mechanical movement into electric energy. A permanent magnetic field is wound with insulated wire coils in the dynamo. When the magnet rotates, it creates a changing magnetic field, which causes the wire to generate electricity. The bicycle dynamo remains attached to a fixed part of the bicycle. A dynamo consists of a rotatory part, rotor and a stationary part, stator. Moreover, it also has the permanent magnets which is connected with wire spools that rotates in their poles. The dynamo mainly works on the fundamental principle of electromagnetism. The current is induced here through copper wire coils under the influence of rotating magnetic fields. The permanent magnet spins at the center of several wire coils inside the dynamo. Sliding rings are not required when the magnet is turned instead of the coils. The wire coils generate electricity by changing the magnetic field created by the rotating magnet. When the bike travels, the upper half of the dynamo is in contact with the rotating tire circle. In this way we get electrical energy through the help of dynamo from bicycle.

5.3.3 Alternative to a Dynamo: An Alternator

Alternator is also a generator which converts mechanical energy to electrical energy but it changes in form of alternating current. The structure of alternator is mainly with a stationary armature using rotatory magnetic field. Alternator is larger and heavier than dynamo. However, an alternator can produce much more energy than dynamo. Alternator is more efficient. The output energy of dynamo is very low and it is used for powering low powered device. For powering up high powered devices an alternator should be a viable substitute of a dynamo. The alternator should be placed by removing the carrier, other than that there is no way to place a

dynamo as it is large in size. The alternator shaft pulley drives the alternator through a belt. The shaft of an alternator should be connected to the back tire of bicycle and there should be a belt over the shaft on one end and the other end rolls over a cylindrical structure. Therefore, when the wheel of the bicycle rotates the alternator also rotates and produces energy. The rotating magnetic field induces an Ac voltage in the stator windings. A three-phase current is produced here so three sets of stator winding is available. An automatic voltage controller is available to limit the voltage so that it does not give more than usual voltage. Moreover, the ac current can be rectified 6-diode rectifier and convert the ac output voltage to dc output voltage. The shaft of alternator can be connected in another way by making the shaft roll over the tire but it can slip if there is no grip. Hence, a grip is to be placed and it can be placed with the help of a rubber. The first way will be more productive but the bicycle needs to be in stationary state.

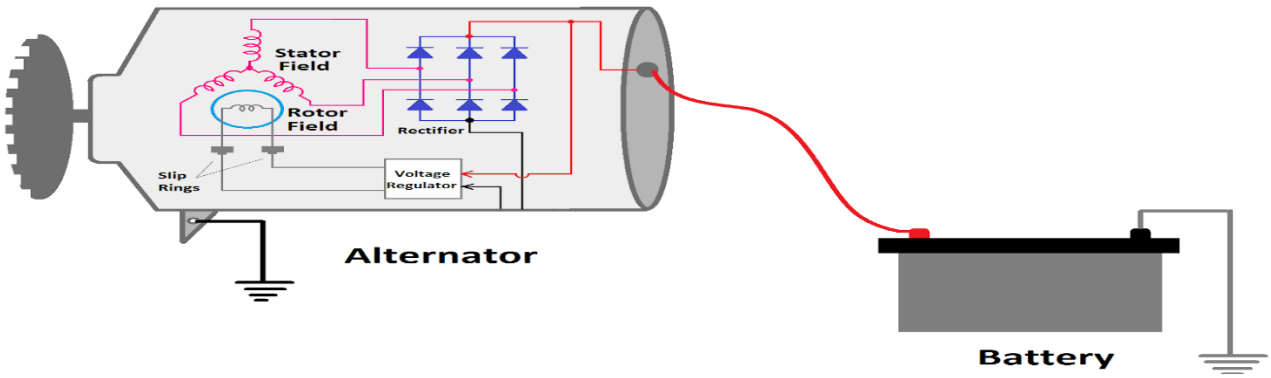

Figure 5.27: Alternator with battery. (Source: Google)

The alternator is able to produce more power, the rectifier and filter should not undergo any alternation. The regulator part will regulate a voltage of 15V through the use of IC7815. The alternator can be welded to avoid stealing.

5.3.4 Human Power

Through an activity such as pedaling or turning a crank generator, human power may be utilized to spin an armature in a generator, generating electricity, which can be used to power other devices. While engaging in any intense activity, the typical fit individually can generate between 50 and 150 watts of power, while an exceptional athlete may generate up to 400 watts of power for an hour of continuous exercise. Considering that the average human's daily energy expenditure is approximately 2792 watt-hours, it opens up the possibility of developing a device to capture this energy in order to power electrical devices [45]. As heat and motion are both sources of energy release, it creates possibility of developing a device to capture this energy in order to power electrical devices. Many businesses are researching ways to turn the energy that people waste while exercising at the gym on exercise equipment such as stationary bikes and ellipticals into power by connecting the equipment to generators.

5.3.5 Lead Acid Battery

The battery that we will incorporate with the dynamo is a lead acid battery. The lead acid battery is the first rechargeable battery that was invented in 1859. It is a battery with lowest current density but has the ability to provide high value current. Therefore, it can be said the cell provides low energy to weight ratio and a low energy to volume ratio.

5.3.5.1 Chemistry behind lead acid battery [26]:

Discharge, negative plate reaction:

$Pb(s) + HSO_4^-(aq) \rightarrow PbSO_4(s) + H^+(aq) + 2e^-$

Discharge, positive plate reaction:

$PbO_2(s) + HSO_4^-(aq) + 3H^+(aq) + 2e^- \rightarrow PbSO_4(s) + 2H_2O(l)$

Discharge, the whole reaction:

$Pb(s) + PbO_2(s) + 2H_2SO_4(aq) \rightarrow 2PbSO_4(s) + 2H_2O(l)$

Charge: negative plate reaction:

$PbSO_4(s) + H^+(aq) + 2e^- \rightarrow Pb(s) + HSO_4^-(aq)$

Charge: positive plate reaction:

$PbSO_4(s) + 2H_2O(l) \rightarrow PbO_2(s) + HSO_4^-(aq) + 3H^+(aq) + 2e^-$

Figure 5.28: Lead Acid Battery (Source: Google)

The charge time of a sealed lead acid battery is 12-16 hours. For the large batteries approximately 36-48 hours is needed. Through high current method or multi-stage charge method, we can lessen the required charge time and bring it to 10 hours.

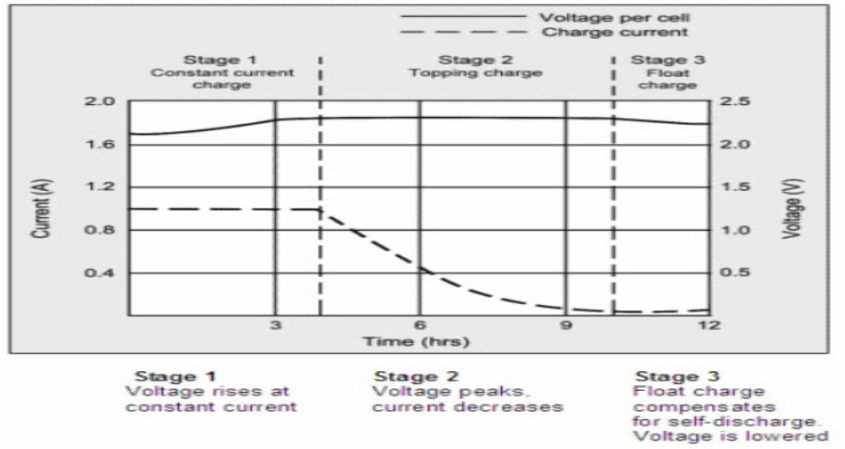

Figure 5.29: Charging state of lead acid battery (Source: Google)

To complete the charging phase, lead acid batteries need to complete 3 stage that is shown in Figure 5.29 -

In the constant current charge stage, the cell receives a huge amount of charge within a short period of time. The topping charge phase gives the saturation level and provides lower current. Finally, as the cells get discharged, the float charge protects the cell from self-discharging.

Some specific details of lead acid battery are [26]-

- Specific energy: 30-40 Wh/kg
- Energy density: 60-75 Wh/L
- Specific power: 180 W/kg
- Charge/discharge efficiency: 50-92%
- Energy/consumer price: 7-to-18 Wh/$
- Self-discharge rate: 3-20%/month
- Cycle durability: up to 800 cycles (500 typical)
- Nominal cell voltage: 2.1 volts
- Float-charge voltage per cell: 2.23 (gel), 2.32 (flooded), 2.25(AGM).

- Cutoff voltage: 1.75 volts per cell (loaded)
- Charging temperature: -40°C (min) to +49°C (max); see specific manufacturer for more details

5.3.6 Bicycle Dynamo Generator Designed for the Project

A pedal powered bicycle generator is a technology that generates electricity by using the energy of the user to act as the second renewable energy source. An alternator is implemented as the power generator in this instance. It is connected to a pulley that is rotated by a belt and chain-sprocket system that is part of a bicycle frame. It is the paddle that receives the input power, and it is the alternator rotor that achieves the ultimate rotating speed. The majority of the components of the portable pedal power generator are based on existing innovations, both contemporary and historic in nature.

Using it as a helpful energy source for a small family in our country's villages, where the family members themselves may generate power by paddling for a short amount of time each, has shown to be a success. Aside from the cheap initial cost, the ‘Paddle Powered Generator' has extremely low operating and maintenance costs, making it a viable source of renewable energy for large-scale implementation.

5.3.6.1 Alternator Selection

Following a series of surveys and discussions with representatives from the local markets, the ND (NIPPON-DENSO) alternator was chosen at the beginning for our project. It is a manual alternator (without an integrated circuit regulator) that is often seen in Japanese automobiles (Toyota). It is an alternating current component that also produces direct current (DC) as a result of rectifier circuits. The following are the most significant benefits of automobile alternators:

- They are readily accessible

- They are small in size
- They have a cheap repair cost.

Figure 5.30: Car Alternator we acquired

The alternator that is shown in Figure 5.30 is mostly chosen because of the ease with which it can be mounted on the setup. Because an automobile battery is used as a storage device, connecting it is a simple process for anyone. The output, on the other hand, is dependent on both the rotor speed and the Field current. This issue may be readily resolved with a permanent magnet generator (DC generator), which has terminal voltage that is only dependent on the fluctuation of the motor speed. After taking all of these factors into account, we have decided to proceed with our project involving the DC generator.

Figure 5.31: DC Generator (Source: Google)

5.3.6.2 Prototype Bicycle Generator Case Design

As previously stated in chapter 3, the kind of generator that will be installed on the bicycle will be one that operates with a roller on the sidewall of the tire. The overall form of the generator casing, f is one of several variables that must be addressed before the implementation for final generator design. The shape of the generator may have an impact on its performance and long-term dependability. The feasibility of various bicycle generator case designs as a bicycle generator was therefore investigated, as shown in the illustration below. In order to choose the best potential generator form, based on its practicality, each of these alternatives was examined for its benefits and drawbacks, as indicated in Table 5.12. Following a thorough examination of each option, the best potential generator shape was selected.

Figure 5.32: Generator Option 1, 2, 3, respectively (Source: Google)

Body Shape	Advantages	Disadvantages
Option 1	• simple case construction • ease of manufacture • ease of availability	• much of the moving shaft is exposed • the edge of the case top might hit the bicycle's tire if the shaft is not long enough and is mounted on the bicycle
Option 2	• shaft is not exposed • case will not hit the tire due to bottle shape	• difficult to create the prototype
Option 3	• shaft is not exposed • case will not hit the tire due to bottle shape • roller will be closer to the tire	• Roller is not in line with the motor, which means gear would be required to transfer power to motor shaft, resulting in a wide case

Table 5-12: Generator Options Advantages and Disadvantages

Even though Option 2 seemed to have the greatest chance of success owing to benefits, which include having a covered rotating shaft and a design that would prevent the bicycle tire from rubbing against the casing, it was ultimately unsuccessful. That is why following a thorough

examination of these considerations for each case option, we determined that Option 1 was the best choice. It is due to the fact that it is readily available during these epidemic periods.

5.3.6.3 Working Principle of the bicycle dynamo generator (Option 1)

A DC Hub dynamo generator (option 1) , with a rated output of 24V, has been installed to power our bicycle dynamo in this project. The dynamo is installed on an iron chassis, and the chassis is linked to the bicycle at the back. Additionally, a wooden board has been placed on the iron chassis in order to set the dynamo in proper position. The dynamo is configured in such a manner that when the bike's pedal begins to spin, the dynamo will also start to rotate in tandem with it. The dynamo will start rotating with the assistance of a rubber belt that is attached to the rear tire and has the proper amount of tension.

Figure 5.33: Dynamo mounted on chassis

Figure 5.34: Bicycle with the dynamo

In Figure 5.34 it is shown that an iron pulley has been connected with the dynamo which enables the rubber belt to make a proper connection with the dynamo.

Figure 5.35: Pulley attached with the dynamo

In Figure 5.35 it is shown the pulley that has been attached with the dynamo. It is essential to maintain proper tension in the rubber belt since this will guarantee that the pulley and tire do not slide during rotation of the vehicle. It is determined that there is a 20:4 radius ratio between the rear tire and the pulley. This implies that while the rear tire of the bicycle spins at 20 rpm (revolutions per minute), the pulley will revolve at 80 rpm, which is four times faster than the rear tire of the bike. As a result, while pedaling the bicycle the pulley starts to rotate along with the rear tire which results in induced voltage inside the dynamo due to the presence of a permanent magnet within it. The output voltage varying depending on the rotation of the pulley and the rotation of the tire.

5.3.6.4 Result and Analysis

A whole separate measurement equipment is required in order to determine the connection between speed and current. In this situation, a load is required. In addition, a multimeter and a tachometer will be required. The alternator and the load are connected in series to produce electricity. In addition, the multimeter is linked in series with the load. It is possible to generate power when the user spins the generator. The amount of electricity consumed by the load varies in proportion to the speed. However, owing to the unavailability of a tachometer, the speed is obtained by analyzing the video recording, and the current is determined by using a multimeter instead.

The following table shows the relationship between speed and current.

SPEED (RPM)	CURRENT (A)
380	0.94
400	0.97
420	1.08
470	1.4
500	1.7
520	1.8
570	2.05
600	2.3

Table 5-13: Relationship between speed and current

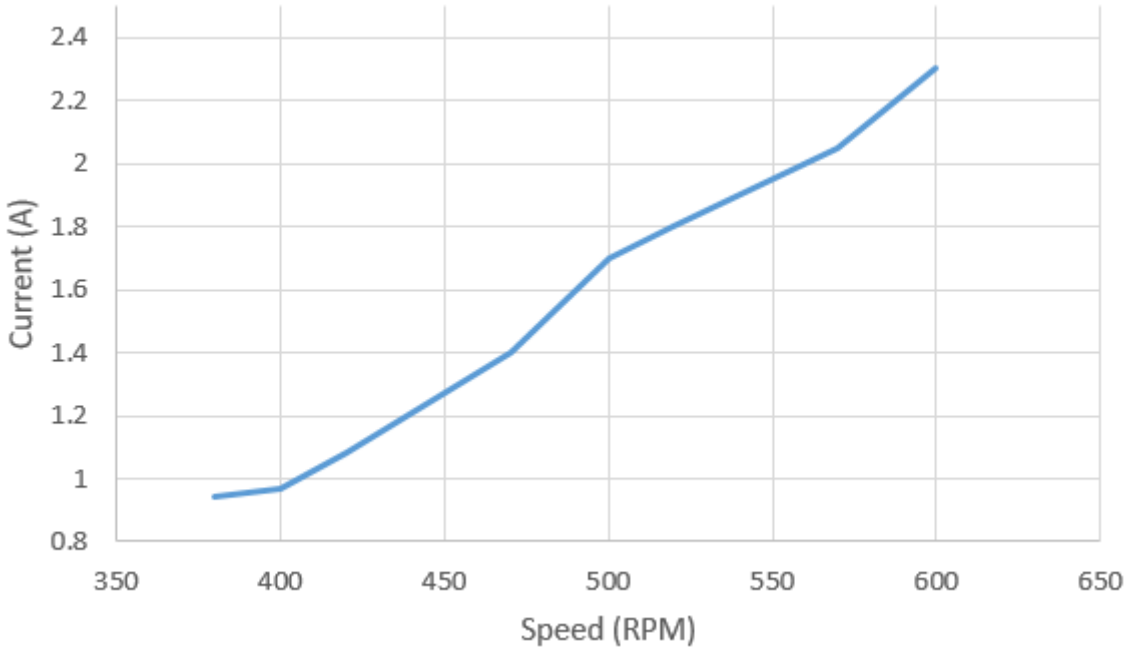

Figure 5.36: Graphical representation for Speed vs Current

In Figure 5.36 the graph illustrates that a motor generator provides more current to the load as the motor speeds up, and as the motor slows down, less current is generated to the load, as seen in the graph.

5.4 Conclusion

The testing and measurement analysis of the Solar PV Panel was carried out on 20 September, 2021 from 07:00 AM up to 06:30 PM. From the meteorological datasheet, we can observe that the months of June to late September have the most rainfall all around the year. We advise that any designers or upcoming researchers/thesis students who would like to study the solar PV panel must conduct the field study either in summer (late January-mid May) or at least in the winter (late October- late January). The rainy season is not the most preferable time to study a solar PV panel. Rather, the solar PV panel analysis can be a little tricky during rainy season and the findings will have a lot of variation because several factors should be in consideration like light-heavy rainfall, dark/thick clouds, humidity, shading etc. For our case, due to a light rainfall and a heavy dark cloudy weather in the morning and also after noon, the open-circuit

voltage readings in our study are not consistent. It has a lot of anomaly. The V_{OC} vs Time curve was supposed to look like a usual bell curve with a maximum concentration of open-circuit voltages during 11:00 AM to 3:00 PM. During field test, there were times when we had to pause the measurement analysis because the sun was not properly showing up. Also, multiple disruptions occurred due to cloud coverage of sunlight.

Since the amount of natural energy available on our planet is decreasing every year, it is imperative that we seek for alternatives. Because bicycles are commonly used in both rural and urban settings, they can be a valuable source of mechanical energy to be converted into electrical energy. The energy we will be able to generate will come from riding the bicycle; the more pressure that is generated, the greater the amount of energy that can be generated. When it comes to energy generating, either a dynamo or an alternator generator can be used effectively. The power that will be generated from this location will have a wide range of applications.

Chapter 6 Simulation and Results Analysis

6.1 Introduction

Several simulation-based tests and calculations are carried out as part of this research. The findings of such tests are described in detail in this chapter. We have used the MATLAB/Simulink software to examine the whole system in order to extract and collect data from simulations for our proposed solution. Simulink is a graphical programming environment for modelling, simulating, and evaluating multidomain dynamical systems that is based on the MATLAB programming language. Its main interface consists of a graphical block diagramming tool and a collection of block libraries that may be customized. In the second chapter, we spoke about the traditional SEPIC DC-DC converter and its advantages and disadvantages. When compared to other types of converters with a traditional construction, the SEPIC converter (Single-Ended Primary Inductor Converter) offers a number of benefits. The SEPIC converter is one of the converters with complicated topologies of fourth order [26], and it is categorized as such. First, we have created a mathematical model of the standard SISO SEPIC, that has been subjected to MATLAB/Simulink simulation in order to conduct a system analysis. In addition, we have finished the development of the modified SEPIC with dual input as well as the MATLAB/Simulink simulation for the system analysis and evaluation.

6.2 Simulation of Mathematical Model of SEPIC based SISO Converter

The first step was to develop a mathematical model of the standard SISO SEPIC, which was then put through its tests in a MATLAB/Simulink simulation to allow us to perform a system analysis.

The parameters for each of the components of the SISO SEPIC converter had been calculated and tabulated in table 6.1 using the equations given in Chapter 3.

Parameters	Values
L1	336 µH
L2	336 µH
C1	504 µF
C2	504 µF
Switching Frequency	32 kHz
Duty Cycle	80.64 %
Load	25 Ω

Table 6-1: SISO SEPIC parameters

We performed the experiment using both a DC voltage source and a PV panel as the voltage input, both of which had the same magnitude of 12V as the DC voltage.

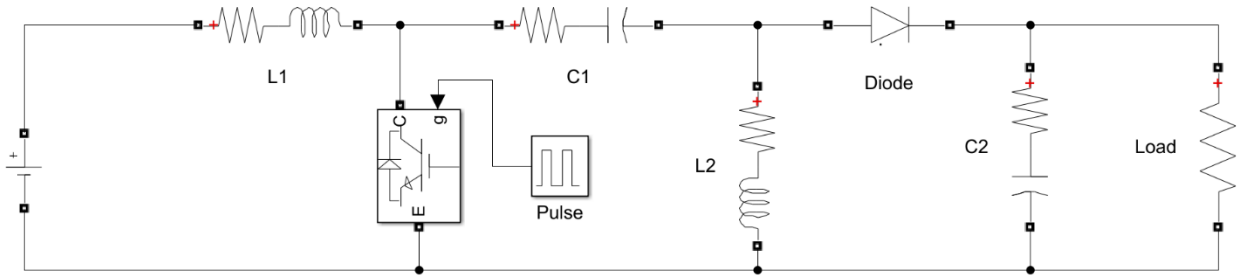

Figure 6.1: Mathematical Model of SEPIC using DC Voltage Source as input

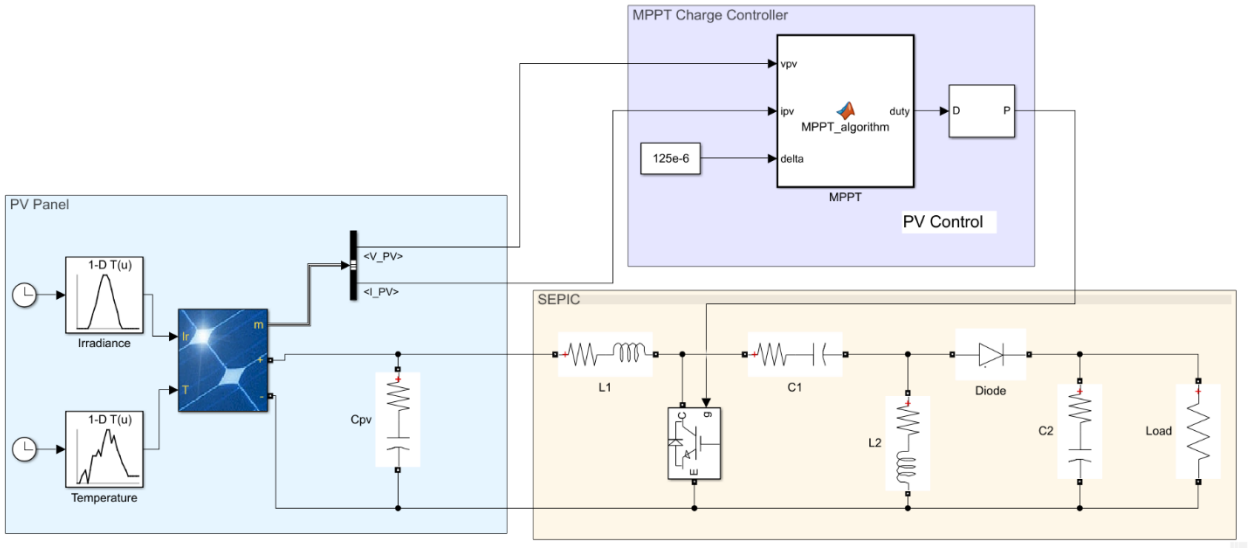

Figure 6.2: Mathematical Model of SEPIC using PV Panel as input

6.2.1 Description of the Individual Components

We will discuss the different components that have been deployed in this project in this part. Solar panels were utilized to obtain solar energy in this project. MPPT charge controllers are used to improve efficiency.

6.2.1.1 PV Array Design Consideration for Software Simulation

PV panels, often known as solar panels, are semiconductor-based electrical devices that use the photovoltaic effect to convert sunlight into electrical energy. Silicon is the most common material used in PV panels. Solar panels are critical to the whole system since their efficiency has a significant influence on the project's overall efficiency. We used 215Wp Soltech solar panels in this project simulation.

.

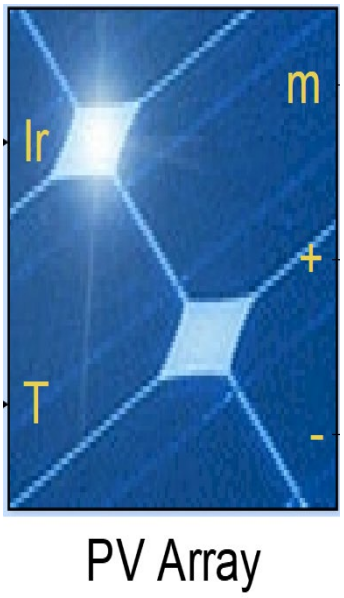

Figure 6.3: Solar Array in Simulation

Figure 6.3 is a visualization of Solar Array from the simulation. In the simulation, the solar panels have two inputs. Solar irradiation is one, and temperature is another. The data on sun irradiance comes from Bangladesh's final report on Solar and Wind Energy Resource Assessment (SWERA). The temperature data comes from the website "weatherspark.com." These data sets are both quite credible

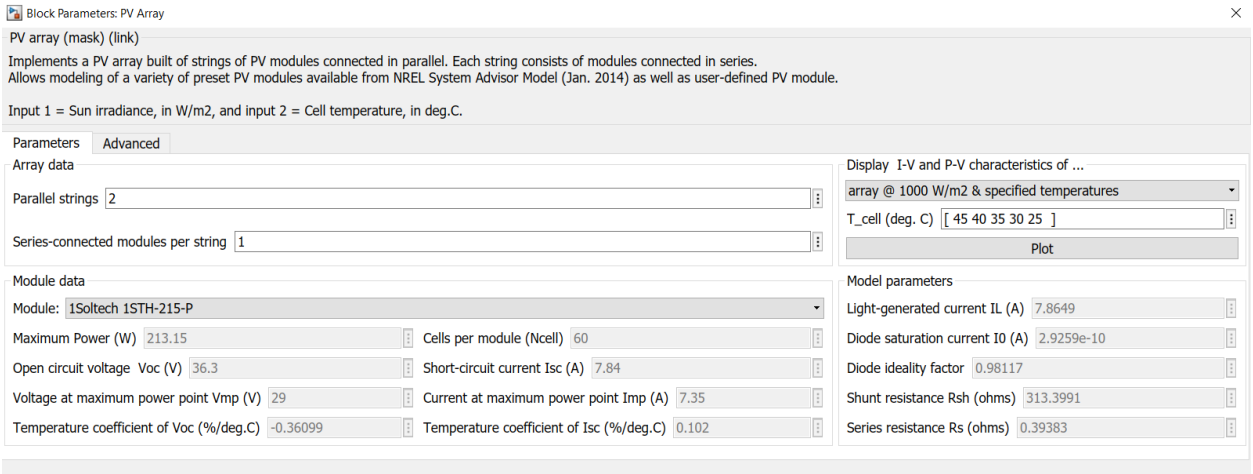

Figure 6.4: Solar Array specifications in Simulink

In Figure 6.4 The specifications in Solar Array in MATLAB/Simulink that needs to considered while performing analysis with Solar panel is shown.

6.2.1.2 MPPT Charge Controller

Throughout this project, the MPPT (maximum power point tracking) charge controller plays a critical function. Due to the fact that solar irradiation fluctuates considerably from season to season and from weather to weather, and even on an hourly basis, the voltage and current produced by the sun are unpredictable. If the voltage coming from the solar panels is greater than the voltage coming from the battery, or if the solar panels are not providing enough voltage and current to charge the battery as a result of inclement weather, the battery's health will degrade rapidly. It keeps track of the maximum power point and the maximum efficiency.

When compared to other charge controllers, MPPT charge controllers perform more effectively since they can enhance the voltage when solar irradiation is insufficient to charge the batteries. MPPT charge controllers are also more expensive. It also bucks or ramps down the voltage when the panels create more voltage than the battery charging voltage limit, which occurs from time to time. In the beginning, the MPPT block senses the voltage and current coming from the PV panels. Consequently, the current and voltage data from the PV panels are sent into this MPPT block as input. The duty ratio will be produced as a result of this block. After that, the duty ratio will be compared to the carrier signal in order to generate a pulse width modulation signal. The signal will then be sent to the gate terminal of the IGBT, which will operate as a switch as a result of its operation.

6.2.2 System Results using DC Voltage Source

6.2.2.1 Relation of the voltage output and the pulse

In this part of the chapter, we will talk about how the output voltage changes as a function of the pulse frequency. The output voltage of the system will be measured once the pulse is generated, thus we will know how well our system worked after it has been simulated.

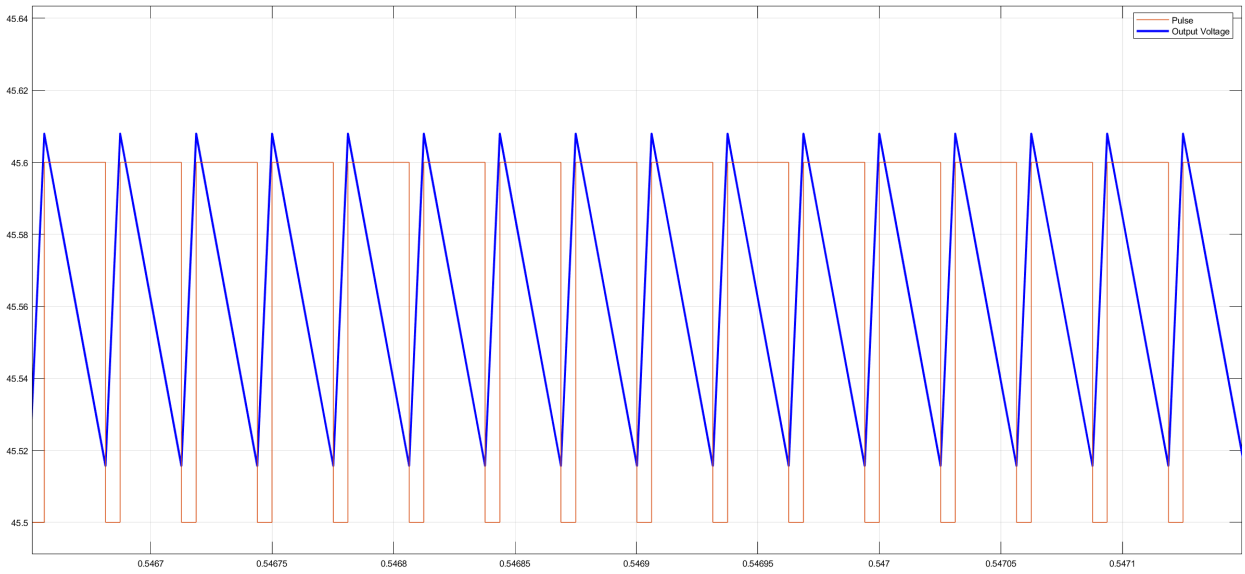

Figure 6.5: Graph of Vout and Pulse

The duty cycle was determined to be 80.64 percent based on the calculations we performed. We used a switching frequency of 32kHz for our project. After running the simulation, we observe in Figure 6.5 that there is a ripple in the output voltage. When the pulse is low, the output ripple spikes up from around 45.52V to close to 45.61V, and when the pulse is high, the output ripple begins to decline again up to around 45.52V.

6.2.2.2 Relation of the Output Capacitor current, Inductor Current with the Pulse

We will observe the ripple in the inductors, as well as how the output capacitor charges and discharges in response to the pulse, in this section. Following the completion of the simulation, we measure the currents flowing through the output capacitor and inductors and see them on the scope. In order to comprehend the impact, we compared it with the switching pulse.

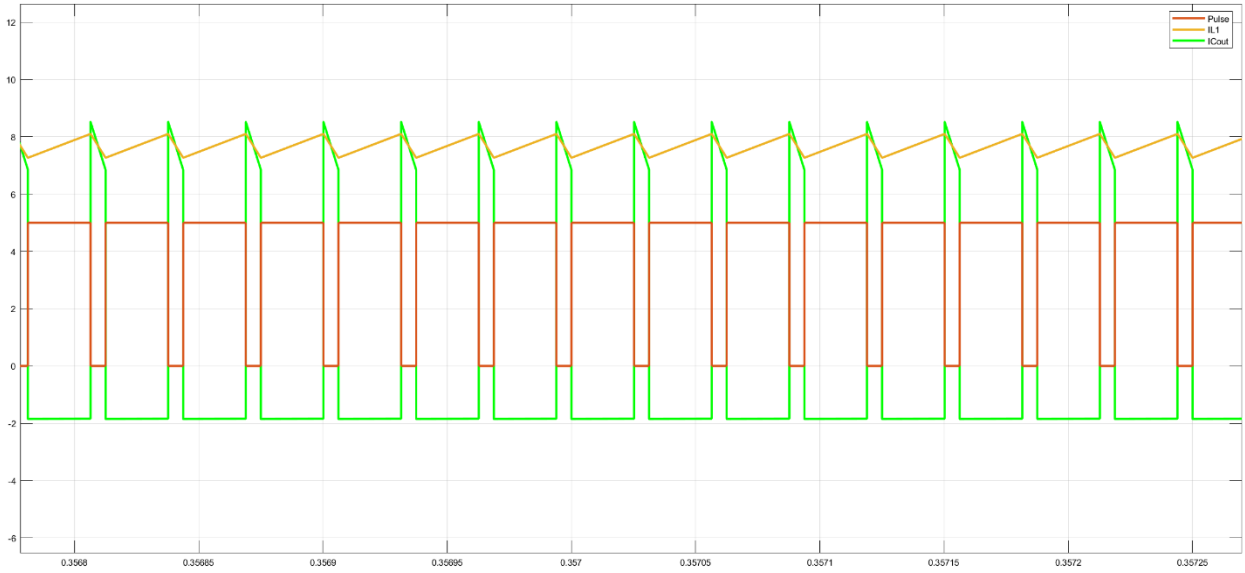

Figure 6.6: Graph of IC_{out}, I_{L1} and Pulse

In Figure 6.6 when the pulse is low, we can see the capacitor is charging. The current in the capacitor increases from around -1.9A to nearly 8A. When the pulse begins to rise, there is a ripple. When the pulse frequency is low, the current of the inductor decreases a bit. As soon as the pulse gets elevated, the inductor current begins to rise gradually.

6.2.2.3 Output Voltage

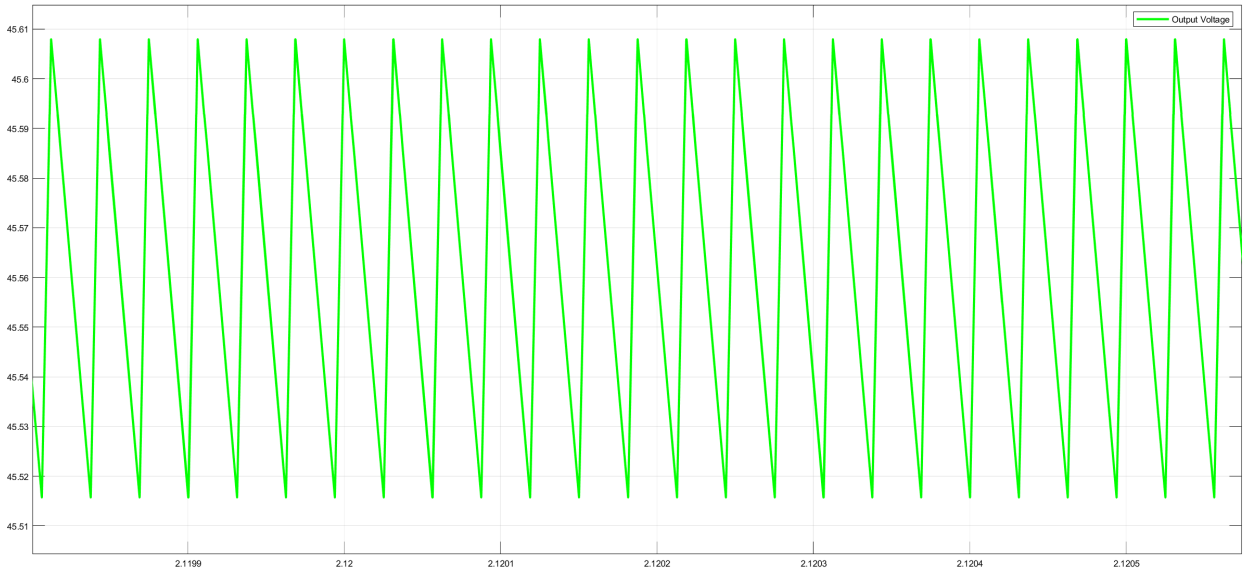

Figure 6.7: *Graph of Vout*

In this project, we are using a SEPIC converter with boost characteristics. The output voltage has been substantially increased which is shown in the graph of figure 6.7. After providing 12V as an input, we can observe that the output voltage was somewhat higher than 45.5V.

6.2.3 PV Panel

The parameters of a photovoltaic generator are determined by the amount of solar light and the temperature of the environment. Temperature fluctuations are responsible for the variability of the maximum power point [26]. In order to improve the accuracy of the simulation, we used data from the final report of the SWERA (Solar and Wind Energy Resource Assessment) project Bangladesh. They investigated data from January 2003 to December 2005 and provided the mean monthly statistics for each month throughout that time period. The real 24-hour solar energy simulation was created using monthly average hourly GHI (Global Horizontal Irradiance) data from April as summer data and December as winter data to create the actual

24-hour solar energy simulation. This chapter demonstrates how solar irradiance changes throughout the day and how this impacts the use of solar energy sources.

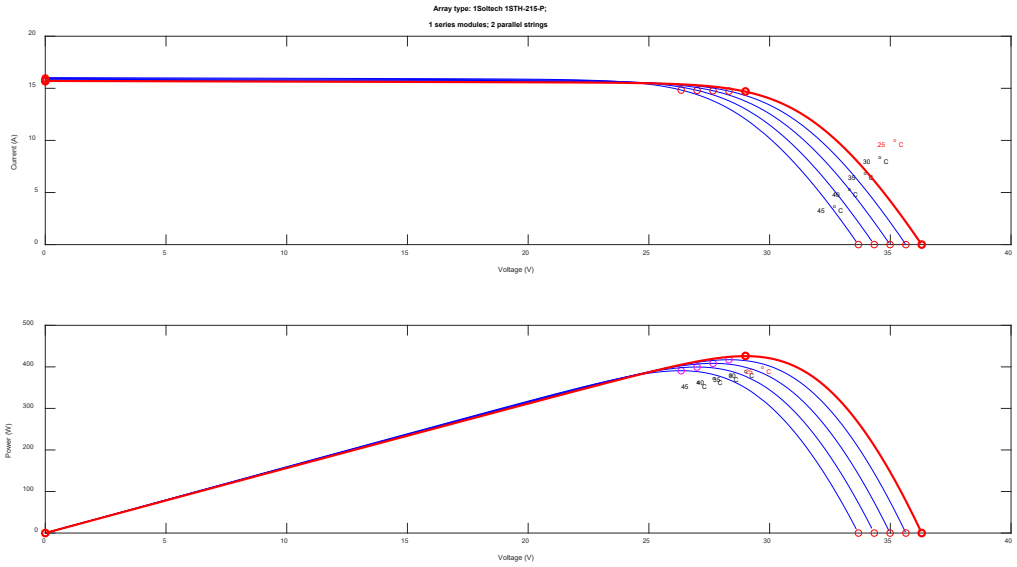

Figure 6.8: I-V & P-V characteristics of PV array

The Soltech 1STH-215-P PV panel model that we have utilized for our simulation is the one that is shown Figure 6.8. It is critical that we make the best use of the PV panels that we have since increasing the efficiency of the array is just one method of extracting more energy from the sun, and it is a significant problem. One method of determining this is to ensure that the PV works at its MPP (Maximum Power Point) under a particular set of irradiance and temperature conditions, among other things.

6.2.4 System Results using PV Panel (Summer)

Summer is when we get the greatest amount of irradiance possible, which is advantageous. In light of the fact that greater irradiance implies that the PV array will operate more efficiently. In this part of the chapter, we will demonstrate the effect that changing the irradiance has on the output of the system.

Using different irradiance data, we ran the system for 24 hours to replicate the system's performance. The average hourly GHI statistics from SWERA were utilized in the simulation system to simulate the system. According to this information, we may create up to 5.46 kWh-day on average by using this much irradiance.

Time	0:00	1:00	2:00	3:00	4:00	5:00	6:00	7:00	8:00	9:00	10:00	11:00
Irradiance W/m²	0	0	0	0	0	5	66	198	354	521	666	751
Time	12:00	13:00	14:00	15:00	16:00	17:00	18:00	19:00	20:00	21:00	22:00	23:00
Irradiance W/m²	764	693	553	402	237	72	4	0	0	0	0	0

Table 6-2: Irradiance data of April by SWERA

6.2.4.1 Relation of the voltage output and the pulse

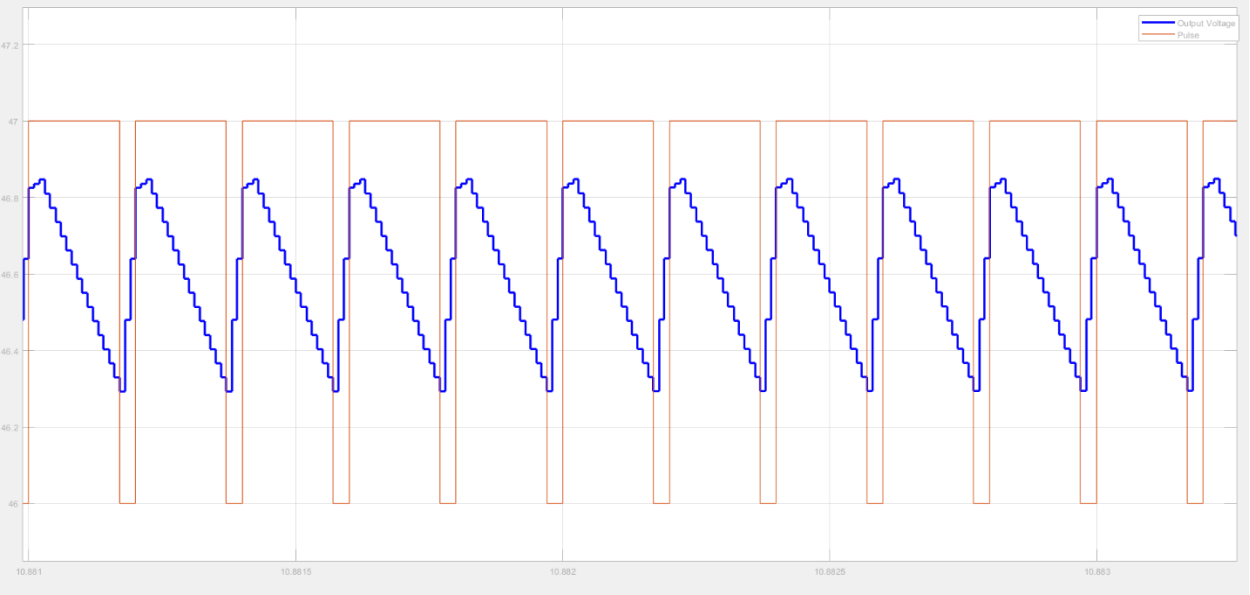

Figure 6.9: Graph of Vout and Pulse

The duty cycle was found to be 80.64 percent, just as it had been previously, based on the calculations we had completed. The switching frequency for our project was 32kHz, which we found to be sufficient for our project. In figure 6.9, The output voltage shows a ripple once we have completed the simulation, as we can see in the image above. In addition, as compared to the prior simulation, the output voltage is a little bit skewed. When the pulse frequency is low, the ripple of output voltage spikes up from around 46.3 V to close to 46.9V, and whenever the pulse frequency is high, the ripple of output voltage begins to decrease again, reaching near 46.3V.

6.2.4.2 Relation of the Output Capacitor current, Inductor Current with the Pulse

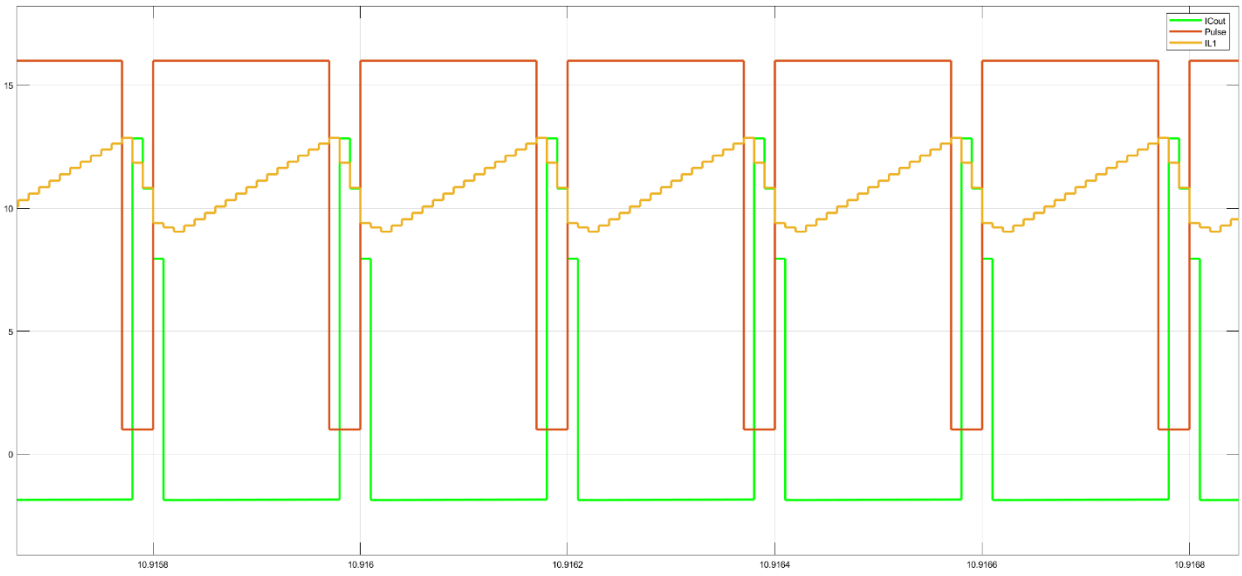

Figure 6.10: Graph of IC_{out}, I_{L1} and Pulse

In figure 6.10, when the pulse is low, we can observe the capacitor is charging. The capacitor's current increases from -2A to 12A as the voltage drops. When the pulse begins to rise, there is ripple and the capacitor starts discharging. Due to the lower frequency of the pulse, the current across the inductor reduces a little bit. The inductor current appears to be more distorted in this

simulation when it is compared to the prior simulation. As soon as the pulse intensity is increased, the inductor current begins to progressively increase.

6.2.4.3 Output Voltage

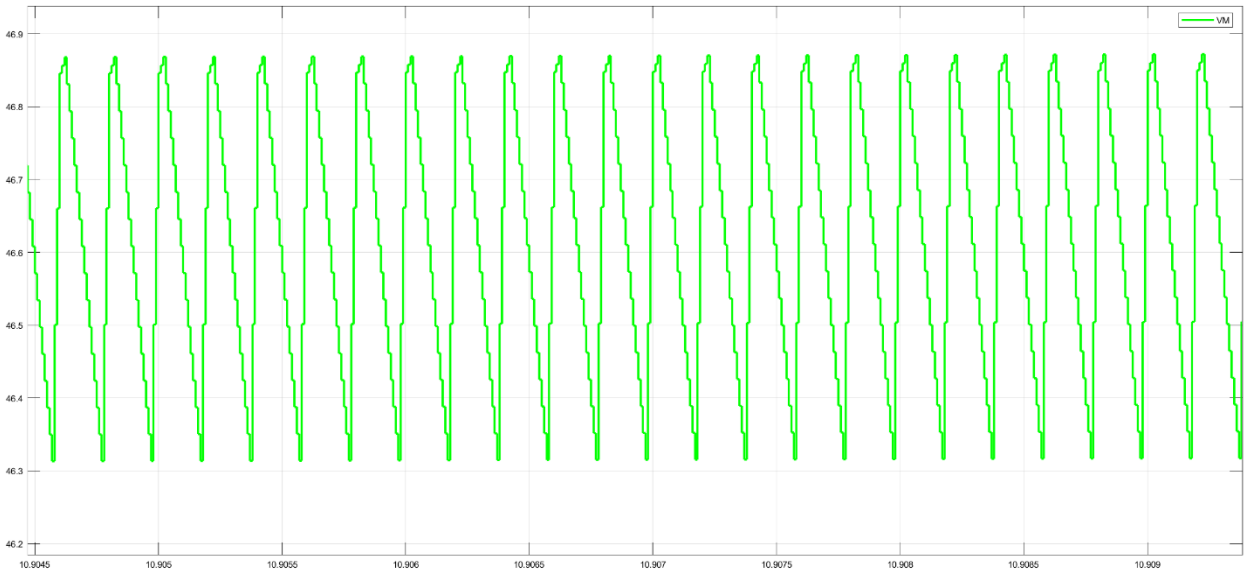

Figure 6.11: Graph of Vout

When we have used a PV panel of 12V as our voltage source instead of a constant dc voltage supply in our SEPIC converter. The output voltage has been substantially increased and gained close to 46.9V which can be seen in figure 6.11. if this output voltage is compared with the output voltage when a dc supply was connected, it can be said that they almost gave the same output voltage.

6.2.4.4 Efficiency

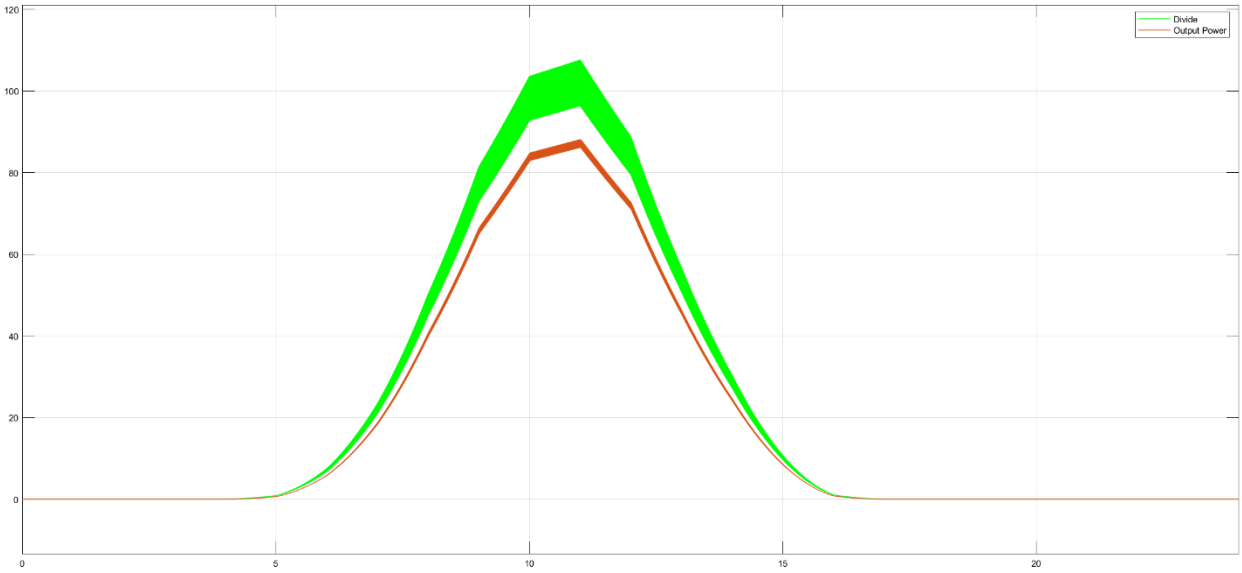

Figure 6.12: Graph of Pout and Pin

Now, we can calculate the power of the input that we get from the solar panel and the output that we get from SEPIC converter when the PV panel is connected in the input side. It is observed in Figure 6.12 the comparison between the input power and output power of the system. Here, we notice that the input power is higher than 100W. On the other hand, the output power is decreased to around 85 watts. Therefore, it can be said that there is a degradation in the efficiency of the system.

6.2.5 System Results using PV Panel (Winter)

For the purpose of determining the system's dependability, simulations based on the summer and winter seasons were performed. We had to set up the system during the winter, when the average irradiance is very low, and we had used it throughout that time. This will demonstrate whether the system is capable of operating at full capacity throughout the year or not.

After setting up the system with varied irradiance data, we ran it for 24 hours to simulate the system's performance. It was decided to use average hourly GHI statistics from SWERA in the simulation system in order to replicate the system in question. In accordance with this

information, we may generate up to 3.17 kWh-day on average by utilizing this amount of irradiance.

Time	0:00	1:00	2:00	3:00	4:00	5:00	6:00	7:00	8:00	9:00	10:00	11:00
Irradiance W/m^2	0	0	0	0	0	0	11	97	237	382	479	498
Time	12:00	13:00	14:00	15:00	16:00	17:00	18:00	19:00	20:00	21:00	22:00	23:00
Irradiance W/m^2	489	426	309	189	54	2	0	0	0	0	0	0

Table 6-3: Irradiance data of December by SWERA

6.2.5.1. Relation of the voltage output and the pulse

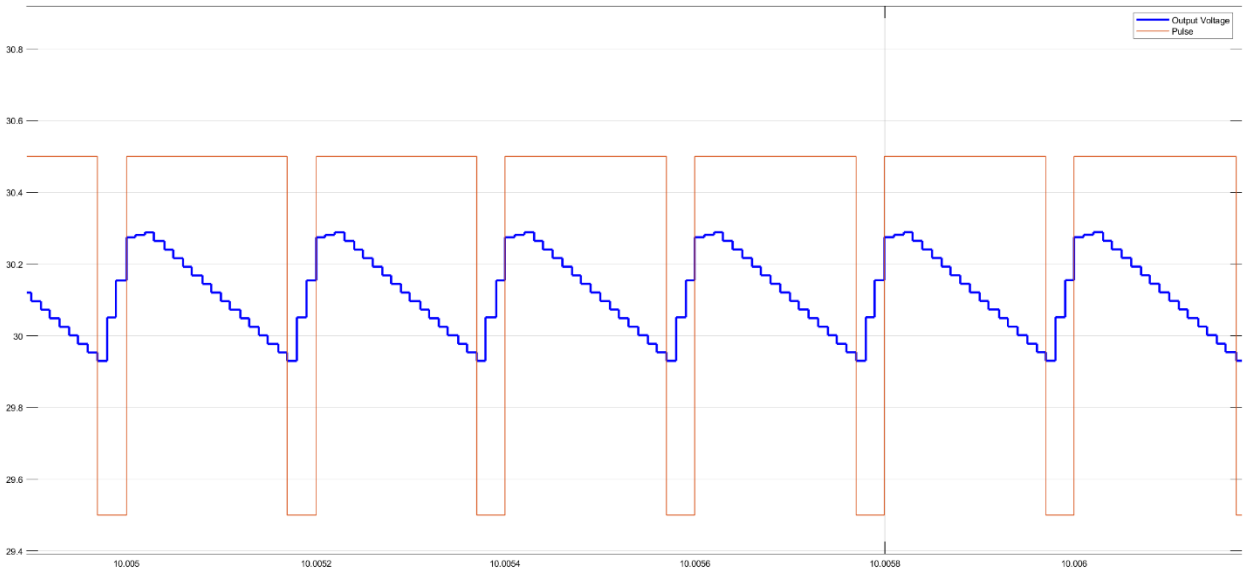

Figure 6.13: Graph of Vout and Pulse

In Figure 6.13, relation between Vout and pulses have been stated. From graph it can be seen that when the pulse is ON, output voltage decreases slowly but when the pulse is OFF, it again rises to its original position.

6.2.5.2. Relation of the Output Capacitor current, Inductor Current with the Pulse

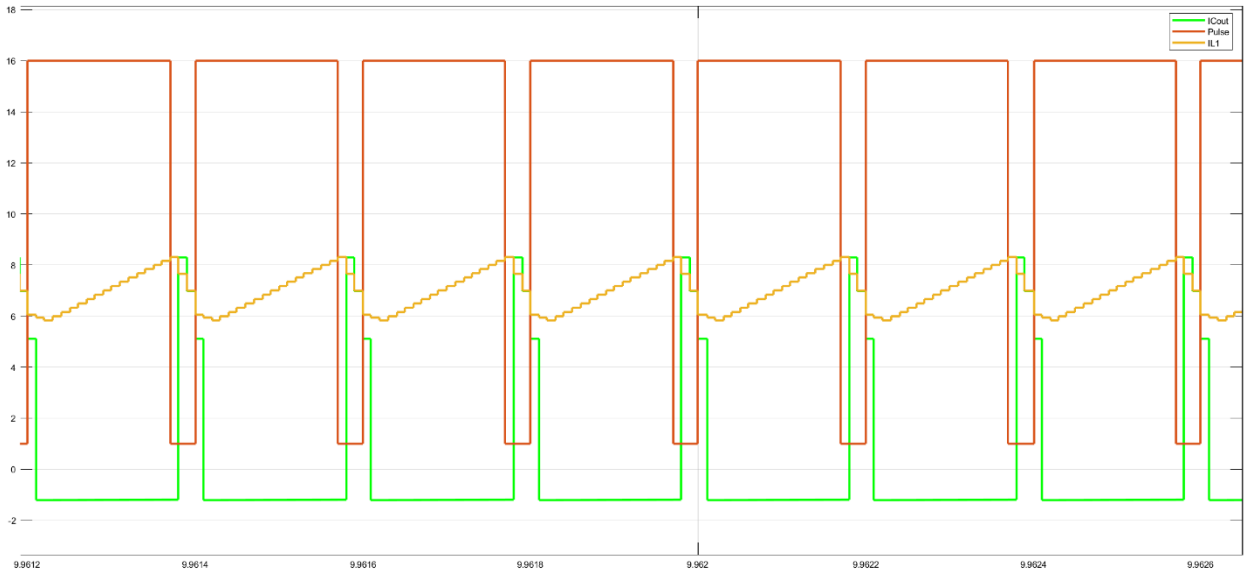

Figure 6.14: Graph of I_{Cout}, I_{L1} and Pulse

In figure 6.14, when the pulse is low, we can observe the capacitor is charging. The capacitor's current increases from around -1A to close to 8.1A as the voltage drops. When the pulse begins to rise, there is ripple and the capacitor starts discharging. It is observed that the current in the capacitor decreased compared to summer simulation. Moreover, Due to the lower frequency of the pulse, the current across the inductor reduces a little bit. As soon as the pulse intensity is increased, the inductor current begins to progressively increase. Furthermore, the current in the inductor also decreased if it is compared it with summer simulation.

6.2.5.3. Output Voltage

Figure 6.15: Graph of Vout

In the figure 6.15, we observe the output voltage has been degraded very largely when we analyzed our system for winter. The output voltage was around 30.3V. During winter the irradiance of the sun is very low compared to summer, as a result the output voltage that we have found is also very low compared to our result of the setup in summer conditions.

6.3 Simulation of Mathematical Model of SEPIC based MISO Converter

Following the development of a mathematical model of the conventional SISO SEPIC and the execution of a MATLAB/Simulink simulation, we revised the circuit to become a Modified MISO SEPIC and conducted a system analysis of the modified circuit. Figure 6.16 shows Mathematical Model of modified Dual Input SEPIC that have been designed.

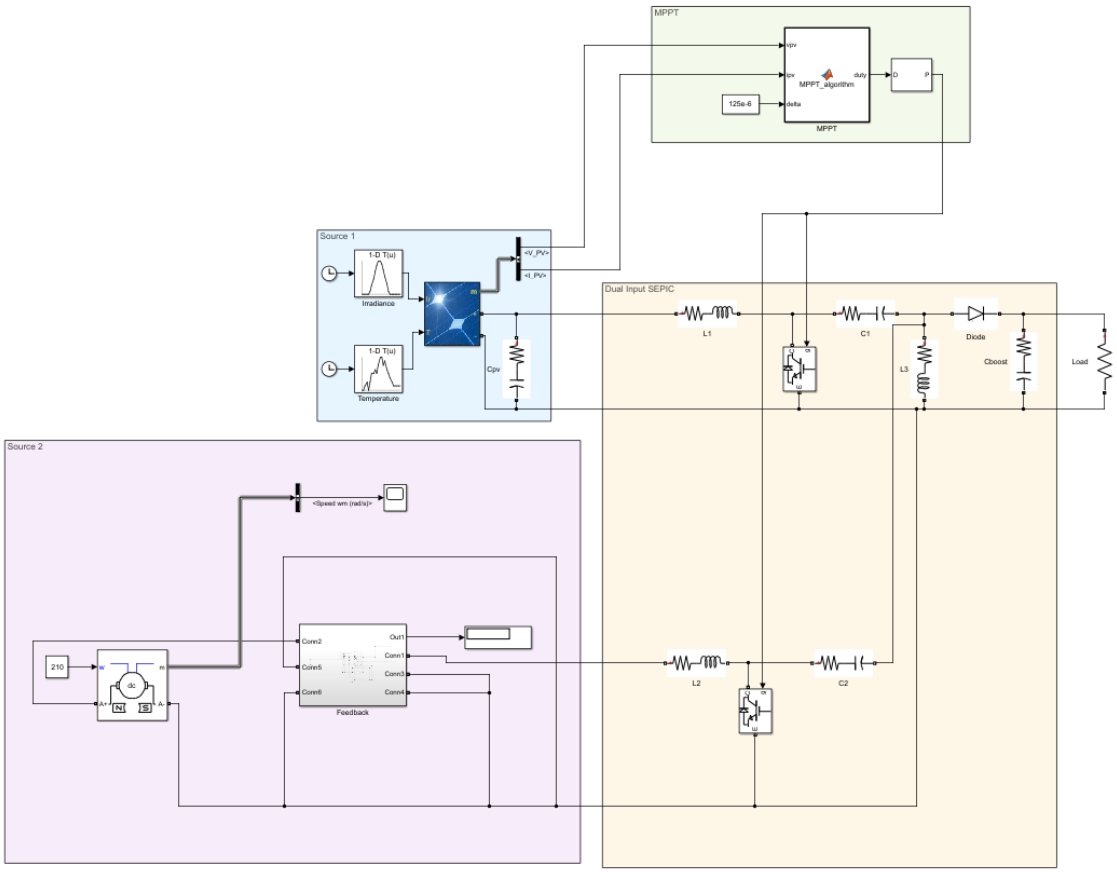

Figure 6.16: Mathematical Model of modified Dual Input SEPIC

6.3.1 Mathematical Model of the Bicycle Dynamo

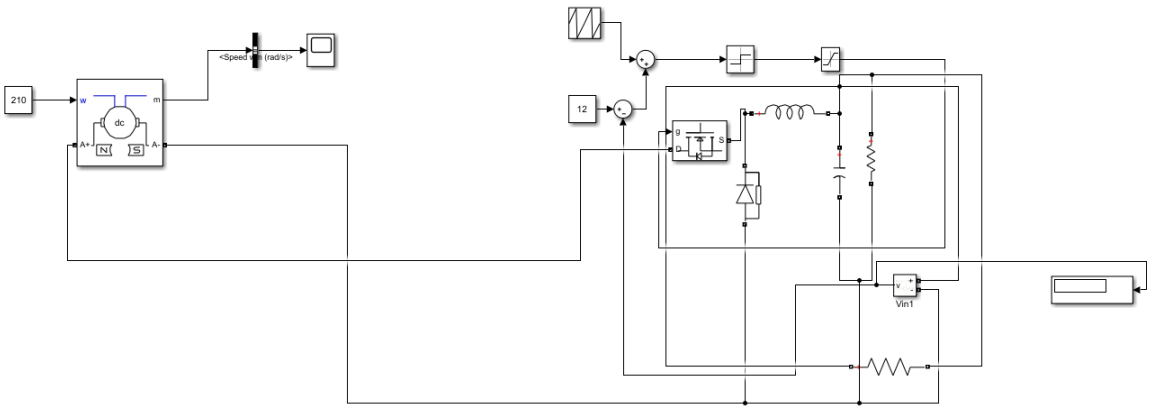

Figure 6.17: Mathematical Model of Bicycle Dynamo Generator

Figure 6.17 illustrates our second source of renewable energy, which is bicycle dynamo, we have developed the system in MATLAB/Simulink. For the dynamo portion, DC machine have been utilized and this DC machine will have permanent magnet inside so that there is no necessity for external voltage to induce flux. The DC machine is equipped with four pins. One of the pins will be utilized to provide input in the form of RPM. In our simulation, the rotating speed is expressed in rad/s, and there is an additional port for measuring parameters such as the rotational speed. The remaining two pins will be utilized to deliver electricity to the circuit that has been converted from mechanical energy. Since, the voltage that we get from the dynamo is directly related to the speed of rotation, the output voltage is highly variable and, in this situation, we need to stabilize it. We have created a feedback system that is integrated with a DC-DC converter in order to make it more stable. As seen in this system, the duty cycle of the converter's MOSFET fluctuates in response to the input voltage, and at its output the system provides a constant output that is then used as an input to our multiport SEPIC converter.

6.3.2 System Result of MISO system (Summer)

Result analysis part has been divided into two portions for Dual Input Multi Output SEPIC circuit where one portion is for summer and another one is for winter. In summer, we receive the solar heat most and so that solar irradiation is greater comparing to the winter season and also due to that efficiency of the PV panel is better in summer but our second renewable source Bi-cycle dynamo isn’t season dependent.

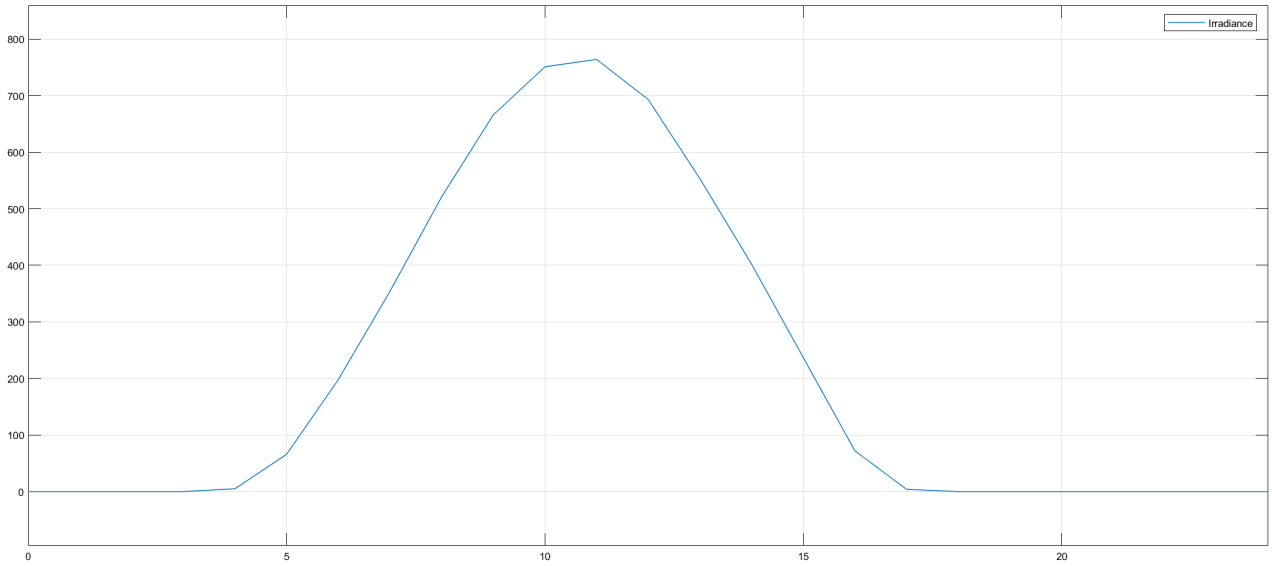

Figure 6.18:Graph of Solar Irradiance (summer) [x-axis(time-hours) and y-axis(irradiation)]

6.3.2.1 PV Voltage and Current

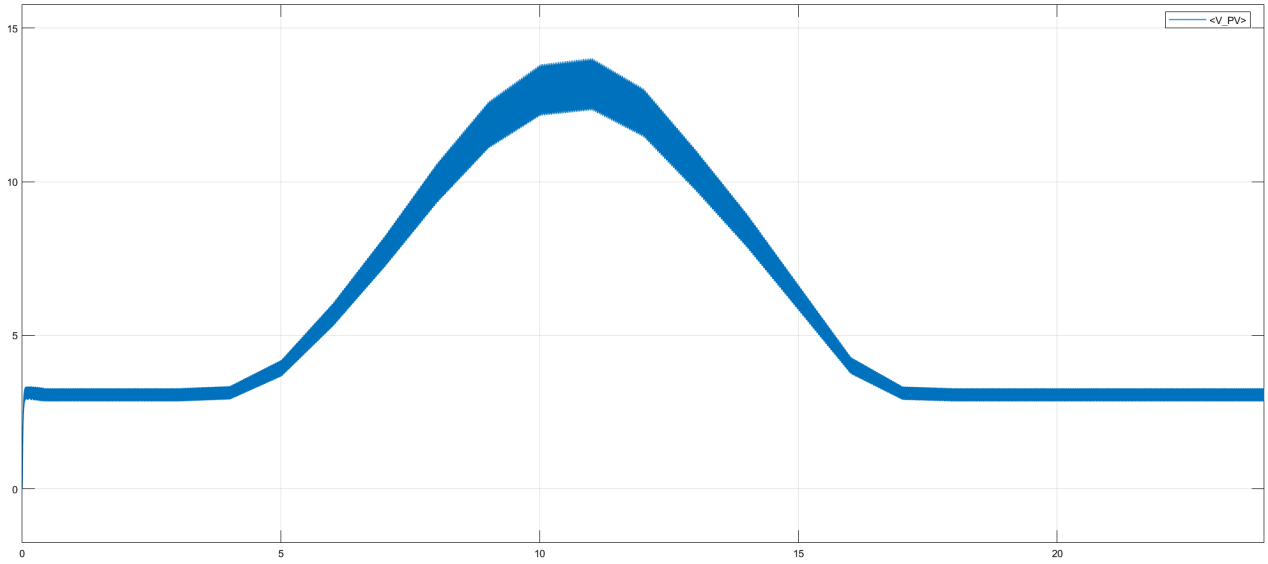

Figure 6.19: Graph of PV voltage (summer) [x-axis(time-hours) and y-axis (Volts)]

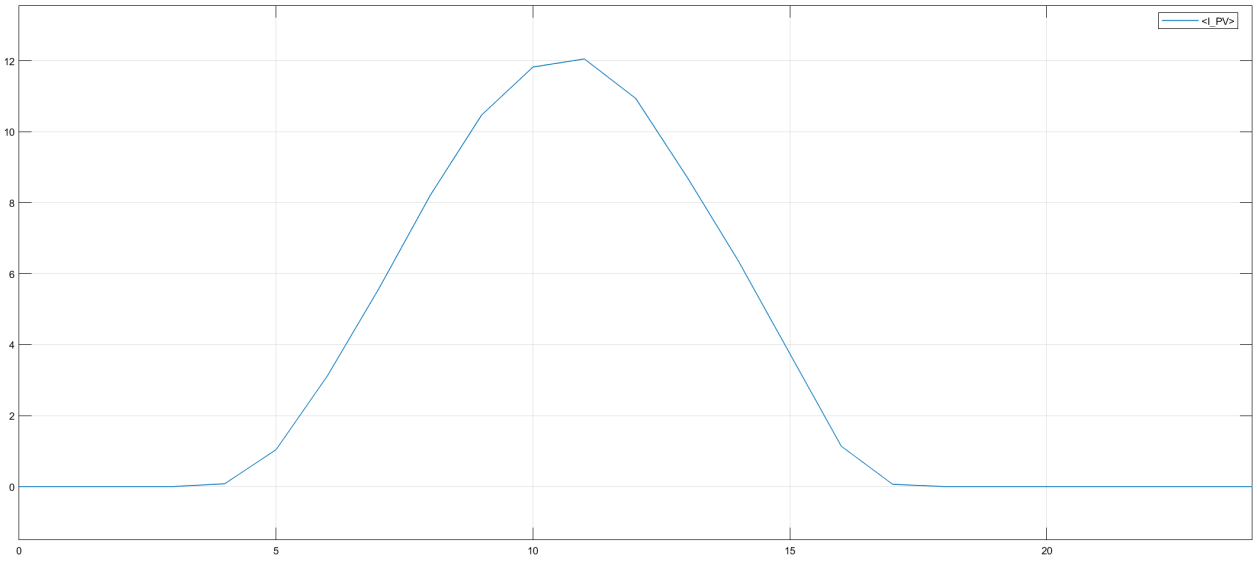

Figure 6.20: Graph of PV Current (summer) [x-axis(time-hours) and y-axis (Amperes)]

In the Figure 6.19 and 6.20 we see that in summer from 5am to 5pm we receive solar irradiance and that's why we have got output voltage and current from PV panel. At 12pm since the solar irradiance is highest also the output voltage from panel is highest.

6.3.2.2 Second source Voltage and Current

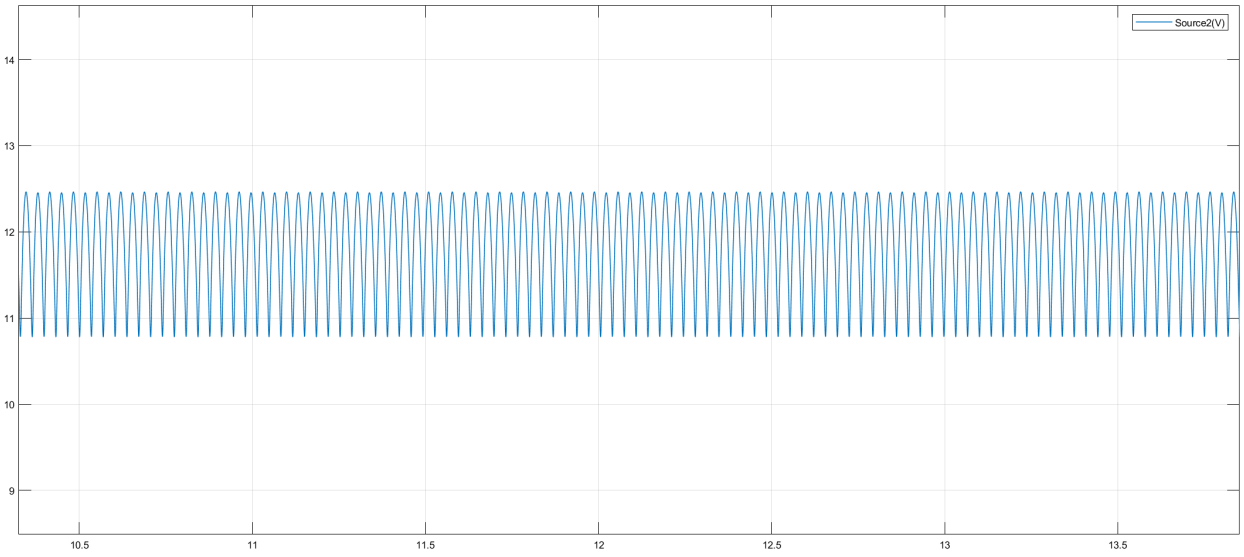

Figure 6.21: Graph of output voltage from second renewable source (summer) [x-axis(time-hours) and y-axis (Volts)]

After successfully implementing the mathematical model in MATLAB/Simulink, we have got our desired result from second renewable source appropriately which is shown in Figure 6.21. As mentioned earlier, there is no effect of solar irradiation unlike the solar PV panel and so that output from second source is almost constant with some ripple.

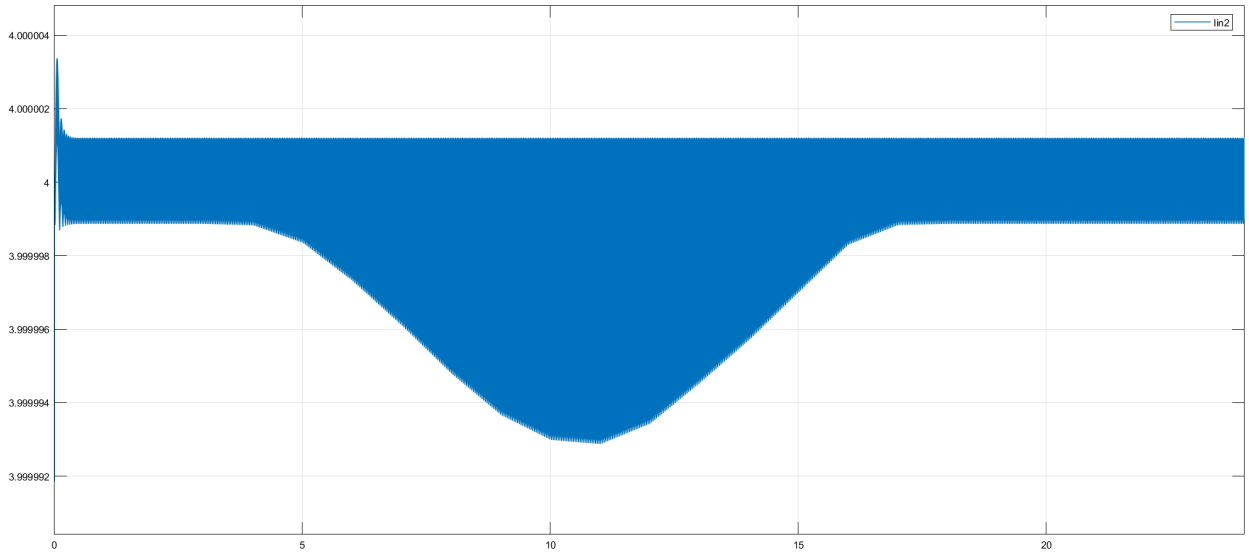

Figure 6.22: Graph of output current from second renewable source (summer) [x-axis(time-hours) and y-axis (Amperes)]

Current from second renewable energy is almost constant, but there is some change that can be seen in Figure 6.22 as we know from 5am to 5pm there is solar irradiation and due to this our PV panel supplies power to the circuit. So, current drawing from second source at that particular time is lower.

6.3.2.3 Output Voltage

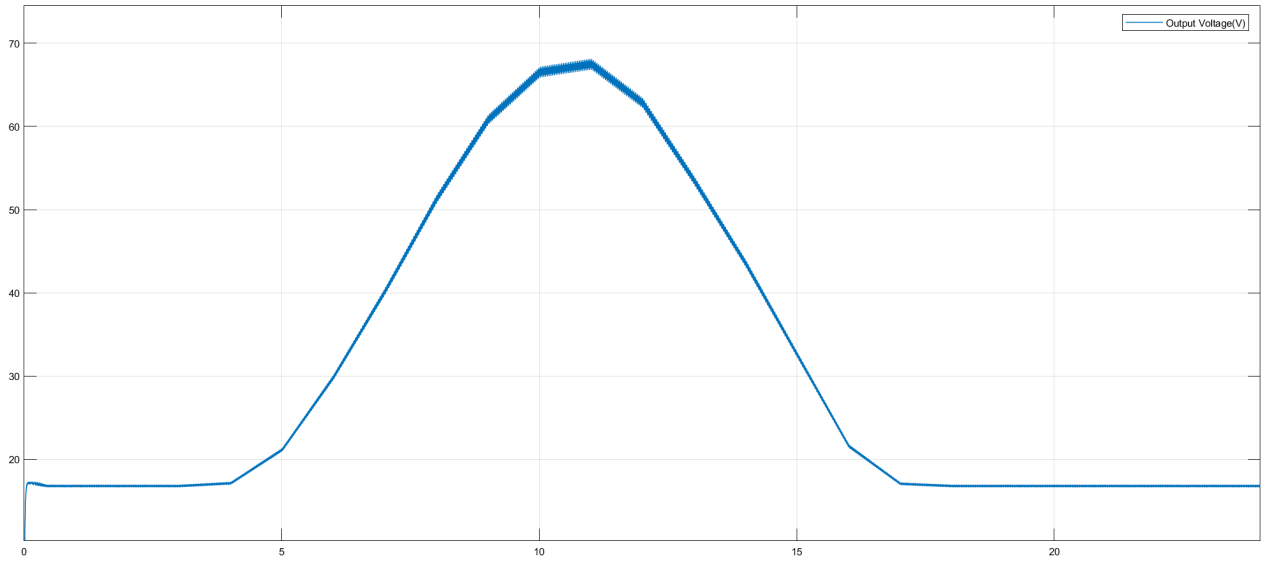

Figure 6.23: Graph of Output Voltage (summer) [x-axis(time-hours) and y-axis (Volts)]

It is shown in Figure 6.23 we see that at the time of solar irradiation, output voltage 68V we get is highest (12pm). When there is no solar irradiation, output voltage from the circuit is almost 18V. And, overall output current also changer with irradiation.

6.3.2.4 Output Current

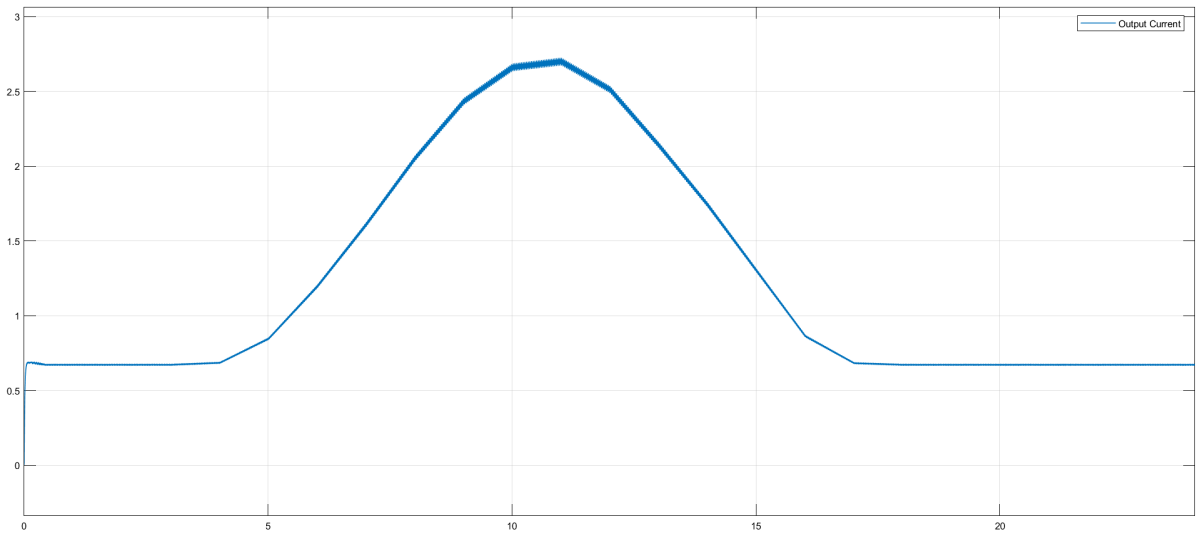

Figure 6.24: Graph of Output Current (summer) [x-axis(time-hours) and y-axis (Amperes)]

6.3.2.5 Output Power

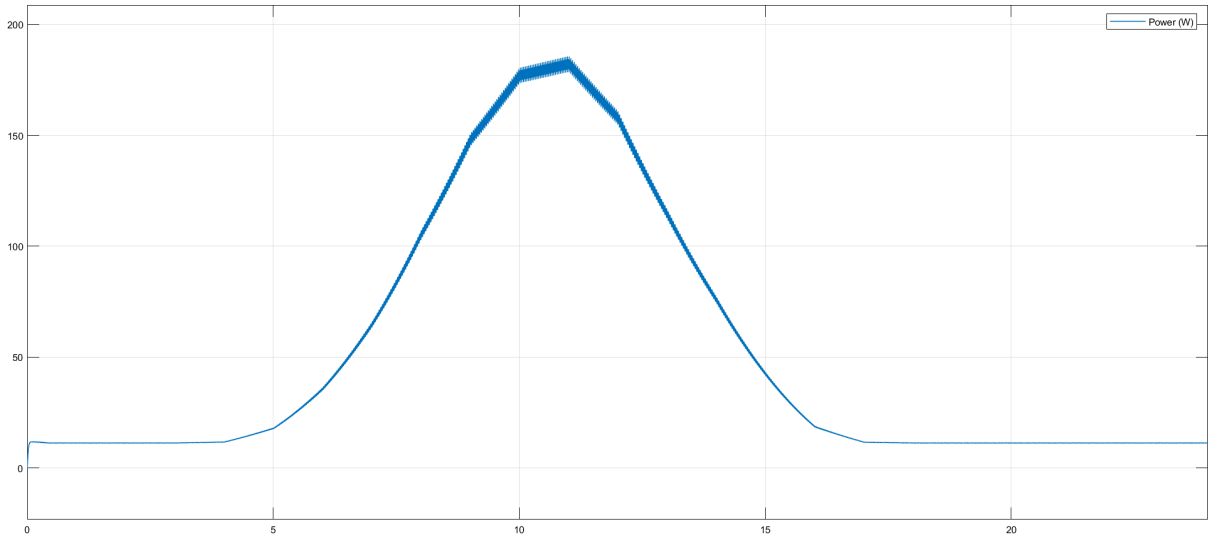

Figure 6.25: Graph of overall output power (summer) [x-axis(time-hours) and y-axis (Watts)]

Overall output power from our system at peak time of the day is almost 180W which is sufficient enough to run a DC fan or lit up DC lights

6.3.2.6 Current and Voltage waveforms for state of operation

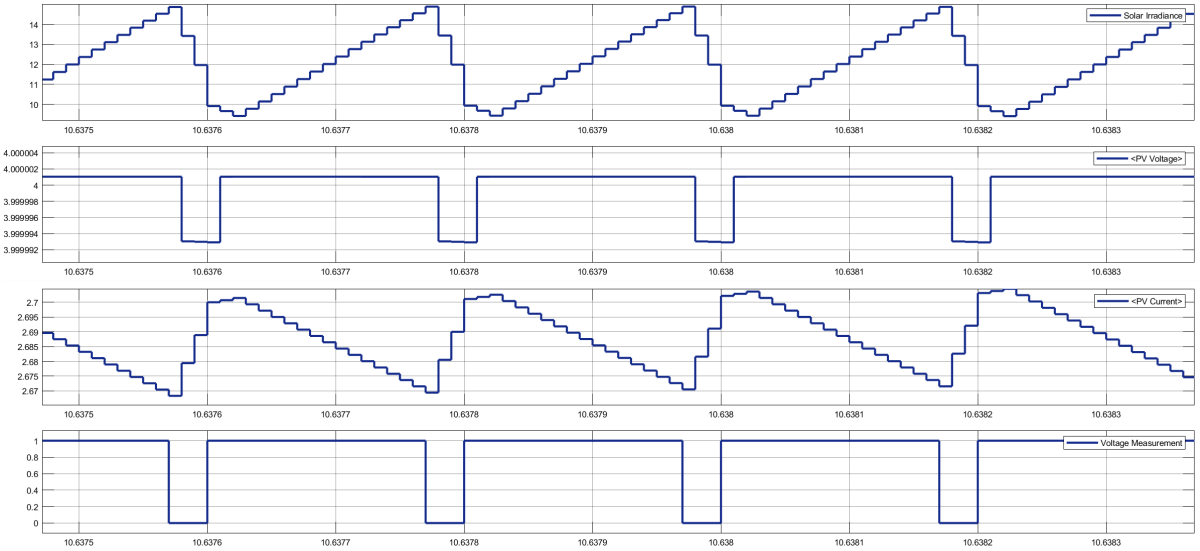

Figure 6.26: Current waveforms for state of operation

A variation in the current flowing through both inductors may be seen when the duty cycle is changed. Because of this, we can observe the ripple effect in the output current when we look at the Scope. Important to remember is that the duty cycle for both switches is the same, which is very important. The IL1 shows an upward ripple when the pulse is at its maximum level, as can be seen in the graph. When the IL1 reaches its maximum, the IL1 level rises from 12A to 14A on the scale. IL2, on the other hand, has a waveform that is comparable to the duty cycle and is near to 4A. The output current has a waveform that is diametrically opposed to the waveform of the IL1 that we can see.

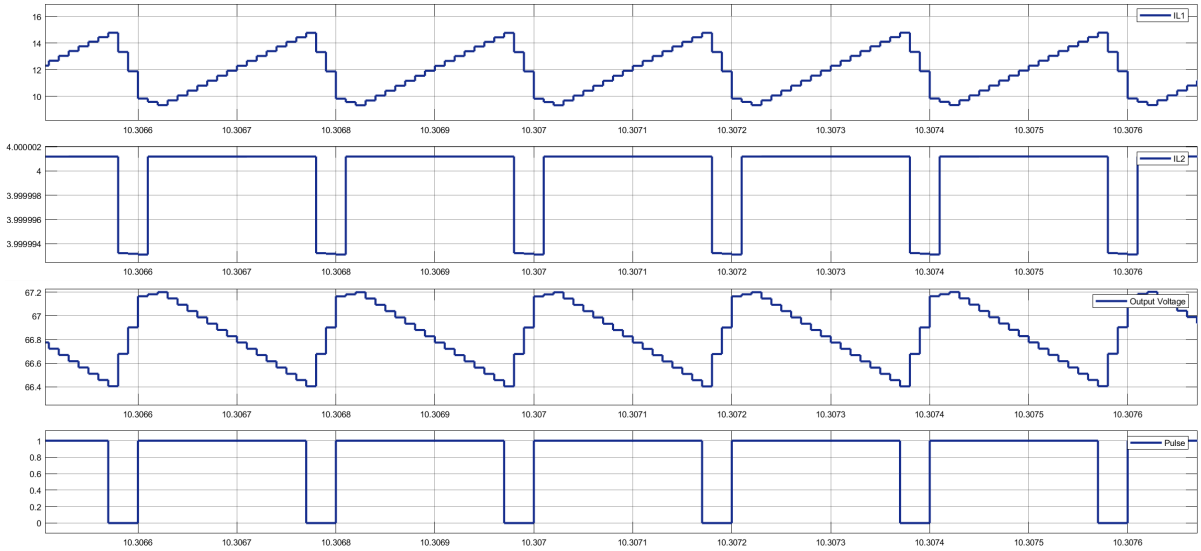

Figure 6.27: Current and voltage waveforms for state of operation

In conjunction with changes in the duty cycle, we can see a fluctuation in the current flowing through both inductors. As a result, we can see the ripple effect in the output voltage. Important to keep in mind is that the duty cycle for both switches is the same. We can see that the IL1 has an upward ripple when the pulse is at its highest level. When the IL1 reaches its maximum, it goes from 12A to 14A. Whereas IL2 have a similar waveform to the duty cycle.

6.3.3 System Result of MISO system (Winter)

At winter season, average solar irradiance is very much lower comparing to summer season and due to this output power also varies tremendously.

6.3.3.1. PV Voltage and Current

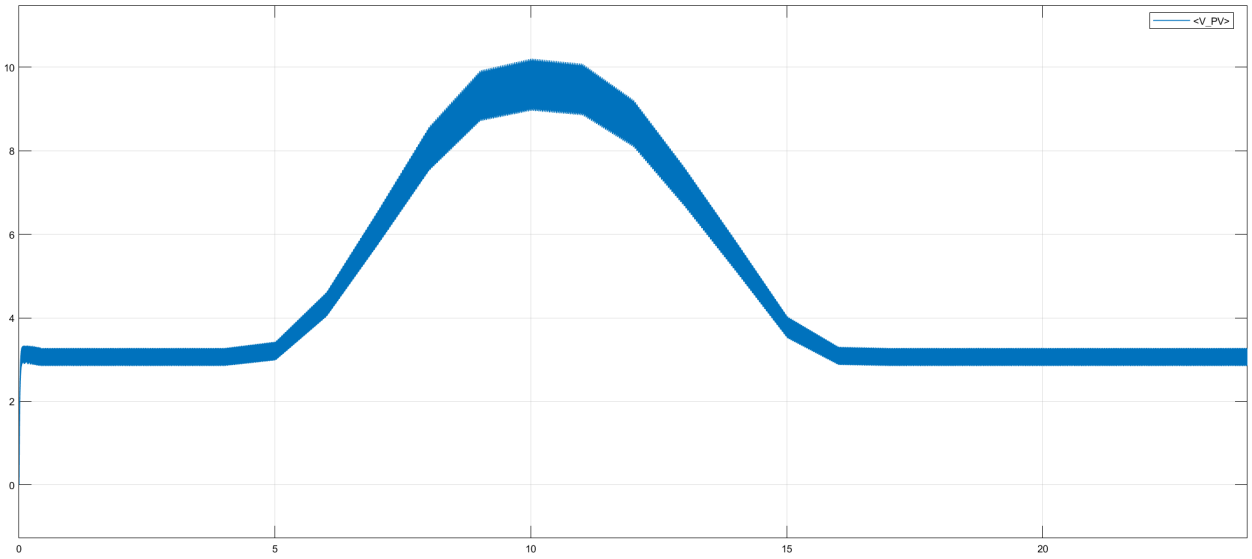

Figure 6.28: Graph of PV voltage (winter) [x-axis (time-hours) and y-axis (Volts)]

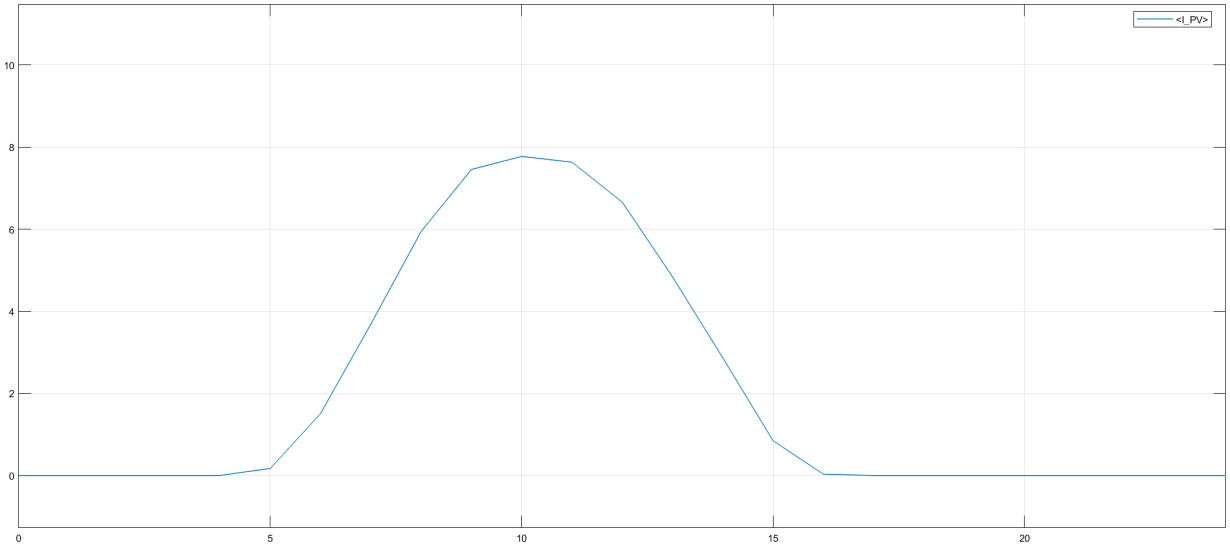

Figure 6.29: Graph of PV current (winter) [x-axis (time-hours) and y-axis (Amperes)]

Looking at the following graphs of voltage and current from PV panel, it can be said that since irradiation is lower than the summer one, voltage and current also lower here.

6.3.3.2. Second source Voltage and Current

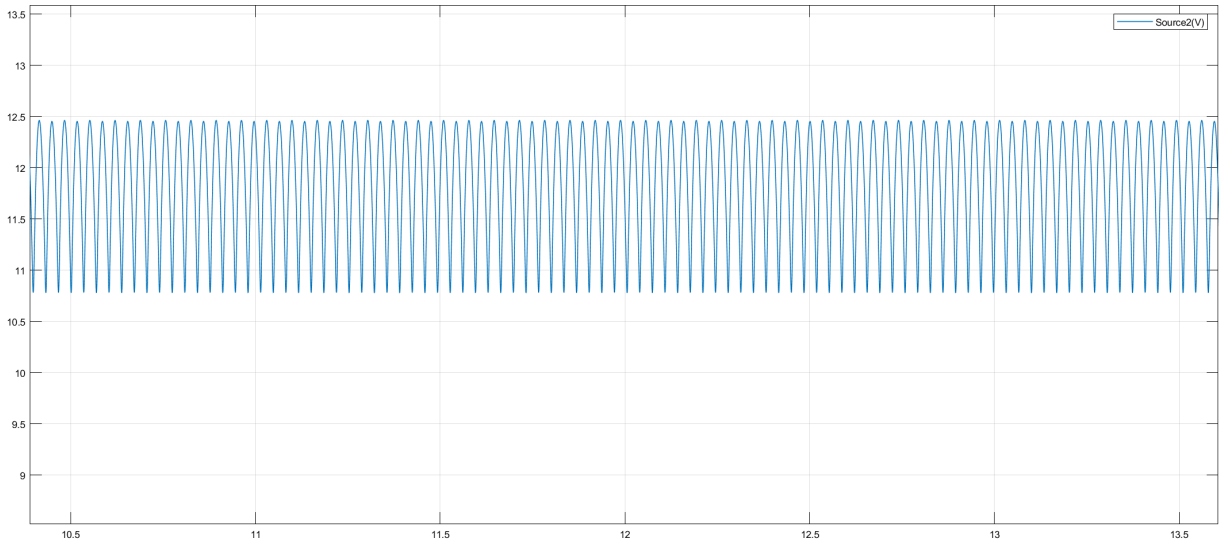

Figure 6.30: Graph of output voltage from second renewable source (winter) [x-axis (time-hours) and y-axis (Volts)]

Unlike the voltage and current from the PV panels, voltage and current from Bi-cycle dynamo is unchanged irrespective of the amount of solar irradiation the system has received.

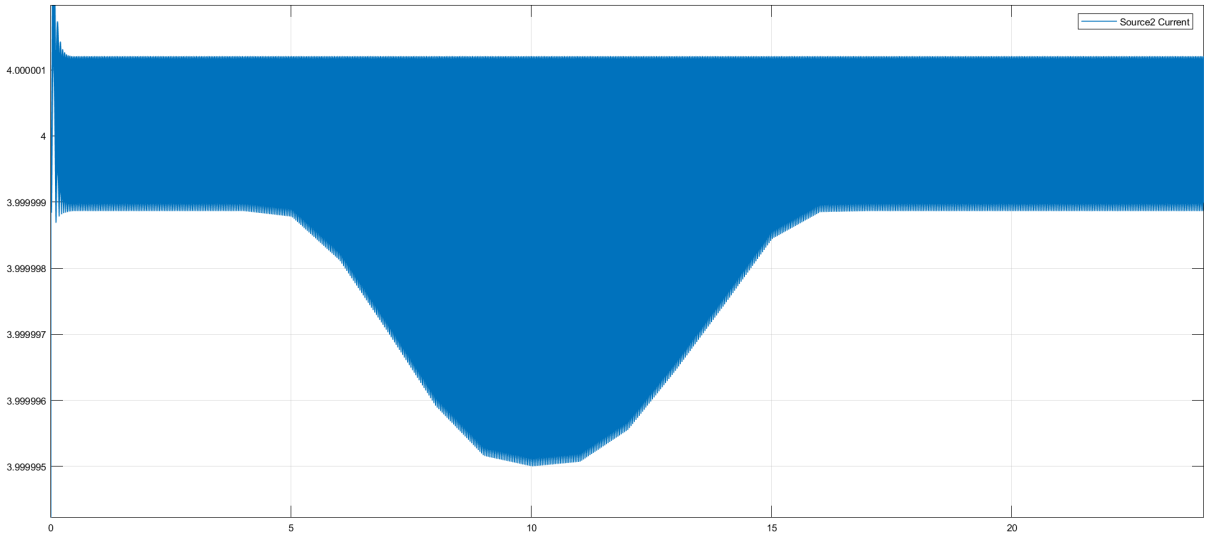

Figure 6.31: Graph of output current from second renewable source (winter) [x-axis (time-hours) and y-axis (Amperes)]

6.3.3.3. Output Voltage and Output Current

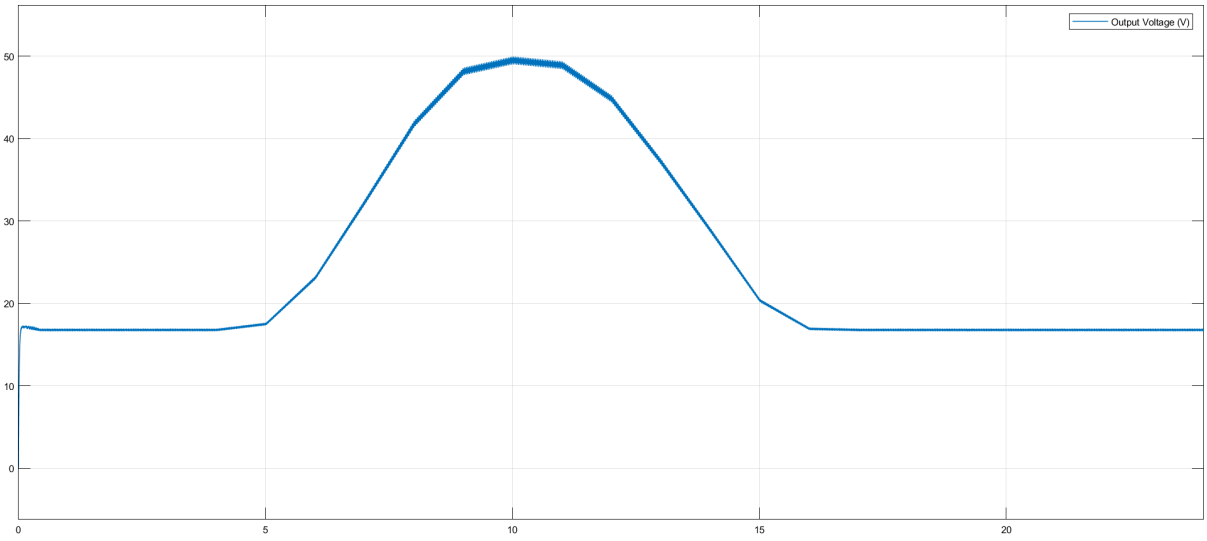

Figure 6.32: Graph of Output Voltage (winter) [x-axis(time-hours) and y-axis (Volts)]

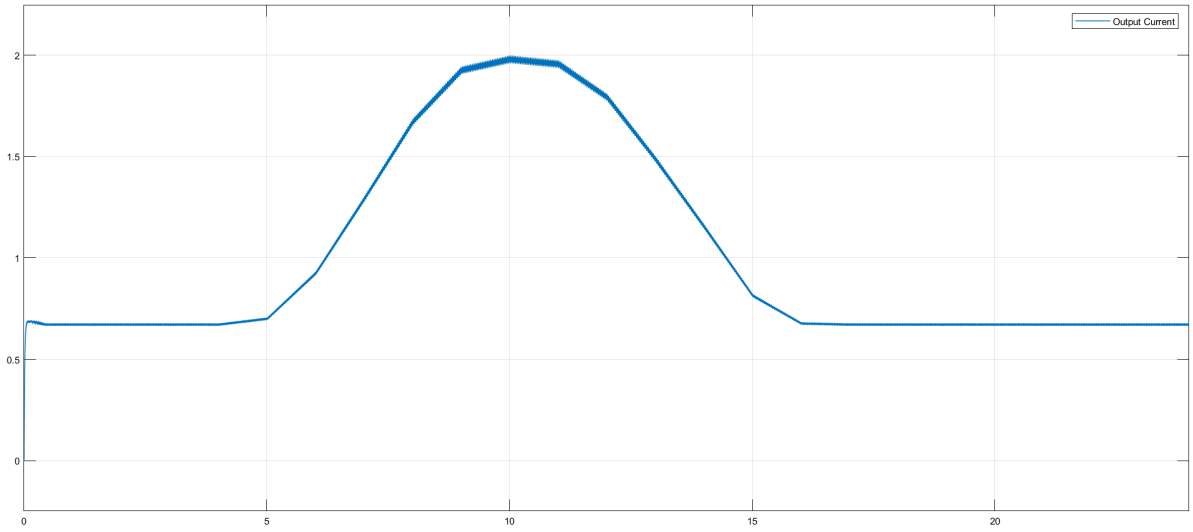

Figure 6.33: Graph of Output Current (winter) [x-axis (time-hours) and y-axis (Amperes)]

Comparing to the summer season, output voltage and current also degrades. Previously the output voltage was almost 68V but now in winter we are getting only 50V at peak and 2A

currents which was approximately 2.7A in summer. And because of these, overall output power which is P=VI falls significantly and in figure 6.34 the power is almost 100W.

6.3.3.4. Output Power

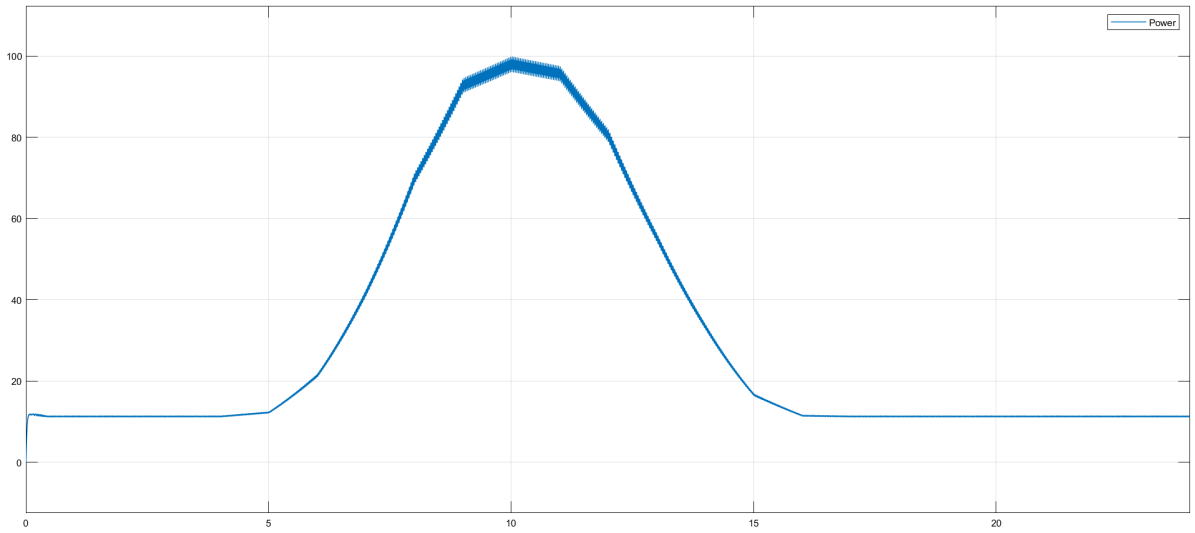

Figure 6.34: Graph of overall output power (winter) [x-axis (time-hours) and y-axis (Watts)]

6.3.3.5. Current and Voltage waveforms for state of operation

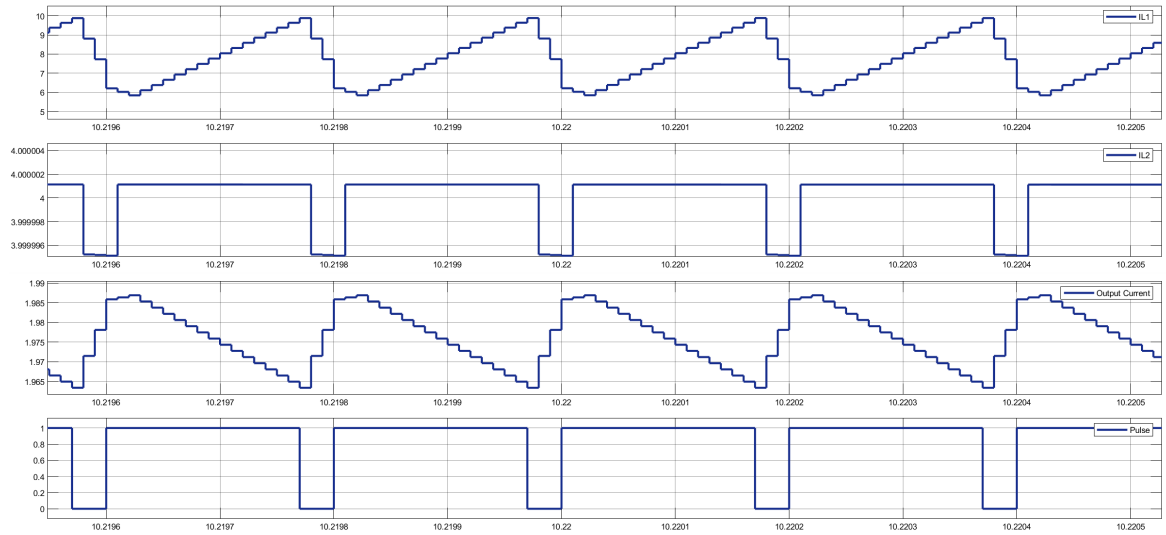

Figure 6.35: Current waveforms for state of operation

The current going through both inductors may vary when the duty cycle is altered, and this may be observed as a result. When we look at the output current with the Scope, we can see the ripple effect that has occurred as a result of this. It's critical to remember that the duty cycle for both switches is the same, which is very essential to know. As can be observed in the graph, when the pulse is at its greatest intensity, the IL1 exhibits an upward ripple in response. When the IL1 concentration reaches its maximum, the IL1 level on the scale rises from 7.5A to 10A. Il2 on the other hand has a waveform that is similar to the duty cycle and is close to 4A in power output. As we can see in the graph, the output current has a waveform that is diametrically opposite to the waveform of the input current (IL1). It is now closer to 2 amps, rather than the 2.5 amps it was throughout the summer months.

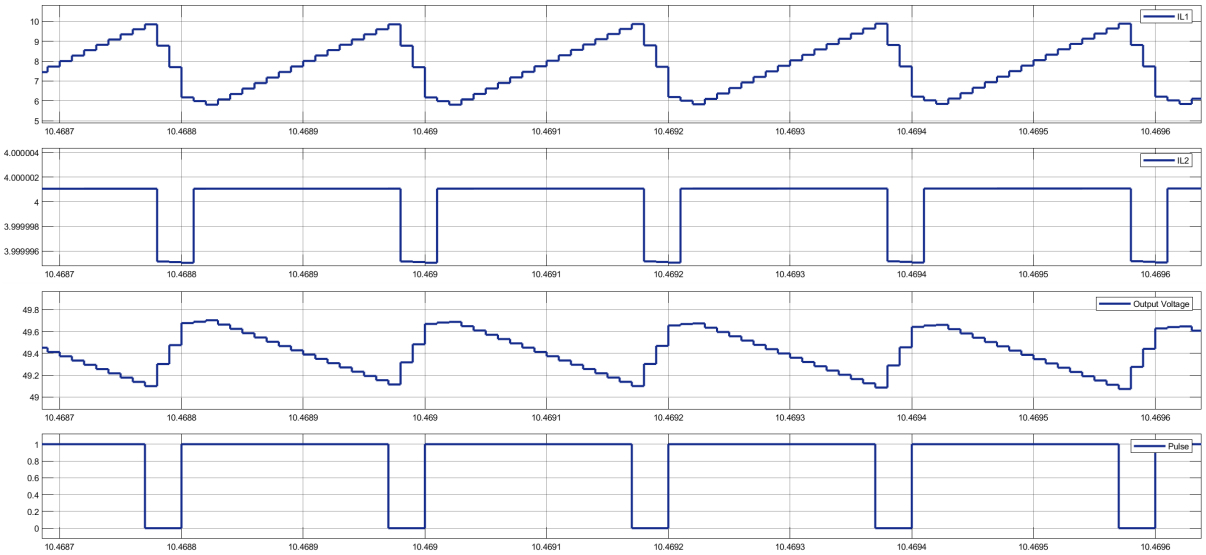

Figure 6.36: Current and voltage waveforms for state of operation

It is shown in Figure 6.36 a change in the current flowing through both inductors may be seen when the duty cycle is changed. Because of this, we can observe the ripple effect in the output voltage when we look at the voltage. Important to remember is that the duty cycle for both switches is the same, which is very important. The IL1 shows an upward ripple when the pulse

is at its maximum level, as can be seen in the graph. IL1 has a value that ranges from 7.5A to 10A at peak periods. IL2 on the other hand, has a waveform that is close to the duty cycle. Moreover, we can see the output voltage how gone lower compared to the output voltages in summer condition

Chapter 7 Practical Field Test and Result Analysis

7.1 Introduction

The SEPIC converter is supplied with a static power from the AC220V-to-DC12V 2A Switching Power Supply module. The input voltage reading was DC12.22V. We used it as an alternative to the PV panel, which will supposedly give similar voltage reading. The SEPIC converter has the capability of either lowering or raising the input voltage. The boost converter mechanism has been incorporated into our project. As a result, the output voltage will increase considerably from its current value of 12.22V. From the field test analysis, we have discovered that the voltage varies between 10.8V to 68V roughly in our experiment. Capacitors may be used as filters in certain situations. Due to the fact that the microcontroller needs 5V of power, we have interfaced a DC12V-to-DC5V regulator to convert the 12.22V DC to a reasonable value of 5V DC. Thus, this voltage has been used to power up the ArduinoUNO microcontroller. We have used a SR540 Schottky Barrier Rectifier diode to curb the voltage drop when it is conducting a forward current [28]. The microcontroller's pin 3, which is a PWM pin, is linked to the gate of the MOSFET, causing it to turn on continuously. The output voltage of the SISO SEPIC converter circuit has been shown in a tabular format. The output voltage was measured with the help of a digital multimeter by varying the 100k potentiometer knob. The potentiometer is basically used to vary the duty cycle of the pulse to the gate of the MOSFET. The potentiometer was controlled manually. As a load, we have used a 10W rated spotlight. In the output side, the resistor that we have used is of 320Ω. Using lower resistor is not feasible. Because, the resistor generates more heat and gets burned during the period when a large voltage is generating at the output side and forcing a large current to flow through the resistor. The two coupling capacitors have been used as rated 47uF respectively. We have used handmade inductor coils assumedly rated at 600uH-630uH each. The secondary coil at the output side was a Ferric Core and Double E-core Flyback Inductor. The initial inductor coil is

a handmade mini inductor coil. We have implemented the circuit in the Veroboard because it has proper holes to mount the heatsink. We previously implemented the SEPIC based SISO converter circuit in a general breadboard. Since, we are using a MOSFET to drive by the switching mode. While implementing the circuit in a breadboard, the continuous switching mode operation of the MOSFET generated a huge current through it. Even though we had used a heatsink in the breadboard, our MOSFET got burned up and dissipated a huge power as heat, resulting a damaged breadboard. That's why we have opted into implementing the circuit in the Veroboard after performing multiple cross-check simulation with the Proteus software.

In this section, two photos have been attached representing the SEPIC based SISO converter circuit topology.

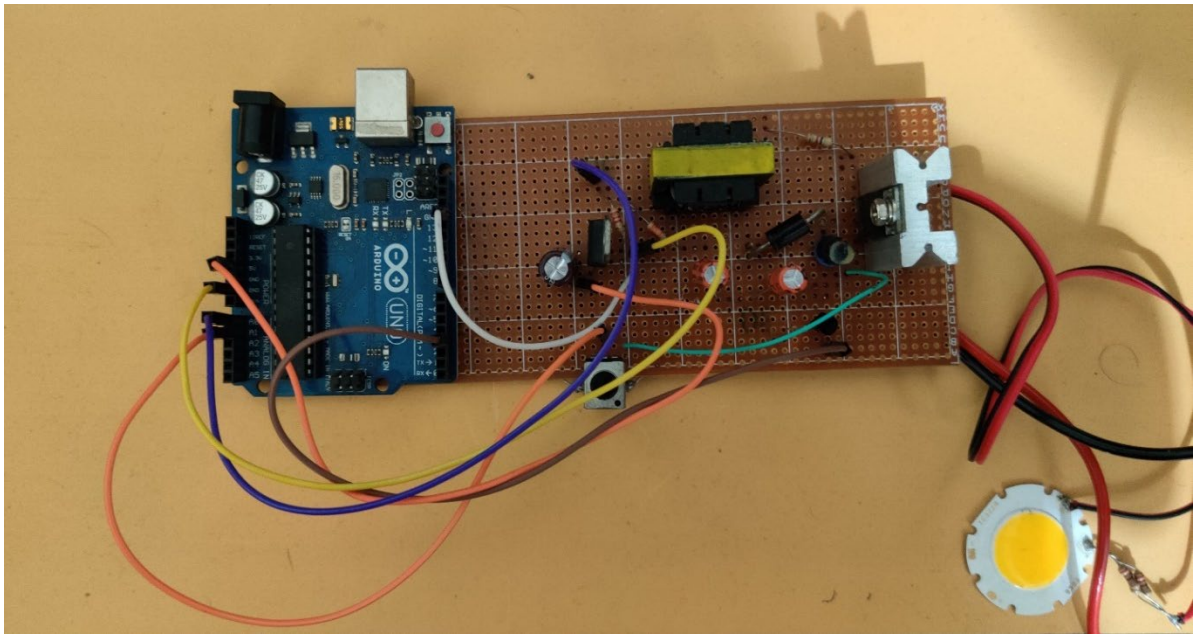

Figure 7.1: Top View of Circuit Setup

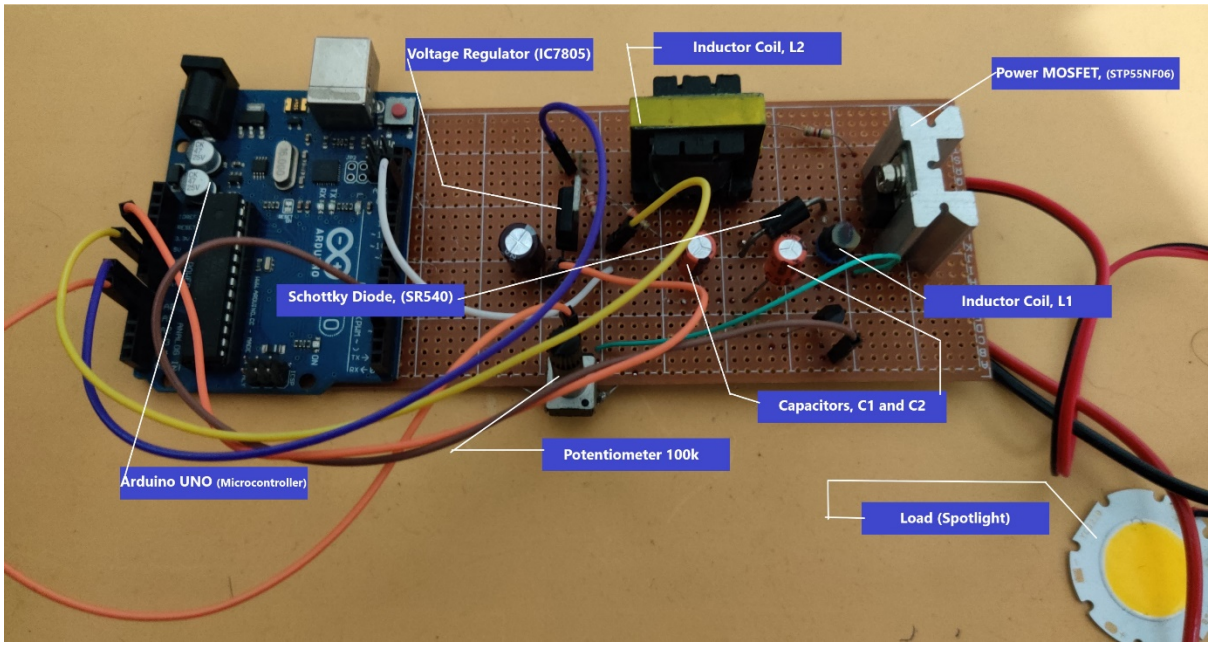

Figure 7.2: Close View of Circuit Setup

7.2 Hardware Implementation and Design Consideration of the SEPIC based SISO Converter Circuit

7.2.1 Components for the SEPIC based SISO Converter Circuit

The following components make up the SEPIC converter's hardware design:

1. **Gate Driver Circuit:** The S8050 is the primary component utilized in the design of the gate drive circuit. The S8050 N-P-N transistor is a general-purpose transistor that is well suited for performing modest and general jobs in electrical circuitry. It may be used as a switch in electronic circuits to switch on various loads, and as a result, it may be utilized in IGBT or power MOSFET applications [29]. A further important characteristic is that it offers electrical isolation between the power circuit and the microcontroller power board or the control circuit of the SISO converter. As a result, the power circuit is protected against surges coming from the supply side.

2. **Microcontroller:** Arduino Uno is a microcontroller that is based on the ATmega328P microcontroller chip [30]. Among its features are 14 digital input/output pins, 6 analogue inputs, a 16MHz quartz crystal, a USB connection, an external power supply connector, an ICSP header, as well as a reset button. The ArduinoUno board is required in this case in order to provide switching pulses to the gate drive circuit, which in turn supplies power to the MOSFET [18]. The duty cycle of the converter is controlled by a 100k potentiometer, and the programmed code is uploaded into the microcontroller. We have set a frequency of 32kHz by using the Timer 2 register and its corresponding values (Following the completion of the connections, the input of the S8050 is linked to one of the fourteen analogue pins on the Arduino and that is pwm pin 3.

3. **Power Circuit:** The SEPIC converter, which consists of two inductors (L_1 and L_2), serves as the power supply in this case. The L_1 inductor is linked to the source side of the circuit, while the L_2 inductor is attached to the coupling capacitor side of the circuit. In this circuit, two capacitors are used: an output capacitor and a coupling capacitor. There is an output Schottky barrier diode and a switch in this circuit; the STP55NF06 is used (power MOSFET). This MOSFET has lower heat dissipation in terms of general N-channel MOSFETs.

4. **DC Voltage Source:** The STP55NF06 MOSFET receives its DC supply from the AC220V-to-DC12V 2A Switching Power Supply module.

7.2.2 Hardware Result

Table 7.1 illustrates the parameters of the components used for the practical field test of the SEPIC based SISO Converter Circuit

SL no	Parameter	Experimental Value
1.	V_{in}	12.22 V
2.	V_{out}	57 V (adjusted)
3.	Load Resistance	320 Ω
4.	Duty Cycle	82.3%
5.	I_{L1}	0.68 A
6.	I_{L2}	0.08 A
7.	Switching Frequency	32 kHz
8.	Load	11 W
9.	I_{load}	0.18A
10.	$I_{load(max)}$	0.21A
11.	I_{C1}	0.67A
12.	I_{C2}	0.43A

Table 7-1: Hardware Parameters of SEPIC based SISO

7.2.2.1 Voltage Gain of the SEPIC based SISO Converter Circuit

Due to the fact that we built a boost integrated SEPIC DC-DC converter. For our case, the converter will act as a boost integrated converter if the duty cycle is over 50%. On the other hand, the duty cycle is less than 50%, the output voltage is lower than the input voltage, resulting in the conversion becoming a buck converter [46]. Various duty cycle variations of

the switch's control pulse have been carried out for D = 0.50 to 0.85, and the value of the converter's voltage gain have been presented and tabulated in Tables 7.2.

Duty Cycle	**V_{in} (V)**	**V_O (V)**	**V_{gain} (V_o/V_{in})**
0.5	12.22	12.22	1
0.55	12.22	14.92	1.220949264
0.553	12.22	15.12	1.237315876
0.6	12.22	18.27	1.495090016
0.65	12.22	22.7	1.857610475
0.7	12.22	28.4	2.32405892
0.75	12.22	36.7	3.003273322
0.79	12.22	48.6	3.977086743
0.809	12.22	52.0	4.255319149
0.812	12.22	52.8	4.320785597
0.82	12.22	55.6	4.549918167
0.823	12.22	57.0	4.664484452
0.83	12.22	59.8	4.893617021

0.84	12.22	64.1	5.245499182
0.847	12.22	68	5.564648118

Table 7-2: The Value of Voltage Gain with changing Duty Cycle for the SISO SEPIC

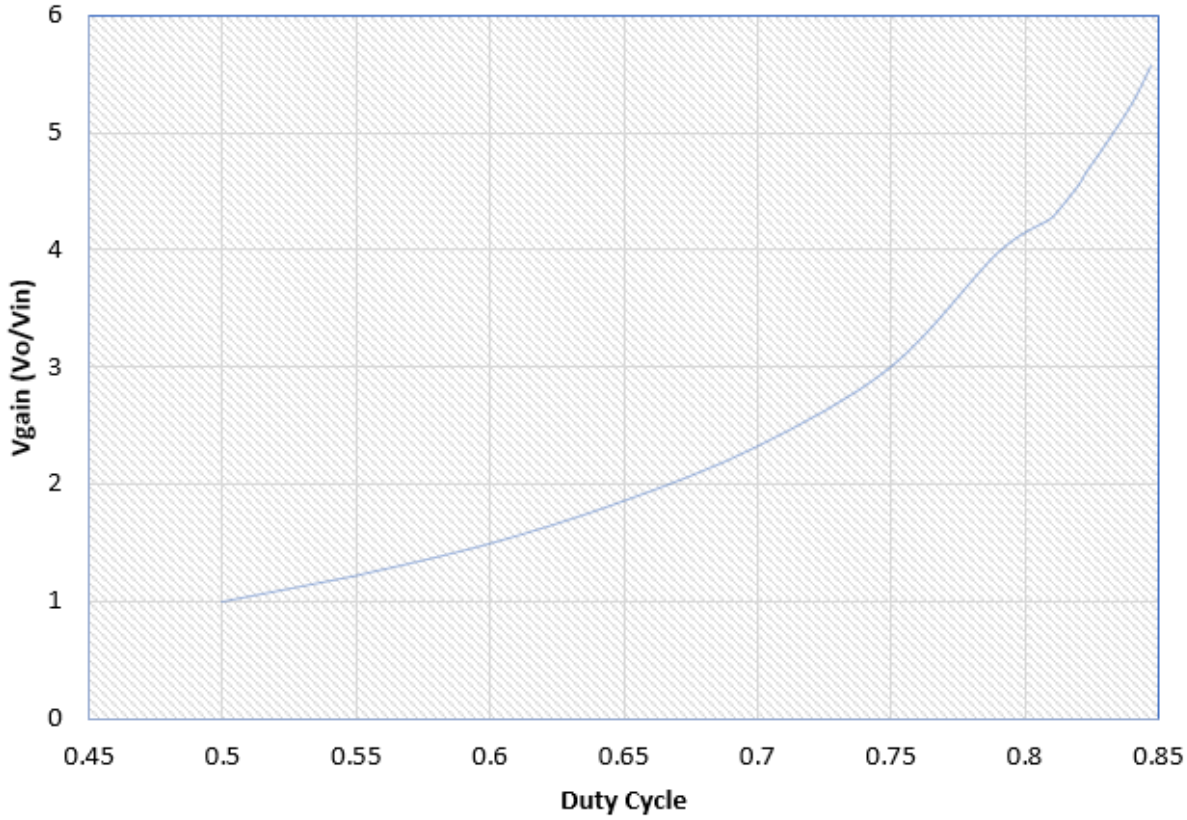

Figure 7.3: Characteristics Curve Gain Vs Duty Cycle for SISO SEPIC

The basic ratio of a system or circuit's output voltage to its input voltage, as we all know, is known as its voltage gain. If the input voltage is a certain value, it specifies the maximum amount of output voltage that may be produced by the device. The duty cycle of a load or circuit is the ratio of the total time the pulse remains high over the time the pulse remains low. The duty cycle, also known as the "duty factor," is represented as a percentage of the total time

spent ON. We will show the exact same analysis for the SEPIC based MISO topology in the next sections.

As shown in Table 7.2 and illustrated graphically in Figure 7.3, the findings of the practical field tests demonstrate that the voltage gain (Vo/Vin) of the converter increases with an increase in the duty cycle of the converter. As soon as the duty cycle reaches 0.847, the voltage gain reaches a maximum of 5.57 is used as the equation for the output voltage.

$$D = \frac{V_O}{V_O + V_S}$$

In theory, when D is greater than 0.5, the Voltage Gain must be greater than 1 up to infinity, which is demonstrated by our results.

7.2.2.2 Efficiency of the SEPIC based SISO Converter Circuit

A number of duty cycle changes of the switch's control pulse have been carried out for D=0.50 to 0.85, and the value of the converter's efficiency has been determined, which is listed in Table 7.3.

Duty Cycle	**V_{in} (V)**	**I_{in} (A)**	**P_{in} (W)**	**V_{out} (V)**	**I_{out} (A)**	**P_{out} (W)**	**Efficiency $\left(\frac{P_{out}}{P_{in}}\right)$**
0.5	12.22	0.65	7.943	12.22	0.038	0.46436	0.05846154
0.55	12.22	0.66	8.0652	14.92	0.04	0.5968	0.07399693
0.553	12.22	0.66	8.0652	15.12	0.047	0.71064	0.08811189
0.6	12.22	0.68	8.3096	18.27	0.057	1.04139	0.12532372
0.65	12.22	0.69	8.4318	22.7	0.07	1.589	0.18845324
0.7	12.22	0.71	8.6762	28.4	0.089	2.5276	0.2913257

0.75	12.22	0.79	9.6538	36.7	0.114	4.1838	0.43338375
0.79	12.22	1	12.22	48.6	0.151	7.3386	0.6005401
0.809	12.22	1.14	13.9308	52	0.16	8.32	0.59723778
0.812	12.22	1.16	14.1752	52.8	0.165	8.712	0.6145945
0.82	12.22	1.23	15.0306	55.6	0.173	9.6188	0.63994784
0.823	12.22	1.29	15.7638	57	0.18	10.26	0.6508583
0.83	12.22	1.34	16.3748	59.8	0.19	11.362	0.69387107
0.84	12.22	1.51	18.4522	64.1	0.2	12.82	0.6947681
0.847	12.22	1.63	19.9186	68	0.23	15.64	0.78519575

Table 7-3: The Value of Efficiency with changing Duty Cycle for the SISO SEPIC

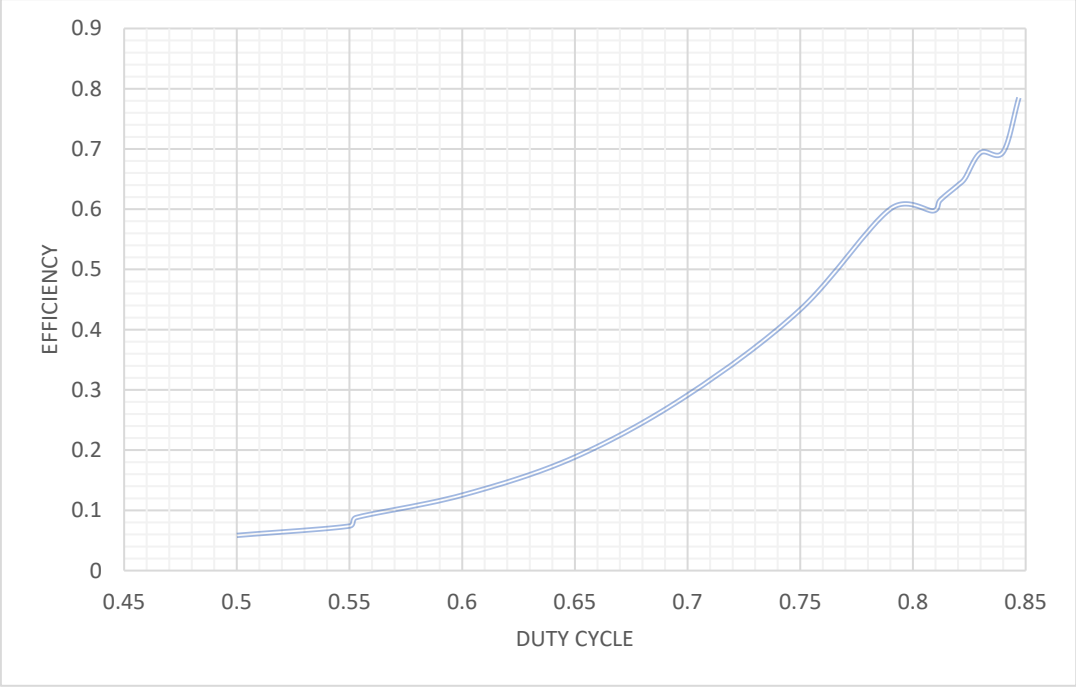

Figure 7.4: Characteristics Curve Efficiency Vs Duty Cycle for SISO SEPIC

Electrical energy efficiency is defined as the decrease in the amount of power and energy required by the electrical system without interfering with the regular operations of buildings, industrial facilities, or any other transformation process in any way. Practical field tests have shown, as stated in Table 7.3 and graphically depicted in Figure 7.4, that the efficiency of the converter improves when the duty cycle of the converter is increased. At 0.847, the voltage gain reaches a maximum of 0.785. The efficiency of our practical DC-DC converter is shown in the graph above, while the efficiency of an ideal DC-DC converter is 100 percent or unity, as is the case with the SEPIC converter.

7.3 Hardware Implementation and Design Consideration of the SEPIC based MISO Converter Circuit

We have shifted from the SISO topology towards the proposed MISO topology because its cost-effective, reliable, flexible and feasible in terms of incorporating multiple variable input sources. The hardware implementation of the proposed model was carried out in consideration of the fact that, the two renewable sources will generate sufficient DC power and that power will be stored into a DC12V 7.5Ah battery during the charging phase. This battery can work as a backup and the output of this battery is boosted up to 53.3V using the SEPIC converter circuit. That reading of the source at the output end of the battery was 12.1V. Although, we have initially proposed that there will be no battery connected with the two sources. But this secondary design approach has been addressed in the simulation analysis of our proposed model where we have shown the detailed impact on the system due to not incorporating a battery to be connected with the two sources. In the simulation analysis, we have considered Source-I as a PV panel with varied voltages due to changes in solar irradiance at different times of the day as well as Source-II as a stabilized output from the bicycle dynamo using a feedback-

controlled block diagram. For our target group, the rural people in the distant islands are mostly deprived of the power from the national grid. They don't have easy access to power during the night time. This is why we felt that if the power is not stored for usage at a later period, the rural people will not be able to get the best out of this proposed project. However, for the accomplishment of a successful study, we have also discussed the secondary design approach of this MISO topology within this section regardless of the fact that we could not implement that due to time-limitations and the additional challenges emerged out of the COVID-19.

For the primary design approach of the hardware implementation, when battery is connected with the two sources, we have used handmade L1 and L2 inductor coils rated at approximately 600uH. Then we have used another coil (Ferric Core and Double E-core Flyback Inductor), L rated an approximate value of 615uH at the output side of the power circuit. Both the source output is 12.1V and they were further fed into the MISO topology. The duty cycle of this design approach was calculated at 81.4% through a reverse calculation once we got the optimum output of 53.3V. The two MOSFETs were switched using the Arduino ProMini at the exact same duty cycle. The frequency was set to 32kHz, just like the SISO topology. We have used a 3 Amp diode 5408, two MOSFETs IRF540, an N-P-N transistor of S8050 as the gate driver circuit of the proposed system. The load is again a 10W spotlight. The load resistor we have used is 282Ω. To control the ripple effect, large coils have been incorporated in this circuit. Likewise, the SISO SEPIC converter circuit, we have also implemented the MISO circuit in a Veroboard. To power up the Arduino, we have used an IC7805 DC12V-DC5V voltage reugulator. We have developed a reverse polarity protection circuit using bridge rectifier. At the load end, we have connected a digital DC Volt-meter. We have used a 100k potentionmeter. Alongside, A switch has been incorporated to either open the circuit or short the circuit.

For the primary design approach, we split the approach into two phases. In the first phase, for testing purposes, we didn't incorporate the Source-II as our input because the Source-II was

actually in one of our thesis member's house and it was quite hard for us to collect the source within a short time. Rather, we took an alternative to the Bicycle Dynamo Generator that is an AC220V-to-DC12V 2A Switching Power Supply module.

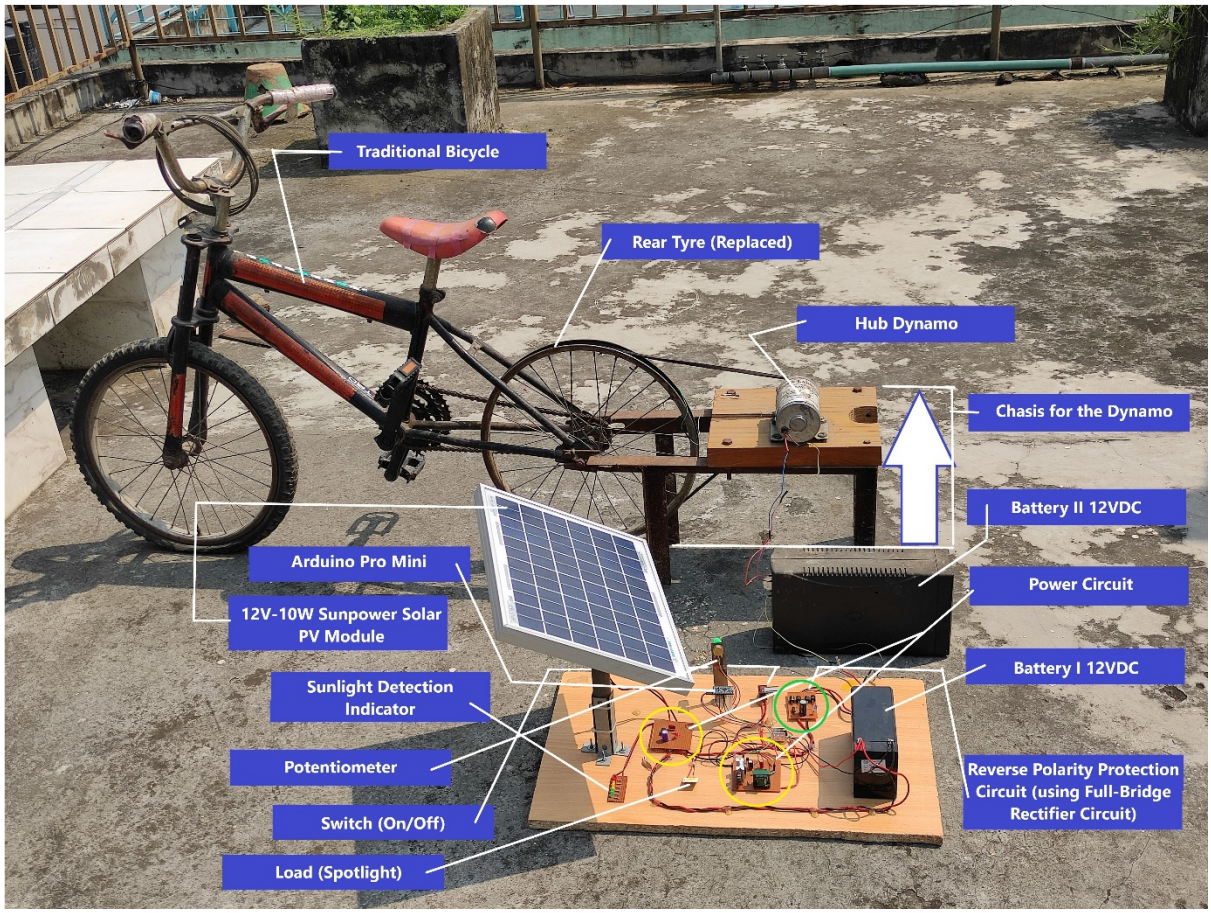

Figure 7.5: Circuit Setup of the Dual Input SEPIC Converter

In the next phase of the primary design approach, we have incorporated the MISO topology with a Solar Panel and a Bicycle Dynamo which is shown in Figure 7.5. A rigorous field-test has been performed on the day of 25th September. The data has been discussed in the upcoming sections.

Figure 7.6: Circuit Setup of the Dual Input SEPIC Converter with a Bicycle Dynamo as the second source

Now, to implement the secondary design approach (without adding a battery that was supposed to be connected to the two sources), we can actually control the system based on these two expressions –

a. When ($V_2 > V_1$), $V_0 = \frac{D2*V2+Deff*V1}{1-D1}$

b. When ($V_1 > V_2$), $V_0 = \frac{D1*V1+Deff*V2}{1-D2}$ ……..... [73]

Here, $D_{eff} = D_2 - D_1$, the value of D_{eff} cancels out from the expression because we will implement the topology by taking same duty cycle of the two sources for ease of application. If we don't take similar duty cycle then we would need to incorporate another microcontroller to drive the second MOSFET of the other source, that will ultimately increase the complexity of the overall proposed project.

From the hardware analysis, we have seen that the bicycle dynamo is giving more or less DC105V. To achieve secondary design approach, first we need to stabilize and fix the output of the bicycle dynamo using different op-amp comparator circuits and ultimately developing a PID controller to stabilize the output. Let us assume that, we adjust the bicycle dynamo output to 24V using a feedback controller. Then at different times of the day, the MISO topology will work based on two phenomena. When the Solar PV panel output voltage exceeds the bicycle dynamo output voltage (>24V), the bicycle dynamo voltage source will be automatically redundant. During this time, the Solar PV panel will dominate the project as a source. This can happen in summer season, from 8AM up to 3PM when the solar irradiance is very high. On the other hand, when the Solar PV panel is less dominant during early morning and late afternoon, the dynamo output will dominate the MISO topology as the most contributing source. This can happen in summer days from 4AM up to 8AM and 3PM up to 6PM. It is to note that, we can adjust the bicycle dynamo output as per our requirements.

7.3.1 Components for the SEPIC based MISO Converter Circuit

i. **Gate Driver Circuit:** Just like the SISO topology, we have used a S8050 as a gate driver circuit of the MISO topology.

ii. **Microcontroller:** In the MISO topology, we are actually using an Arduino Pro Mini based on ATmega328. It has 14 digital pins to be used as either input or outputs, it has six analog inputs, on-board resonator, a reset button and holes for mounting pin headers [72].

iii. **Power Circuit:** The power circuit of the MISO topology consists of two inductor coils at the source side and one inductor coil at the load side. The circuit has two coupling capacitors at the source side along with one capacitor at the load side to sweep the output ripple effect. It has a schottky diode namely ZRB582. The reverse

recovery time of the schottky diode is very small and also the cut-in voltage for a schottky diode is very smaller [74]. We also have a load resistor at the power circuit.

iv. **Reverse Voltage Polarity Protection:** We have used 4 IN4007 diodes to create a Safety Protection Circuit for the reverse-polarity issue, if experienced, from the bicycle dynamo output.

v.

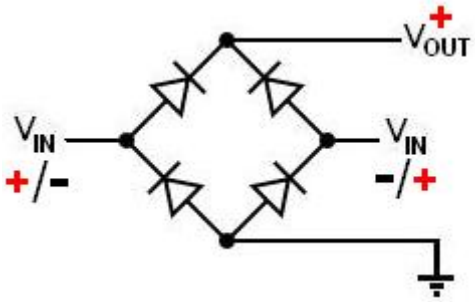

Figure 7.7: The reverse polarity protection circuit using IN4007 diodes as bridge rectifier (source: Google)

The main advantages of creating this circuit is that the polarity of the bicycle dynamo that is shown in Figure 7.7. Generator will not matter that is going as an input to the reverse-polarity bridge-rectifier circuit.

vi. **Mini Digital Volt-Meter:** The voltmeter has three wires. The red, black and a yellow one. The red and black ones are used to power up the voltmeter.

vii. **LEDs:** In our proposed MISO converter circuit, we have also used several RGB LEDs as indicators to the bicycle dynamo generator outpur voltage.

7.3.2 Hardware Result of the SEPIC based MISO Converter Circuit

The hardware parameters used in the practical field test of SEPIC based MISO Converter have been listed in the Table 7-4.

Sl no.	Parameter	Experimental Value
1.	V_{in}	12.1 V
2.	V_{out}	52.8 V (adjusted)
3.	$V_{out(max)}$	53.3V
4.	Load Resistance	282 Ω
5.	Duty Cycle	81.43%
6.	I_{L1}	0.19 A
7.	I_{L2}	0.19 A
8.	V_{L1}	-53.61 V
9.	V_{L2}	-53.61 V
10.	V_L	53.6V
11.	V_{C1}	-12.11V
12.	V_{C2}	-12.11V
13.	V_C	V_0
14.	V_R	52.8V
15.	Switching Frequency	32 kHz
16.	$Load_{(experimental)}$	10.1 W
17.	I_{load}	0.18A
18.	$I_{load(max)}$	0.19A
19.	I_{C1}	0.67A
20.	I_{C2}	0.43A

Table 7-4: Hardware Parameters of SEPIC based MISO Converter Circuit

7.3.2.1 Voltage Gain of the SEPIC based MISO Converter Circuit

D	V_{in}	V_{out}	V_{gain}
0.4716	12.1	10.8	0.892562
0.4916	12.1	11.7	0.966942
0.5141	12.1	12.8	1.057851
0.5273	12.1	13.5	1.115702
0.5434	12.1	14.4	1.190083
0.5568	12.1	15.2	1.256198
0.5754	12.1	16.4	1.355372
0.5953	12.1	17.8	1.471074
0.6046	12.1	18.5	1.528926
0.6183	12.1	19.6	1.619835
0.6253	12.1	20.2	1.669421
0.6399	12.1	21.5	1.77686
0.6543	12.1	22.9	1.892562
0.6611	12.1	23.6	1.950413
0.6694	12.1	24.5	2.024793
0.6833	12.1	26.1	2.157025
0.6968	12.1	27.8	2.297521
0.6998	12.1	28.2	2.330579
0.7119	12.1	29.9	2.471074
0.7186	12.1	30.9	2.553719
0.7238	12.1	31.7	2.619835
0.7269	12.1	32.2	2.661157

0.7346	12.1	33.5	2.768595
0.7392	12.1	34.3	2.834711
0.7458	12.1	35.5	2.933884
0.7515	12.1	36.6	3.024793
0.754	12.1	37.1	3.066116
0.7599	12.1	38.3	3.165289
0.7641	12.1	39.2	3.239669
0.7699	12.1	40.5	3.347107
0.7729	12.1	41.2	3.404959
0.7772	12.1	42.2	3.487603
0.7804	12.1	43	3.553719
0.7866	12.1	44.6	3.68595
0.7911	12.1	45.8	3.785124
0.7917	12.1	46	3.801653
0.7949	12.1	49	4.049587
0.7979	12.1	47.8	3.950413
0.8	12.1	48.4	4
0.8029	12.1	49.3	4.07438
0.8067	12.1	50.5	4.173554
0.8091	12.1	51.3	4.239669
0.8118	12.1	52.2	4.31405
0.8147	12.1	53.2	4.396694
0.8149	12.1	53.3	4.404959

Table 7-5: Voltage Gain for SEPIC based MISO

Figure 7.8: Graphical Representation of Duty Cycle vs Voltage Gain for MISO SEPIC

Figure 7.8 represents the relation of duty cycle and voltage gain of the Multi Input Single Output (MISO) SEPIC converter. The graph states that the relation of duty cycle with voltage gain is directly proportional. That means by increasing the duty cycle we can increase the voltage gain. Since, we know that SEPIC converter with duty cycle less than 50% works as a buck converter and during that time the voltage gain is less than 1 but when we increase the duty cycle by adjusting the potentiometer, voltage gain also increases simultaneously and the gain becomes greater than 1. Maximum output voltage that can be given by our circuit is 53.3V and at that time duty cycle measured is 81.49% and voltage gain becomes slightly greater than 4.

7.3.2.2 Efficiency of the SEPIC based MISO Converter Circuit

Duty Cycle	Vin	Vo	Iin	Io	Po	Pin	Efficiency (%)
0.8149	12.1	53.3	0.9136	0.19	10.127	11.05	91.64
0.8147	12.1	53.2	0.914	0.19	10.108	11.0594	91.39
0.8118	12.1	52.2	0.911	0.19	9.918	11.0231	89.98
0.8091	12.1	51.3	0.910	0.19	9.747	11.011	88.521
0.8067	12.1	50.5	0.908	0.187	9.4435	10.9868	85.95
0.8029	12.1	49.3	0.907	0.183	9.0219	10.9747	82.206
0.8	12.1	48.4	0.905	0.180	8.712	10.9505	79.559
0.7979	12.1	47.8	0.902	0.179	8.5562	10.9142	78.39
0.7949	12.1	47.3	0.899	0.176	8.272	10.8749	76.044
0.7917	12.1	46	0.893	0.174	8.004	10.8053	74.08
0.7911	12.1	45.8	0.890	0.172	7.8776	10.769	73.16

0.7866	12.1	44.6	0.884	0.166	7.4036	10.6964	69.22
0.7804	12.1	43	0.881	0.163	7.009	10.6601	65.75
0.7772	12.1	42.2	0.879	0.161	6.7942	10.6359	63.32
0.7729	12.1	41.2	0.877	0.161	6.6332	10.6117	62.51
0.7699	12.1	40.5	0.876	0.160	6.48	10.5996	61.14
0.7641	12.1	39.2	0.873	0.158	6.1936	10.5633	58.64
0.7599	12.1	38.3	0.872	0.156	5.9748	10.5512	56.62
0.754	12.1	37.1	0.872	0.155	5.7505	10.5512	54.50
0.7515	12.1	36.6	0.870	0.155	5.673	10.527	53.89
0.7458	12.1	35.5	0.866	0.154	5.467	10.4786	52.173
0.7392	12.1	34.3	0.865	0.153	5.2479	10.4665	50.14
0.7346	12.1	33.5	0.865	0.153	5.1255	10.4665	48.97

0.7269	12.1	32.2	0.865	0.153	4.9266	10.4665	47.08
0.7238	12.1	31.7	0.863	0.152	4.8184	10.4423	46.14
0.7186	12.1	30.9	0.862	0.150	4.635	10.4302	44.44
0.7119	12.1	29.9	0.860	0.148	4.4252	10.406	42.525
0.6998	12.1	28.2	0.859	0.148	4.2624	10.3939	41.008
0.6968	12.1	27.8	0.855	0.147	4.0866	10.3455	39.51
0.6833	12.1	26.1	0.854	0.145	3.7845	10.3334	36.63
0.6694	12.1	24.5	0.854	0.144	3.528	10.3334	34.15
0.6611	12.1	23.6	0.853	0.144	3.3984	10.3213	32.93
0.6543	12.1	22.9	0.850	0.143	3.2747	10.285	31.84
0.6399	12.1	21.5	0.849	0.141	3.0315	10.2729	29.51
0.6253	12.1	20.2	0.849	0.140	2.828	10.2729	27.528
0.6183	12.1	19.6	0.846	0.140	2.744	10.2366	26.81

0.6046	12.1	18.5	0.845	0.138	2.553	10.2245	24.97
0.5953	12.1	17.8	0.842	0.137	2.4386	10.1882	23.94
0.5754	12.1	16.4	0.840	0.137	2.2468	10.164	22.11
0.5568	12.1	15.2	0.839	0.135	2.052	10.1519	20.213
0.5434	12.1	14.4	0.836	0.1310	1.8864	10.1156	18.648
0.5273	12.1	13.5	0.835	0.127	1.7145	10.1035	16.969
0.5141	12.1	12.8	0.835	0.125	1.600	10.1035	15.836
0.4916	12.1	11.7	0.830	0.125	1.4625	10.043	14.562
0.4716	12.1	10.8	0.829	0.123	1.3284	10.0309	13.243

Table 7-6: The values of Efficiency with changing Duty Cycle for the MISO SEPIC

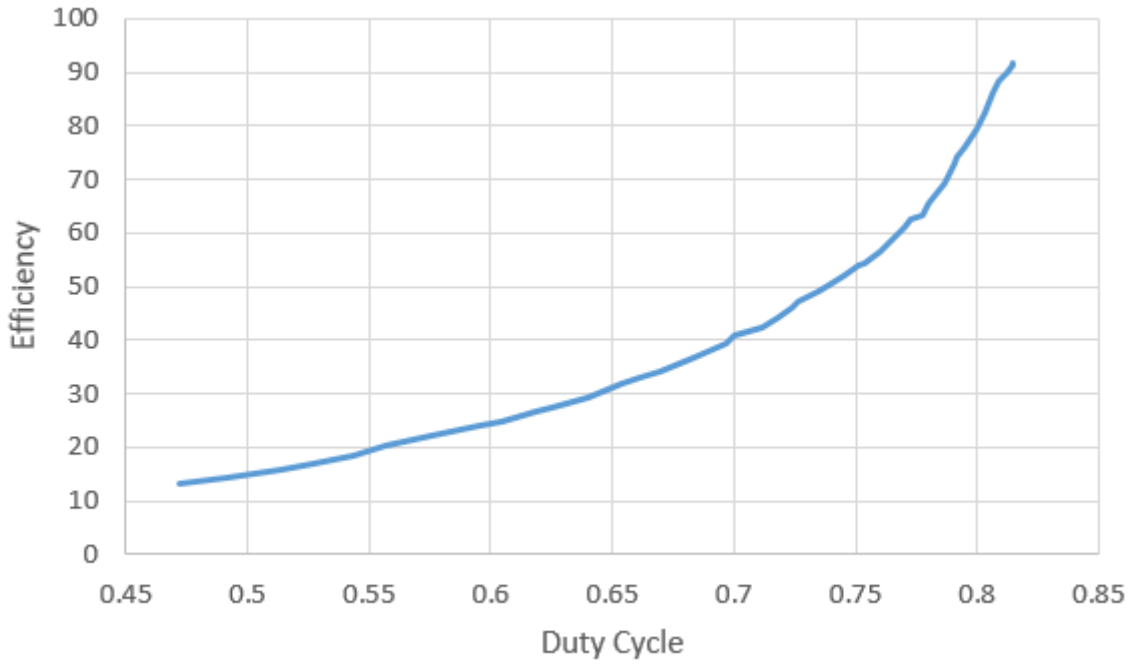

Figure 7.9: Characteristics Curve Efficiency Vs Duty Cycle for MISO SEPIC

In our MISO system, efficiency changes positively with the increasing of duty cycle. Figure 7.9 shows the direct proportional relation between duty cycle and efficiency. Our maximum efficiency of the system is 91.64% when the adjusted duty cycle is 81.49% and efficiency of the system decreases with decrement of duty cycle.

Chapter 8 Conclusions and Future Work

8.1 Conclusion

This paper proposes a Multi-Input–Single-Output (MISO) DC-DC SEPIC converter. The suggested converter's functioning has been thoroughly investigated. The suggested topology has several advantages, including a high voltage gain, decreased current stress, and a higher rating for the power switches, among others. Furthermore, it should be noted that the converter under consideration offers an increased switching duty cycle spectrum. Because of this, a more flexible control strategy may be implemented.

By comparing simulation and actual findings, we were able to confirm that the specific procedures in many instances, as well as design principles and theoretical assessments, were correct. In addition, experimental data offered to demonstrate the feasibility and validity of the converter under consideration. Because of the advantages gained from the suggested topology, it is a suitable converter for clean energy generating systems, such as those that use MPPT on PV modules or operate in hybrid energy generation systems, among other applications.

8.2 Future Work

As we have built a Multi Input Single Output (MISO) SEPIC. The sources that we have used are solar PV panel and bicycle dynamo generator to give supply power to dc loads. Nevertheless, we can use other sources too, to supply the required power. For example, we can combine our national grids with the solar PV panel in our MISO SEPIC prototype. As a result, the loads can get a constant power supply from the national or from the solar power. The prototype can be developed in such a way that, when there is presence of sunlight and it can give adequate energy to the solar panel to meet the demand of the load till that the load will receive power from solar panel and will not receive power from the grid. The grid will mainly be in cutoff position when the availability of sunlight is satisfactory. However, it’s not possible

to have sunlight throughout the whole day adequately. Especially during winter, the sunlight is unable to produce enough heat. Moreover, the sun starts to set at evening and completely disappears at night. In these scenarios, the grid will supply the power when the solar panel will be unable to provide required amount of power. On that account, getting adequate power from solar panel will be our first priority and grid will be an optional source. If the solar panel fails to provide required energy, then the grid will act as optional power source. As the system will be planned to construct without the presence of battery. It is because batteries cannot be afforded by everyone and the cells will be needed to change when it crosses its expired date. A system without the battery will be less hectic, affordable and user friendly. As the sources will be alternate to each other a controller is needed to be placed which can switch the power the automatically. The controller will control the sources in such a way that, during the sufficient amount of day light it will allow the power to be supplied from solar panel to the load and disallow power form the grid at that time. On the other hand, when there is absence of adequate sunlight the controller will switch the system towards grid and the system will receive power from grid. The controller that can be used here is a fuzzy logic controller.

Fuzzy logic controller system is one of the intelligent methods of energy management system that aims at conserving energy. The effectiveness of fuzzy logic controller is depending on set of restrictions, linguistic variables, values, and number of probabilistic combinations of resources to formulate the rules [24]. It is an intelligent switch which can shift the load to available resource. The fuzzy logic controller is based on fuzzy logic which is closed to human thinking. This controller is an intelligent management tool, which serves to manage the energy for energy saving. To maximize the supply from solar panel and save the energy of national grid, this controller can play a very vital role. It can save up to 80% energy of national grid during day time [24]. A rule-based control system of this controller will be a suitable way to use this to compare the load demand at the various times a day with the availability of the

resources by giving the priority to the solar panel. A written rule can be applied to maximize the use of solar panel. It is a multi-valued logic, between 1 and 0 it can consider the decimal numbers too for different conditions. Therefore, the system can understand various conditions of the sun and function accordingly.

Moreover, it is seen that the solar panel sometimes produces more power than it is required for the load. The excess power can be feedback to the utility grid if a battery is fixed with the transformer by the utility company. The extra energies can be stored there. Then the owner of the solar panels can sell the extra energies to the utility companies with a reasonable price. Through this way both the utility company and the seller will be profitable. In addition, since we have used two renewable resources in our system, but we can use here more than two renewable resources. In future this system can be used for supplying power to higher load if multiple sources are connected with this system. More renewable energy sources can be connected with proper design of the required parameters of the system. For example- Windmill, Biomass, Geothermal etcetera can be connected here as additional sources to this system which will be able to supply more energy to the load.

The sole target of this system will be to save energies of national grid and provide sufficient electricity to the people of remote areas, in their range of affordability. All these things will be possible if we maximize the use of solar panel, as the energy that we will get from here is free so it will be our first priority but we should also consider an alternate source to supply constantly to the load when solar panel fails to provide necessary amount of energy. Therefore, we can observe here that, we won't be needing a battery and also constant supply from the grid also not required. Thus, through this process the electricity can be made affordable for the people of remote areas and the pressure from the grid can also be reduced. The energy production will also be more.

References

[1] M. Banaei, H. Ardi, R. Alizadeh and A. Farakhor, "Non-isolated multi-input–single-output DC/DC converter for photovoltaic power generation systems", *IET Power Electronics*, vol. 7, no. 11, pp. 2806-2816, 2014. Available: 10.1049/iet-pel.2013.0977

[2] R. Gules, W. dos Santos, F. dos Reis, E. Romaneli and A. Badin, "A Modified SEPIC Converter With High Static Gain for Renewable Applications", *IEEE Transactions on Power Electronics*, vol. 29, no. 11, pp. 5860-5871, 2014. Available: 10.1109/tpel.2013.2296053

[3] C. Anuradha, N. Chellammal, M. Saquib Maqsood and S. Vijayalakshmi, "Design and Analysis of Non-Isolated Three-Port SEPIC Converter for Integrating Renewable Energy Sources", *Energies*, vol. 12, no. 2, p. 221, 2019. Available: 10.3390/en12020221

[4] R. Moradpour, H. Ardi and A. Tavakoli, "Design and Implementation of a New SEPIC-Based High Step-Up DC/DC Converter for Renewable Energy Applications", *IEEE Transactions on Industrial Electronics*, vol. 65, no. 2, pp. 1290-1297, 2018. Available: 10.1109/tie.2017.2733421

[5] G. Mohanty, "SEPIC Based Multi Input Dc-Dc Converter", *2019 IEEE 5th International Conference for Convergence in Technology (I2CT)*, 2019. Available: 10.1109/i2ct45611.2019.9033886

[6] H. Ardi and A. Ajami, "Study on a High Voltage Gain SEPIC-Based DC–DC Converter With Continuous Input Current for Sustainable Energy Applications", *IEEE Transactions on Power Electronics*, vol. 33, no. 12, pp. 10403-10409, 2018. Available: 10.1109/tpel.2018.2811123

[7] Y. Hsieh, J. Chen, T. Liang and L. Yang, "Novel High Step-Up DC–DC Converter With Coupled-Inductor and Switched-Capacitor Techniques", *IEEE Transactions on Industrial Electronics*, vol. 59, no. 2, pp. 998-1007, 2012. Available: 10.1109/tie.2011.2151828

[8] Megalingam, Rajesh Kannan & Sreedharan Veliyara, Pranav & Prabhu, Raghavendra & Katoch, Rocky. (2012). Pedal Power Generation. 7.

[9] Ruichen Zhao and A. Kwasinski, "Multiple-input single ended primary inductor converter (SEPIC) converter for distributed generation applications", *2009 IEEE Energy Conversion Congress and Exposition*, 2009. Available: 10.1109/ecce.2009.5316295

[10] "Attaining renewables generation target still elusive", *Dhaka Tribune*, 2021. [Online]. Available: https://www.dhakatribune.com/bangladesh/2021/06/26/attaining-renewables-generation-target-still-elusive. [Accessed: 06- Jul- 2021].

[11] "Sustainable finance presents Bangladesh with verdant possibilities", *The Daily Star*, 2021. [Online]. Available: https://www.thedailystar.net/opinion/news/sustainable-finance-presents-bangladesh-verdant-possibilities-2118645. [Accessed: 06- Jul- 2021].

[12] Z. Rehman, I. Al-Bahadly and S. Mukhopadhyay, "Multiinput DC–DC converters in renewable energy applications – An overview", *Renewable and Sustainable Energy Reviews*, vol. 41, pp. 521-539, 2015. Available: 10.1016/j.rser.2014.08.033

[13] D. Sangalad, Hemalatha J N, Hariprasad S.A. and Anitha G.S., "Design and analysis of dual input SEPIC converter for renewable energy sources", *2015 International Conference on Emerging Research in Electronics, Computer Science and Technology (ICERECT)*, 2015. Available: 10.1109/erect.2015.7499041

[14] S. Haghighian, S. Tohidi, M. Feyzi and M. Sabahi, "Design and analysis of a novel SEPIC-based multi-input DC/DC converter", *IET Power Electronics*, vol. 10, no. 12, pp. 1393-1402, 2017. Available: 10.1049/iet-pel.2016.0654

[15] Nath, V., & Mandal, J. K. (2020). *Proceedings of the Third International Conference on Microelectronics, Computing and Communication Systems: MCCS 2018 (Lecture Notes in Electrical Engineering, 556)* (1st ed. 2019 ed.). Springer.

[16] R. Meenadevi and L. Premalatha, "A Novel bridgeless SEPIC Converter for Power Factor Correction", Energy Procedia, vol. 117, pp. 991-998, 2017. Available: 10.1016/j.egypro.2017.05.220.

[17] W. Gu and D. Zhang, "Designing A SEPIC Converter", 2008.

[18] M. Verma and S. Kumar, "Hardware Design of SEPIC Converter and its Analysis", *2018 International Conference on Current Trends towards Converging Technologies (ICCTCT)*, 2018. Available: 10.1109/icctct.2018.8551052

[19] H. Pathirathne and P. Maduranga, "Design & Simulation of a SEPIC Converter for Home Solar PV Systems", in *27th IET Annual Technical Conference*, Colombo, Sri Lanka, 2020.

[20] R. Wai, C. Lin and B. Chen, "High-Efficiency DC–DC Converter With Two Input Power Sources", *IEEE Transactions on Power Electronics*, vol. 27, no. 4, pp. 1862-1875, 2012. Available: 10.1109/tpel.2011.2170222

[21] J. Duran-Gomez, E. Garcia-Cervantes, D. Lopez-Flores, P. Enjeti and L. Palma, "Analysis and Evaluation of a Series-Combined Connected Boost and Buck-Boost DC-DC Converter for Photovoltaic Application", *Twenty-First Annual IEEE Applied Power Electronics Conference and Exposition, 2006. APEC '06.*. Available: 10.1109/apec.2006.1620657

[22] R. Wai, C. Lin, L. Liu and Y. Chang, "High-efficiency single-stage bidirectional converter with multi-input power sources", *IET Electric Power Applications*, vol. 1, no. 5, p. 763, 2007. Available: 10.1049/iet-epa:20060500

[23] T. Gibson, "These Exercise Machines Turn Your Sweat Into Electricity", *IEEE Spectrum*, 2011. [Online]. Available: https://spectrum.ieee.org/these-exercise-machines-turn-your-sweat-into-electricity. [Accessed: 20- Aug- 2021].

[24] A. Nebey, "Energy management system for grid-connected solar photovoltaic with battery using MATLAB simulation tool", *Cogent Engineering*, vol. 7, no. 1, p. 1827702, 2020. Available: 10.1080/23311916.2020.1827702

[25] I. Cowie, "All About Batteries, Part 3: Lead-Acid Batteries", *EETimes*, 2014. [Online]. Available: https://www.eetimes.com/all-about-batteries-part-3-lead-acid-batteries/. [Accessed: 23- Aug- 2021].

[26] S. Mouslim, M. Oubella, M. Kourchi and M. Ajaamoum, "Simulation and analyses of SEPIC converter using linear PID and fuzzy logic controller", *Materials Today: Proceedings*, vol. 27, pp. 3199-3208, 2020. Available: 10.1016/j.matpr.2020.04.506

[27] S. Gorji, H. Sahebi, M. Movahed and M. Ektesabi, "Multi-Input Boost DC-DC Converter with Continuous Input-Output Current for Renewable Energy Systems", *2019 IEEE 4th International Future Energy Electronics Conference (IFEEC)*, 2019. Available: 10.1109/ifeec47410.2019.9014953

[28] B. Baliwant, A. Gothane and V. Waghmare, "Hardware Implementation of DC-DC SEPIC Converter For Applications of Renewable Energy Using PWM Based Charge Controller", *2019 3rd International conference on Electronics, Communication and Aerospace Technology (ICECA)*, 2019. Available: 10.1109/iceca.2019.8822229

[29] P. Rani and S. Saravanan, "Simulation and modeling Of SEPIC converter with high static gain for renewable application", *2017 Asian Conference on Energy, Power and Transportation Electrification (ACEPT)*, 2017. Available: 10.1109/acept.2017.8168573

[30] ARDUINO Datasheet

[31] A. Deshpande, "Coupled Inductor and Voltage Doubler Circuit for High Step-Up DC-DC Converter", 2021. Available: 10.20944/preprints202104.0717.v1

[32] S. Saravanan and N. Babu, "A modified high step-up non-isolated DC-DC converter for PV application", *Journal of Applied Research and Technology*, vol. 15, no. 3, pp. 242-249, 2017. Available: 10.1016/j.jart.2016.12.008

[33] M. Al, J. Van and H. Gualous, "DC/DC Converters for Electric Vehicles", *Electric Vehicles - Modelling and Simulations*, 2011. Available: 10.5772/17048

[34] P. Anbarasi, S. Priya and D. Poongodi, "Voltage Regulator Dc_Dc Converter Based On Filter for Low Power Analysis", *IOSR Journal of Electronics and Communication Engineering*, vol. 9, no. 2, pp. 19-23, 2014. Available: 10.9790/2834-09251923

[35] https://www.philadelphia.edu.jo/academics/mlazim/uploads/chapter04.pdf. [Accessed: 20- Aug- 2021].

[36] https://www.electrical4u.com/lc-circuit-analysis/#:~:text=An%20LC%20circuit%20%28also%20known%20as%20an%20LC,circuit%2C%20or%20tuned%20circuit.%20An%20LC%20%E2%80%93%20Circuit

[37] F. Asadi and K. Eguchi, "Dynamics and Control of DC-DC Converters", *Synthesis Lectures on Power Electronics*, vol. 6, no. 1, pp. 1-241, 2018. Available: 10.2200/s00828ed1v01y201802pel010

[38] W. Storr, "Magnetism, Magnetic Flux and Magnetic Materials", *Basic Electronics Tutorials*, 2018. [Online]. Available: https://www.electronics-tutorials.ws/electromagnetism/magnetism.html. [Accessed: 04- Sep- 2021].

[39] M. Brain, W. Harris and R. Lamb, "How Electricity Works", *HowStuffWorks*, 2021. [Online]. Available: https://science.howstuffworks.com/electricity.htm. [Accessed: 05- Sep- 2021].

[40] "Generators and Dynamos", *Edisontechcenter.org*, 2021. [Online]. Available: http://edisontechcenter.org/generators.html. [Accessed: 06- Sep- 2021].

[41] "How the charging system works", *How a Car Works*, 2021. [Online]. Available: https://www.howacarworks.com/basics/how-the-charging-system-works. [Accessed: 07- Sep- 2021].

[42] S. Hymel, "Alternating Current (AC) vs. Direct Current (DC) - learn.sparkfun.com", *Learn.sparkfun.com*, 2021. [Online]. Available: https://learn.sparkfun.com/tutorials/alternating-current-ac-vs-direct-current-dc. [Accessed: 09- Sep- 2021].

[43] B. Lamp, "Basics of the Car Electrical System", *NAPA Know How Blog*, 2018. [Online]. Available: https://knowhow.napaonline.com/car-electrical-system-basics/. [Accessed: 08- Sep- 2021].

[44] "Dynamo", *De Fietssite.nl*, 2016. [Online]. Available: https://defietssite.nl/dynamo/?lang=en. [Accessed: 08- Sep- 2021].

[45] W. McArdle, F. Katch and V. Katch, *Essentials of exercise physiology*. .

[46] N. Baharudin, T. Mansur, F. Hamid, R. Ali and M. Misrun, "Performance Analysis of DC-DC Buck Converter for Renewable Energy Application", *Journal of Physics: Conference Series*, vol. 1019, p. 012020, 2018. Available: 10.1088/1742-6596/1019/1/012020

[47] "RE Generation Mix | National Database of Renewable Energy", *Renewableenergy.gov.bd*, 2021. [Online]. Available: http://www.renewableenergy.gov.bd/index.php?id=4. [Accessed: 20- Sep- 2021].

[48] "List of power stations in Bangladesh - Wikipedia", *En.wikipedia.org*, 2021. [Online]. Available: https://en.wikipedia.org/wiki/List_of_power_stations_in_Bangladesh#Solar_PV. [Accessed: 21- Sep- 2021].

[49] "Solar Park | National Database of Renewable Energy, SREDA", *Renewableenergy.gov.bd*, 2021. [Online]. Available: http://www.renewableenergy.gov.bd/index.php?id=1&i=1&pg=1. [Accessed: 21- Sep- 2021].

[50] M. Alauddin, "Introducing floating solar PV technology in Bangladesh", *The Financial Express*, 2020. [Online]. Available: https://thefinancialexpress.com.bd/national/introducing-floating-solar-pv-technology-in-bangladesh-1589818193. [Accessed: 21- Sep- 2021].

[51] V. Fthenakis, "Overview of Potential Hazards", 2021.

[52] https://www.sciencedirect.com/topics/engineering/solar-radiation

[53] "Air mass (solar energy) - Wikipedia", *En.wikipedia.org*, 2021. [Online]. Available: https://en.wikipedia.org/wiki/Air_mass_(solar_energy). [Accessed: 21- Sep- 2021].

[54] "AM1.5 Reference Solar Spectral Irradiance | Everything about solar energy", *Everything about solar energy | Solar energy, helio systems, solar panels, collectors, equipment for water heating and space heating using solar energy and everything about solar energy.*, 2021. [Online]. Available: http://energyprofessionalsymposium.com/?p=5611. [Accessed: 21- Sep- 2021].

[55] "Temperature Coefficient of Solar PV Module", *Linkedin.com*, 2021. [Online]. Available: https://www.linkedin.com/pulse/temperature-coefficient-solar-pv-module-ada-wang. [Accessed: 21-

[56] M. M. Hossain, S. Barua and M. A. Matin, "A pre-feasibility study for electrification in Nijhum Dwip using hybrid renewable technology," 2015 International Conference on Electrical & Electronic Engineering (ICEEE), 2015, pp. 225-228, doi: 10.1109/CEEE.2015.7428262.

[57] T. G. Patil and A. Asokan, "A proficient solar panel efficiency measurement system: Using current measurements," 2016 International Conference on Communication and Electronics Systems (ICCES), 2016, pp. 1-6, doi: 10.1109/CESYS.2016.7889927.

[58] R. B. Nazmul, "Calculating Optimum Angle for Solar Panels of Dhaka, Bangladesh for Capturing Maximum Irradiation," 2017 IEEE International WIE Conference on Electrical and Computer Engineering (WIECON-ECE), 2017, pp. 25-28, doi: 10.1109/WIECON-ECE.2017.8468880.

[59] "What is an LC Filter? | Coilcraft", Coilcraft.com, 2021. [Online]. Available: https://www.coilcraft.com/en-us/edu/series/what-is-an-lc-filter/. [Accessed: 21- Sep- 2021].

[60] "LC Filter Calculator - How LC filters work - ElectronicBase", ElectronicBase, 2021. [Online]. Available: https://electronicbase.net/lc-filter-calculator/#:~:text=The%20LC%20filter%2C%20also%20called%20the%20LC%20filtering, cutoff%20frequency%20is%20a%20key%20element%20of%20this. [Accessed: 21- Sep- 2021].

[61] T. Taufik, K. Htoo, and G. Larson, "Multiple-input bridge converter for connecting multiple renewable energy sources to a DC system," Future Technologies Conf., FTC 2016, 6-7 Dec., San Francisko, USA, pp. 444-449

[62] K. Muddineni, P. Chamarthi, and V. Agarwal, "A new solar PV fed

multiple-input converter for DC micro grid application," 2017 IEEE 44th

Photovoltaic Specialists Conference, PVSC, pp. 1-5

[63] R. Zhao and A. Kwasinski, "Efficiency improvement of a low-power multiple-input converter with forward-conducting-bidirectional blocking switches," 2013 IEEE Energy Conversion Congress and Expo (ECCE), pp. 5566-5573

[64] A Thesis Report on "Sepic Converter Design and Operation"

[65] Smrity, A. Kumar, N. Bajoria and A. Alam, "Multiple-Input-Single-Output Converter for Hybrid Renewable Sources," 2019 International Conference on Vision Towards Emerging Trends in Communication and Networking (ViTECoN), 2019, pp. 1-5, doi: 10.1109/ViTECoN.2019.8899579.

[66] S. J. Chiang, H. Shieh and M. Chen, "Modeling and Control of PV Charger System With SEPIC Converter," in IEEE Transactions on Industrial Electronics, vol. 56, no. 11, pp. 4344-4353, Nov. 2009, doi: 10.1109/TIE.2008.2005144.

[67] Maglin, J.R, R. Ramesh, and Vaigundamoorthi."Design and Analysis of SEPIC Converter Based

MPPT for Solar PV Module with CPWM." J Electr Eng Technol 9.4 (2014).

[68] A. Tomar, P. H. Nguyen and S. Mishra, "SEPIC-MISO Converter Based PV Water Pumping System- An Improved Performance Under Mismatching Conditions," 2020 IEEE 9th Power India International Conference (PIICON), 2020, pp. 1-5, doi: 10.1109/PIICON49524.2020.9112907.

[69] "Wind Energy: Advantages and Disadvantages", Large.stanford.edu, 2021. [Online]. Available: http://large.stanford.edu/courses/2014/ph240/lloyd2/#:~:text=The%20two%20major%20disadvantages%20of%20wind%20power%20include,High%20cost%20of%20energy%20can%2C%20in%20part%2C%20be. [Accessed: 21- Sep- 2021].

[70]https://arena.gov.au/renewable-energy/bioenergy/#:~:text=What%20is%20bioenergy%20and%20energy%20from%20waste

%3F%20Bioenergy,also%20include%20combustible%20components%20of%20municipal%20solid%20waste.

[71] M. M. Hossain, S. Barua and M. A. Matin, "A pre-feasibility study for electrification in Nijhum Dwip using hybrid renewable technology," 2015 International Conference on Electrical & Electronic Engineering (ICEEE), 2015, pp. 225-228, doi: 10.1109/CEEE.2015.7428262.

[72] https://www.arduino.cc/en/pmwiki.php?n=Main/ArduinoBoardProMini

[73] Anuradha, C., N. Chellammal, Md Saquib Maqsood, and S. Vijayalakshmi 2019. "Design and Analysis of Non-Isolated Three-Port SEPIC Converter for Integrating Renewable Energy Sources" *Energies* 12, no. 2: 221. https://doi.org/10.3390/en12020221

[74] Difference Between Schottky and Zener Diode (pediaa.com)

Appendix A.

Code for MPPT Algorithm:

```
function duty = MPPT_algorithm(vpv,ipv,delta)
% I used the MPPT algorithm in the MATLAB examples
% I only modify somethings.
duty_init = 0.8064;
% min and max value are used to limit duty between
% 0 and 0.85
duty_min=0;
duty_max=0.85;

persistent Vold Pold duty_old;
% persistent variable type can store the data
% we need the old data by obtain difference
% between old and new value
if isempty(Vold)
    Vold=0;
    Pold=0;
    duty_old=duty_init;
end
P= vpv*ipv; % power
dV= vpv - Vold; % difference between old and new voltage
dP= P - Pold; % difference between old and new power

% the algorithm in below search the dP/dV=0
```

```
% if the derivative equal to zero
% duty will not change
% if old and new power not equal
% &
% pv voltage bigger than 30V
% the algorithm will works
if dP ~= 0 && vpv>30
    if dP < 0
        if dV < 0
            duty = duty_old - delta;
        else
            duty = duty_old + delta;
        end
    else
        if dV < 0
            duty = duty_old + delta;
        else
            duty = duty_old - delta;
        end
    end
else
    duty = duty_old;
end

%the below if limits the duty between min and max
if duty >= duty_max
    duty=duty_max;
elseif duty<duty_min
```

```
    duty=duty_min;
end

% stored data
duty_old=duty;
Vold=vpv;
Pold=P;
```

Appendix B.

Arduino Datasheet:

The Arduino Datasheet has been attached.

8-bit serial-in/serial or parallel-out shift register with output latches; 3-state **74HC/HCT595**

FEATURES

- 8-bit serial input
- 8-bit serial or parallel output
- Storage register with 3-state outputs
- Shift register with direct clear
- 100 MHz (typ) shift out frequency
- Output capability:
  - parallel outputs; bus driver
  - serial output; standard
- I_{CC} category: MSI.

APPLICATIONS

- Serial-to-parallel data conversion
- Remote control holding register.

DESCRIPTION

The 74HC/HCT595 are high-speed Si-gate CMOS devices and are pin compatible with low power Schottky TTL (LSTTL). They are specified in compliance with JEDEC standard no. 7A.

The "595" is an 8-stage serial shift register with a storage register and 3-state outputs. The shift register and storage register have separate clocks.

Data is shifted on the positive-going transitions of the SH_{CP} input. The data in each register is transferred to the storage register on a positive-going transition of the ST_{CP} input. If both clocks are connected together, the shift register will always be one clock pulse ahead of the storage register.

The shift register has a serial input (D_S) and a serial standard output (Q_7') for cascading. It is also provided with asynchronous reset (active LOW) for all 8 shift register stages. The storage register has 8 parallel 3-state bus driver outputs. Data in the storage register appears at the output whenever the output enable input (OE) is LOW.

QUICK REFERENCE DATA

GND = 0 V; T_{amb} = 25 °C; $t_r = t_f$ = 6 ns.

SYMBOL	PARAMETER	CONDITIONS	TYP.		UNIT
			HC	HCT	
t_{PHL}/t_{PLH}	propagation delay	C_L = 15 pF; V_{CC} = 5 V			
	SH_{CP} to Q_7'		16	21	ns
	ST_{CP} to Q_n		17	20	ns
	$\overline{MR}$ to Q_7'		14	19	ns
f_{max}	maximum clock frequency SH_{CP}, ST_{CP}		100	57	MHz
C_I	input capacitance		3.5	3.5	pF
C_{PD}	power dissipation capacitance per package	notes 1 and 2	115	130	pF

Notes

1. C_{PD} is used to determine the dynamic power dissipation (P_D in μW):
   $P_D = C_{PD} \times V_{CC}^2 \times f_i + \Sigma (C_L \times V_{CC}^2 \times f_o)$ where:
   f_i = input frequency in MHz
   f_o = output frequency in MHz
   $\Sigma(C_L \times V_{CC}^2 \times f_o)$ = sum of outputs
   C_L = output load capacitance in pF
   V_{CC} = supply voltage in V
2. For HC the condition is V_I = GND to V_{CC}; for HCT the condition is V_I = GND to V_{CC} − 1.5 V.

ORDERING INFORMATION

TYPE NUMBER	PACKAGE		
	NAME	DESCRIPTION	VERSION
74HC595N	DIP16	plastic dual in-line package; 16 leads (300 mil); long body	SOT38-1
74HC595D	SO16	plastic small outline package; 16 leads; body width 3.9 mm	SOT109-1
74HC595DB	SSOP16	plastic shrink small outline package; 16 leads; body width 5.3 mm	SOT338-1
74HC595PW	TSSOP16	plastic thin shrink small outline package; 16 leads; body width 4.4 mm	SOT403-1
74HCT595N	DIP16	plastic dual in-line package; 16 leads (300 mil); long body	SOT38-1
74HCT595D	SO16	plastic small outline package; 16 leads; body width 3.9 mm	SOT109-1

PINNING

SYMBOL	PIN	DESCRIPTION
Q_0 to Q_7	15, 1 to 7	parallel data output
GND	8	ground (0 V)
Q_7'	9	serial data output
$\overline{MR}$	10	master reset (active LOW)
SH_{CP}	11	shift register clock input
ST_{CP}	12	storage register clock input
$\overline{OE}$	13	output enable (active LOW)
D_S	14	serial data input
V_{CC}	16	positive supply voltage

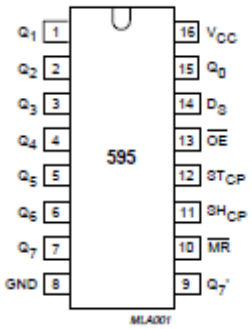

Fig.1 Pin configuration.

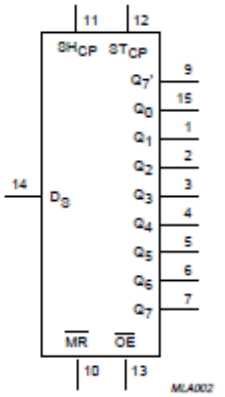

Fig.2 Logic symbol.

Arduino Code uploaded in SISO SEPIC Practical Circuit:

```
int a;

void setup () {

TCCR2B=TCCR2B&B11111000|B00000001; // 31.6khz (PWM Signal)

//TCCR0B = TCCR0B & B11111000 | B00000001; // for PWM frequency of 62500.00 Hz

Serial.begin (9600);

pinMode (A0, INPUT); //pot

pinMode (3, OUTPUT);

}



void loop () {

  // put your main code here, to run repeatedly:

 a = analogRead (A0);

 a = map (a,1023,0,255,0);

 analogWrite (3, a);

 Serial.println (a);

}
```

Arduino Code uploaded in MISO SEPIC Practical Circuit:

```
int potentiometer = A1;

int feedback = A0;

int PWM = 3;

int pwm = 0;

void setup () {

  pinMode (potentiometer, INPUT);

  pinMode (feedback, INPUT);

  pinMode (PWM, OUTPUT);

}

void loop () {

  float voltage = analogRead (potentiometer);

  float output = analogRead (feedback);

  if (voltage > output)

    {

     pwm = pwm+1;

     pwm = constrain (pwm, 1, 254);

    }



  if (voltage < output)
```

```
  {
   pwm = pwm-1;
   pwm = constrain (pwm, 1, 254);
  }
  analogWrite (PWM, pwm);
}
```

Appendix C.

SWERA Data for Monthly average hourly GHI:

Table 1: Monthly averaged hourly GHI (Wh/m^2)

Hours/month	Jan	Feb	Mar	Apr	May	Jun	Jul	Aug	Sep	Oct	Nov	Dec
5:30			1	5	17	19	11	7	3			
6:30	3	8	29	66	106	93	86	66	58	46	31	11
7:30	57	93	148	198	252	200	198	180	165	169	157	97
8:30	175	254	318	354	406	321	355	288	303	324	331	237
9:30	300	424	489	521	561	416	438	433	435	473	490	382
10:30	411	573	629	666	681	494	503	514	485	487	580	479
11:30	494	672	712	751	727	532	548	537	485	520	614	498
12:30	518	701	722	764	711	543	570	535	486	488	573	489
13:30	483	646	657	693	641	500	503	482	441	406	510	426
14:30	379	528	541	553	577	451	463	453	385	323	377	309
15:30	236	353	377	402	419	329	372	356	281	208	204	183
16:30	94	175	204	237	257	215	244	231	164	76	57	54
17:30	10	37	55	72	93	93	107	89	45	6	1	2
18:30			2	4	11	17	18	8	1			
Daily average (kWh/m^2-day)	3.16	4.46	4.88	5.28	5.46	4.22	4.42	4.18	3.74	3.53	3.92	3.17

Note: 5:30 represents the period between 5am to 6am

Appendix D.

Originality Report Check:

Similarity Index: 13%